Millipede-Inspired Locomotion for Rumen Monitoring through Remotely Operated Vehicle

Anthony Jon Chanco Garcia

Dissertation submitted to the faculty of the Virginia Polytechnic Institute and State University in partial fulfillment of the requirements for the degree of

Doctor of Philosophy

In

Mechanical Engineering

Shashank Priya, Chair
Rolf Mueller
Bahareh Behkam
Andrew J. Kurdila
Paul Marek

August 10, 2018
Blacksburg, VA

Keywords: Millipede Locomotion, Bio-Inspiration, Bio-Mimetic, Miniature Robotics

Millipede Inspired Locomotion for Rumen Monitoring through Remotely Operated Vehicle

Anthony Jon Chanco Garcia

Abstract

There has been a growing interest in development of nature-inspired miniature mobile robotics, for navigating complex ground scenarios, unknown terrains, and disaster-hit areas. One application is the development of a remotely operated vehicle (ROV) for rumen monitoring to improve our understanding of microbiology, and real-time physical changes and correlations with health. This interest is being driven from the desire to improve the safety and efficiency of food production by improving precision animal agriculture, which involves understanding the digestive system of ruminant animals and responding to the biochemical and physical changes. Most miniature robotic locomotion methods have taken inspiration from insects and have focused on adopting approaches that results in improved gait performance with respect to stability, velocity, cost-of-transport, and ability to navigate uneven surface terrains. In order to operate in the rumen environment, the locomotion mechanism should have the ability to handle large frictional and viscous forces in the direction of motion performing submerged burrowing-like action. The rumen environment consists of varying stiffness content with different fluidic concentration across the layers, reaching high viscosity and densities similar to wet soil or mud. Taking inspiration from millipedes for a locomotion mechanism to function in such an environment is attractive as these organisms have evolved to be proficient burrowers in similar substrates.

In this dissertation, the bio-mechanics of millipedes were investigated in-depth and modeled using analytical approaches. Multiple experiments were conducted on real animals to gain fundamental understanding of their locomotive abilities under varying environmental conditions. From this understanding, their gait behavior was emulated on a robotic platform to confirm the predicted dynamics and practically demonstrate the phenomena of modulating thrust force. The robotic models were also utilized to validate the parametric analysis and gain insight of the burrowing ability in varying gait behavior and body morphology. The primary features that govern the millipede behavior for effective burrowing were analyzed and utilized to design a locomotion mechanism for a rumen ROV. The design of the locomotion mechanism was tested in rumen-like media consisting of a wet mud mixture, where both locomotion thrust and steering ability were demonstrated.

Millipede Inspired Locomotion for Rumen Monitoring through Remotely Operated Vehicle

Anthony Jon Chanco Garcia

General Audience Abstract

In this dissertation, the movement of millipedes utilize to traverse effectively within an environment that provides significant resistance is studied. Through various experimental observations and mathematical modeling, we are able to develop an understanding of the techniques millipedes use to be effective burrowers. To validate our model and understanding the millipede movement techniques, a robot was designed to emulate a millipede's body structure and movement behavior. The performance of the millipede robot was found to be consistent with that of the biological creatures, indicating that we are able to emulate their behavior to achieve desirable tasks.

With this developed understanding of the fundamental concepts that allow millipedes to effectively move against large resistances, we introduce the ability to design robots or devices that can achieve similar performance for various applications ranging from search and rescue to health inspection. One such application is a device that traverse within the stomach (rumen) of dairy cows to investigate its biological features and characteristics for improvement in animal agricultural efficiency. The fundamental concepts of millipede motion are translated to a rumen monitoring vehicle design, which would operate in a wet-soil-like environment, similar to millipedes. The device motion techniques are demonstrated, an indication of successfully transferring the fundamental mechanism used by millipedes for an engineering application.

Acknowledgments

I would like to express my sincere gratitude to my advisor, Dr. Shashank Priya, for the opportunity to join his group and accomplish the work in this dissertation, as well as several other engaging research projects. Thank you for the providing the environment that challenged me, while giving me the freedom to pursue my ideas. I would not be where I am today without his efforts in supporting me.

I wish to thank my committee, Dr. Behkam, Dr. Mueller, Dr. Kurdila, and Dr. Marek for providing their suggestions and valuable time to improve this research.

I wish to express my appreciation to the CEHMS and BMDL laboratories for their valued support, insight, and collaboration on various research efforts. It has been a great experience working along-side a group of very dedicated and intelligent colleagues.

I would also like to thank all my friends who have helped me throughout my academic career to get to where I am today.

Without the love and support of my family, I would not have been able to accomplish any of my pursuits. Thanks to my parents, who have always supported me and made willing sacrifices in their lives for anything and everything I have striven for. Thanks to my brothers and sisters, for being there and all the encouragement they have given me.

Table of Contents

List of Figures

List of Tables

Chapter 1 – Introduction

1.1 Problem Statement

There is a growing need for miniature mobile robots that can navigate through difficult scenarios, unknown terrains, and dangerous areas of interest. Whether autonomous or actively/remotely operated, such robotic devices can be used for a range of purposes such as inspection, sample collection, remote delivery, remote sensing etc. In this dissertation, the focus is on developing an effective locomotion technique for a remotely operated vehicle (ROV) that will gather data in the rumen environment. This data will improve the analysis on prediction of health conditions and in turn improve the efficiency of food production. There has been significant investment and research on precision crop agriculture that has provided production boost across the range of crops. However, precision animal agriculture is still in early stages and there is much fundamental research needs to be done to provide a foundation for technology to be developed and implemented. One likely factor hindering the further developments is the difficulty in actively monitoring and responding to the digestive systems of ruminant animals, where the greatest efficiency losses occur during digestion. A better understanding of the biology and environment of the rumen could provide insight for sustainable food production because ruminants have the unique capacity to ferment fiber into energy usable by the animal very affectively. Thus, remote monitoring of the rumen environment of individual animals could enable individualized feeding strategies that minimize energetic losses associated with digestion, and therefore improve feeding efficiency and whole-system environmental impact.

Developing a remotely operated vehicle to navigate the rumen is challenging, because it is a complex heterogeneous environment stratified vertically and horizontally, reflecting the variation in density of feed particles, microbes, pH, O_2, and fermentation products. Furthermore, the content experiences random forces due to large violent contractions of the rumen during digestion. The ROV developed in this thesis provides structure and locomotion technique that is capable of traversing a variety of stiffness environment while handling the complex surrounding and dynamic pressures.

1.2 Background and Previous Research

1.2.1 Rumen environment and monitoring technology

The cow rumen is a specialized large digestive chamber that converts low quality food (like grain and hay) to usable energy [1]. The typical volume of a lactating cow rumen ranges from 60 to 100 L, depending on body size. For a mature cow, the rumen can hold about 90kg of material, which is approximately 14% of its body weight. The rumen environment is constantly perturbed by fluid flow and muscle contractions (mixing or primary contractions occur ~1 to 3 times/minute). During bouts of rumination, more forceful secondary contractions occur every few minutes. These secondary contractions sharply contract the muscles of the abdomen to move the gas bubble at the top of the rumen next to the esophagus to facilitate eructation, as failure to eructate can cause health problems for the animal that could be potentially fatal (Figure 1.1A).

The rumen content ranges from a consistency similar to water to that of oatmeal or mud, resulting in varying densities that stratifies vertically. The pH of the rumen environment varies throughout the day, in association with meals, and is generally between 5 and 7 with rumen pH near 6.5 considered normal. Rumen temperature tends to be maintained around 40 ^{o}C.

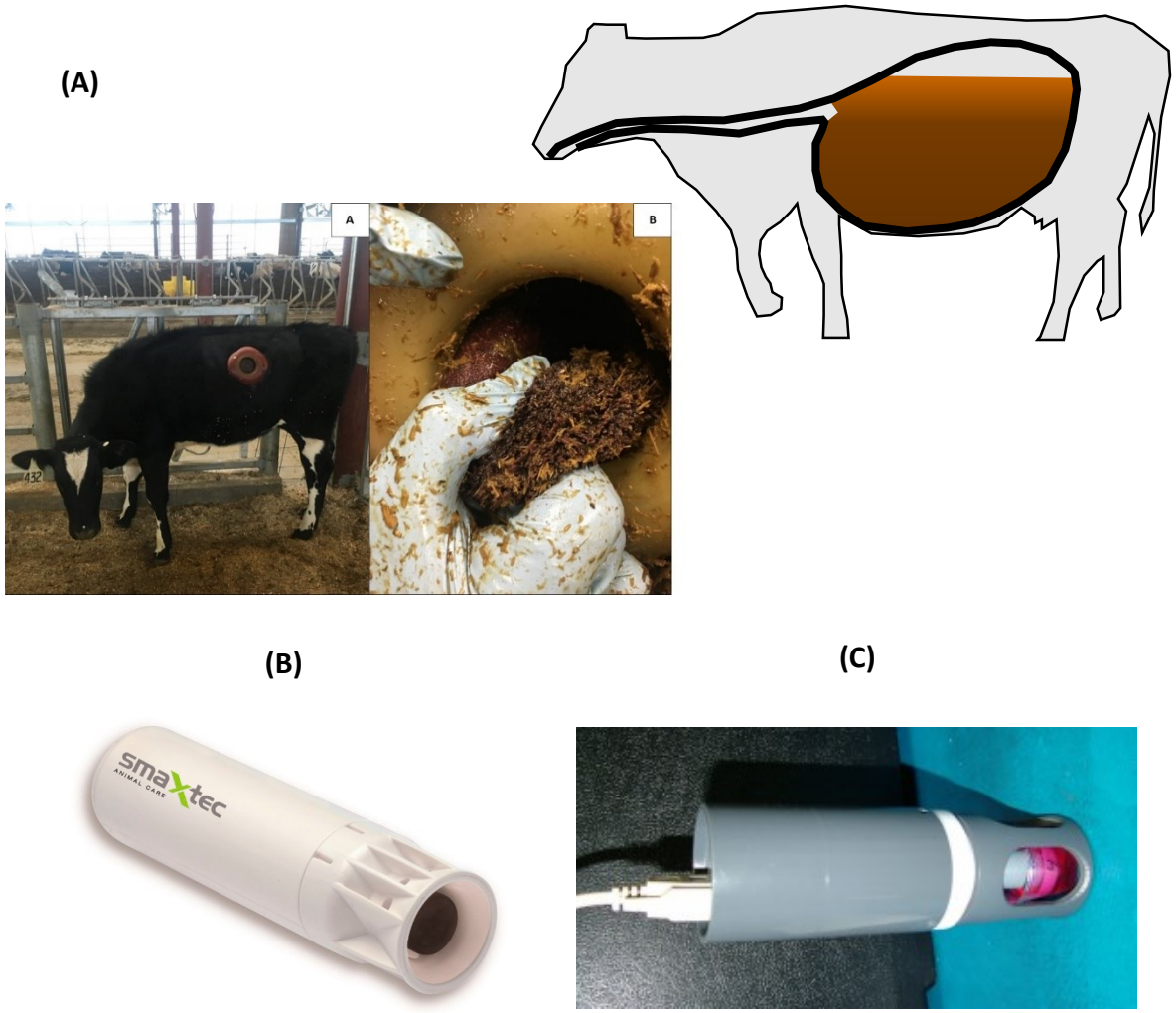

Figure 1.1: [fair use]
(A) Illustration of cow rumen digestion chamber (right), Picture of cow with cannulae to access the rumen (left), (B) Smaxtec bolus-based pH and temperature monitoring device [2], (C) Dascor bolus-based pH and temperature monitoring device [3]

In animal nutrition experiments, access to the rumen is typically obtained through rumen cannulae. Sampling through this orifice is physically difficult and is thought to result in mixing of naturally stratified (vertical and horizontal) rumen contents when perturb by the sampler. The physical difficulty in sampling the rumen prevents researchers from being able to precisely monitor difficult-to-reach areas of the rumen. Additionally, disrupting the rumen environment through sampling, physically or chemically, alters the unique microclimates within the rumen and thus

precludes accurate and representative sampling. Collectively, these challenges make accessing unique microclimates within a rumen a difficult task.

Currently, there are two primary bolus-based real-time pH and temperature monitoring technologies commercially marketed for use in ruminants (Smaxtec [2], Wastiangasse, Austria and Dascor [3], Escondido, CA). These are both pure data loggers and possess no ability to actively locomote inside the animal or even detect actual location. The first type (Smaxtec) is designed to sample pH for 6 months, and the device is swallowed by the animal. The second type (Dascor) is inserted into the rumen via the cannula, and tracks pH and temperature for short period of time (about 2 weeks). This data logger tends to drift over the time period and must be carefully calibrated before and after use to account for this drift. Both loggers tend to sink to one of the compartment ([2], [3]) within the rumen and although they appear to remain in the same location consistently, this cannot be confirmed without constant physical monitoring or tracking. Although these tools have been widely adopted in ruminant research, they are cumbersome to use and fail to provide the detailed information necessary to model the rumen biology.

An effort towards development of platform required for understanding of rumen biology is the work of Nogami et al. [4], where a three-axis accelerometer was implemented on a miniature bolus-type sensor node. The accelerometer provided distribution of forces during rumen contraction. However, similar to the commercially available devices, the sensor node is static or traverses passively within the rumen, unable to monitor or access (without invasive means) desired regions. Besides manual sampling there is no known technology available that allows for both controlled locomotion within the rumen and collection and storage of fluid and/or tissue samples from various locations. This inability to sample the rumen environment non-disruptively limits our understanding of the interplay between tissue morphology, microbial populations, and their overall

contributions to whole animal feed efficiency. Poor sample collection also precludes identification of microbial species present in unique microclimates within the rumen which may be critical to our overall understanding of ruminant metabolism and efficiency of fiber fermentation.

1.2.2 Miniature bio-inspired locomotion robotics

In response to the growing need of mobile devices that are capable of navigating through difficult scenarios, unknown terrains and danger-prone areas, researchers have attempted to develop miniature robotic vehicles with effective locomotion. While standard vehicle designs utilize mechanisms such as wheels and propellers, such approaches fall short in meeting desired specifications when scaled down to miniature robotics. For instance, wheels for terrestrial locomotion have been proven to be an effective locomotion technique, however, they are generally limited to smooth terrain. This becomes a significant issue when traversing complex surfaces, particularly at small scales. In the last decade or so, there has been a growing amount of research performed for the development of miniature robots that can traverse over a variety of terrains. For operations at the mesoscale (centimeter range), many researchers have started to take inspiration from biological creatures, such as insects and other arthropods (such as arachnids and myriapods), for developing compatible locomotion techniques.

Most work in the field of miniature legged ambulatory robot systems have looked to develop quadrupedal or hexapedal platforms. Such systems take inspiration from insects that have rigid bodies. As we will see, the variations and choices between quadrupeds and hexapods relate to the degree of complexity desired for the system and the actuation depending on the type of gait utilized. A few examples of these systems include work done by Ho et al. [5], Vaidynnathan et al. [6], Goldfarb et al. [7], Birkmeyer et al. [8], Hoover et al. [9], and Avirovik et al. [10], [11]. All of these robots use a variety of actuators and mechanisms to generate a forward locomotion.

Few of these robotic platforms are operated using simply a single drive motor. Vaidyanathan et al. [6] demonstrated the terrestrial locomotion inspired by the crawling motions of a cockroach, which utilizes a tripod gait. One of the main challenges in their miniature robotic platform was the inability to traverse real world obstacles such as a steps of a staircase. By observing how cockroaches adjust their gaits and handle such obstacles, as shown in Figure 1.2, they implemented a wheel-leg type mechanism called "Whegs". These "Whegs" were operated by using a single drive motor. This specific platform [6] however was developed for traversing both aerially and terrestrially, and thus for such an application the implementation of many legged mechanism would likely add weight to the platform. Another robot "DASH" developed by Birkmeyer et al. [8], was also inspired by the cockroach tripod gait and achieves locomotion by means of a single drive motor.

While choice of the actuator is dependent on the scale of the mechanism for a given application, conventional rotary DC motors would start to suffer with regards to its efficiency at microscales, due to their low power density and rotating components. Use of smart material actuators such as

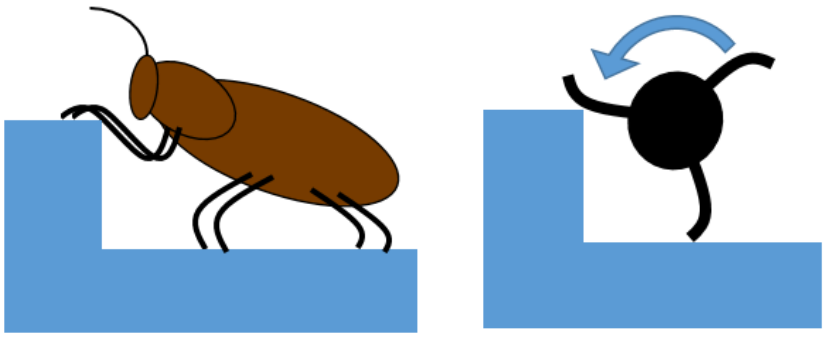

Figure 1.2: Concept illustrations of cockroach inspired Whegs design for locomotion combining advantages of wheels and legs [6]

ionic polymer-metal composites (IPMC), shape memory alloys (SMA) and piezoelectric ceramics, is attractive as they perform more favorably when scaled down. One example of a microrobotic

platform that utilizes SMA's for actuation is the RoACH system developed by Hoover et al. [9]. Again, as seen in the platform name, this robot was inspired by the cockroach, and exhibits common tripod gait seen in many insects. SMAs with respect to robotic locomotion suffer from hysteresis and cannot operate at high frequencies which is necessary for repeatability and speed.

The most commonly used actuation mechanism in crawling robots has been piezoelectric transducers. A few examples of quadrupedal robots that have implemented such transducers include the work done by Avirovik et al. [9, 10]. In their work, two robotic locomotion platforms were developed using similar piezoelectric transducers. In Ref. [10], the use of piezoelectric bimorphs in an L-shaped configuration was presented. The bimorphs with their degrees of freedom perpendicular to one another resulted in the free-end tracing a circular/elliptical motion when excited with two sinusoidal signals of the same frequency but with a phase difference of 90˚. The robot utilized the gait most commonly seen in four legged creatures. In Ref. [11], the same principle was used in the development of a U-shaped piezoelectric motor (Figure 1.3A). Four of these motors were placed in a sequence, resulting in a partial traveling wave motion observed from

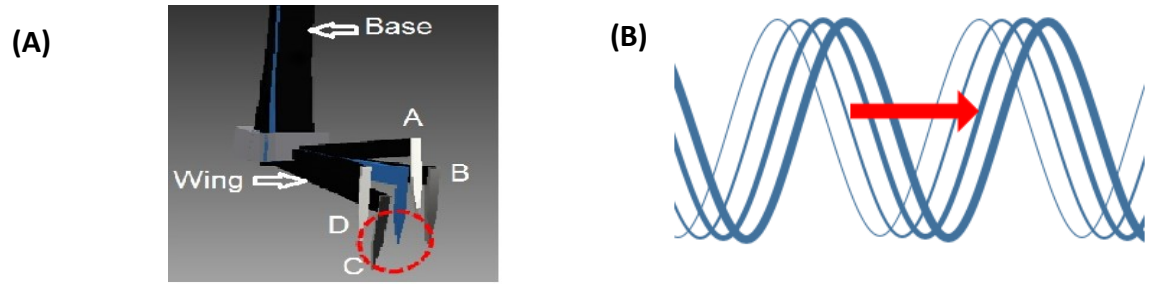

Figure 1.3: (A) L-shaped piezoelectric leg actuator used by Avirovik et al. [10], for walking robot, (B) Traveling wave mechanism concept used for locomotion by Avirovik [16] and Zarrouk [18]

the side. Goldfarb et al. [7] also used piezoelectric bimorphs to achieve locomotion, however these piezoceramics were used to drive a 5-bar linkage configuration for each leg to achieve a similar elliptical motion. Ho et al. [5] also used piezoelectric device to drive the locomotion of their

microrobot, however unlike the previous designs mentioned in this chapter, it did not require two piezoelectric bimorphs to achieve the circular two degree of freedom motion. Instead adjusting the geometry of the legs resulted in tilting of the body at an angle causing an asymmetry stance of the robot. When actuated by the piezoelectric bimorph along its single degree of freedom, the asymmetric configuration would result in forward locomotion. In addition to bending type piezoelectric transducers (e.g. bimorphs), piezoelectric stacks exhibiting longitudinal motion have also been utilized. Eigoli et al. [12] developed an A-shaped transducer that consists of two beams attached together by a piezoelectric stack. The piezoelectric stack when actuated moves the beams along its horizontal degree of freedom, resulting in the sliding of the contact point of the device on the ground. From this motion, friction based locomotion can be achieved by several means, creating a "stick-slip" mode of motion. The friction locomotion is achieved by either manipulating the friction coefficient of the contact points or the contact normal forces (by asymmetry). Such locomotion exhibits displacements when operated close to its resonant frequency with a high resolution. However with such small deflections, it is not useful for a biomimicking crawling robot. Despite the advantages offered by piezoelectric actuators that include repeatability and high frequency operating range, they do have limitations that includes limited strain and high operating voltages.

Above discussion focused on the miniature robotic platforms inspired by rigid body insects that are primarily effective on the flat or complex surface, utilizing a variety of different types of actuators depending upon the application requirements. However, for an ROV that can operate within the cluttered and viscous environment of the rumen, additional burrowing capabilities are of interest. Looking at biology, small creatures that are effective burrowers such as earth-worms and caterpillars, utilize their elongated bodies to generate peristaltic or traveling wave movements

for locomotion. Multiple researchers have considered such traveling wave locomotion for designing microbots including Daltorio et al. [13], Calderon et al. [14], Yuk et al. [15], Avirovik et al. [16], and Zarrouk et al. [17], [18].

Yuk et al. built a robot using SMA's to replicate the locomotion of a *Caenorhabditis elegans* worm that uses body undulations to effectively traverse while burrowing, much like snakes or *Scincus scincus* (sandfish). While effective, *C. elegans* uses large body dynamics which requires more complex control schemes which are not desirable in building miniature robots. Earthworm inspired robots that use peristaltic locomotion have been explored in literature. Daltorio et al. [13] developed "Softworm" which is a robot comprising of deformable helical mesh structure driven by a single driver motor. Calderon et al. [14] built a earthworm-inspired multi-material multi-actuator soft robot that is pneumatically-driven to capture the peristaltic locomotion through axial and radial actuator components. Zarrouk et al. [17] used a screw-like axis mechanism to sequence and coordinate cells, creating a modular segmented peristaltic motion with a single motor actuator. However, these robots appear to be effective on the surface or in a tubular setting. Furthermore, these locomotion designs being radial in nature, the mechanism would make it very difficult to implement sensors on board the same device.

Locomotion using traveling waves has also been explored by Avirovik et al. [16]. In their work, excitation of piezoelectric ceramics generated mechanical traveling waves along a beam to generate motion. However, for applications in viscous and complex environments, the limited strain offered by piezoelectric actuators would likely not be effective. Zarrouk et al. [18] developed a large amplitude traveling wave locomotion device driven by a single DC motor, by use of a helix and a series of links to essentially capture the projection of the spinning helix, creating a traveling wave. The effective thrust that the traveling wave can generate towards locomotion is completely

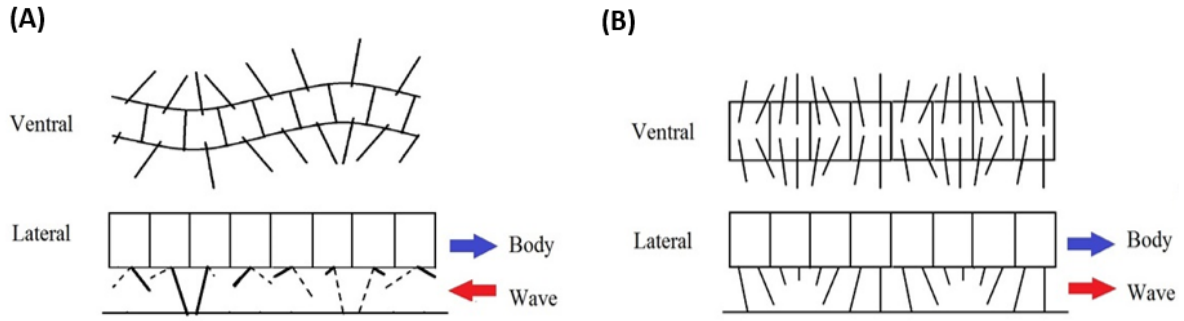

Figure 1.4: (A) Schematic of ventral and lateral view of a centipede gait, (B) Schematic of ventral and lateral view of a millipede gait

frequency dependent (Figure 1.3B). While these peristaltic and traveling wave locomotion mechanisms are biologically inspired by earthworms and caterpillars, which are effective burrowers, they are generally much slower and do not demonstrate the same complex terrain locomotive capabilities as the legged mechanisms discussed earlier.

A group of arthropoda that possess all the advantageous qualities in the miniature robotic platform locomotion discussed this far are the myriapoda. Myriapoda like other arthropods have legs that allow them to walk effectively on complex uneven terrains with reasonable velocity, but like earthworms and caterpillars have elongated flexible bodies and generally use a wave-like behavior for locomotion. Desired features that make such a morphology advantageous, in comparison to the rigid body insects, include stability (many legs, therefore many points of contact with the ground), flexibility (having a flexible spine would allow conformity with a given surface) and robustness (if one leg breaks, limited or no change of gait is needed to keep moving).

Probably the most commonly found myriapod in terms of application of robotic inspiration is the centipede. Centipedes are known for their long bodies and many legs, and demonstrate very impressive speed and flexibility resulting from their evolution as predators needing to hunt and capture prey. A few examples of centipede inspired robots that have been developed include the

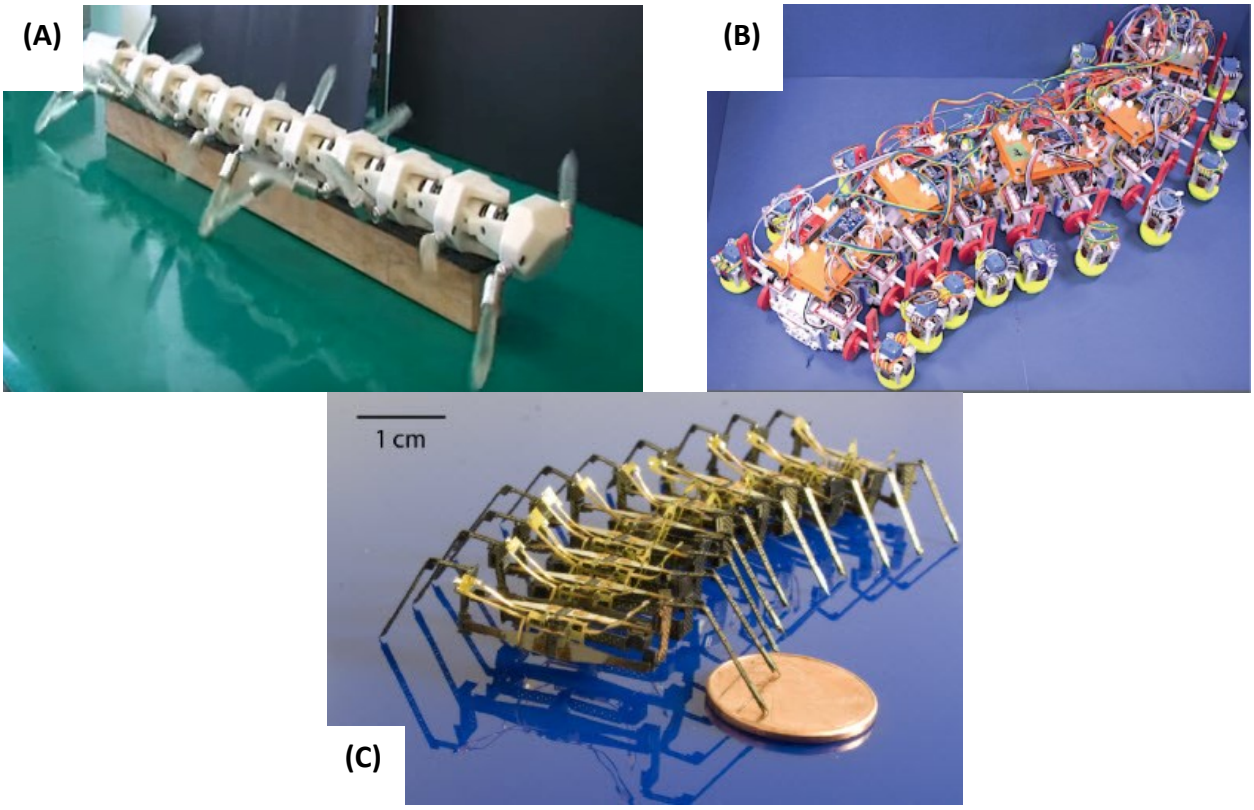

Figure 1.5: [used with permission]
(A) Zinedyn centipede robot [19], (B) Millipede robot to investigate decentralized control scheme from ground reaction force [27][28], (C) Centipede-inspired millibot [20][21]

work done by Koh et al. [19], and Hoffman et al. [20], [21]. Koh et al. [19] demonstrated a centipede robot platform "Zinedyn" having length of 73cm that emulated the walking locomotion pattern of a centipede (Figure 1.5A). This robotic system is far larger in dimension than the corresponding biological creature. This platform is not a microrobotic system and in operating at the macroscale, it uses conventional motors and gear systems. Hoffman et al. [20], [21] developed a centipede inspired robot which is relatively much smaller in scale (Figure 1.5C). In their work, both experimental and simulation model of microrobotic centipede was developed. The locomotion of this robot was achieved by using piezoelectric bimorphs in combination with four-bar SCM structures. Like the quadrupedal and hexapedal robot platforms discussed earlier, the leg actuation system is effective by moving in a circular/elliptical motion. Being a many legged robot,

it did not exhibit the same gaits as discussed earlier, instead it mimicked the gait of centipedes. Centipedes have a single pair of legs per body segment, with each of those legs 180˚ out of phase with each other. Each pair of legs is only slightly out of phase with the pair of legs of the adjacent body segments, creating a traveling wave moving opposite to the body motion. As a result, centipede exhibits body undulations during its gait as seen in Figure 1.4A, which is desirable for speed. The undulation seen along the centipede requires that the segments of the robotic platform be capable of relative motion with one another. Hoffman et al. achieved this requirement by use of sarrus linkages between the robots' body segments, in combination with flexures at the joints [21]. Another myriapod, often confused as a centipede, is the millipede. Similar to the centipede, the millipede also has a long body made of many segments and are known for their many legs. However, there are distinct differences that make the development of a millipede-inspired robotic platform relevant for a rumen ROV.

1.2.3 Millipede locomotion and robots

In Manton's study of the chilopoda (centipedes) [22] and diplopoda (millipedes) [23], there is much useful information related to structure, habits and evolution. Amongst all their distinguishing features, the two main distinctions between the millipede and the centipede are the number of legs and their functional habits. As previously mentioned, centipedes are built for speed, however millipedes have evolved to be effective burrowers. Naturally roboticists have been interested in emulating the speed in traversing different terrains displayed by the centipede. In nature, even though the millipede naturally does not display the same speed, on a robotic platform the speed is highly related to the frequency which actuators operate. The centipede gait is designed to avoid all obstacles, but a millipede gait allows them to burrow through certain substrates, which is more desirable in the rumen ROV design.

The superior ability to burrow effectively comes from its gait and morphology. Millipedes have 2 leg pairs per body segment, and in having more legs they have more stability and can apply more anchoring force. Across all species of millipedes, fully grown specimens have a range from 22 to 750 legs [24], [25], while centipedes range from 30 to 382 legs [26]. The gait of millipede also differs in comparison to a centipede (Figure 1.4B). A pair of legs on a millipede operate in phase with each other, not 180˚ out of phase, resulting in more thrust in the direction of motion [23]. Like centipedes, there is a slight phase difference between leg pairs along the body resulting in a metachronal wave when crawling. The generated traveling wave moves in the same direction as the body motion. Furthermore, millipedes will adjust only their gait in cases they encounter resistance, while centipedes do not exhibit such behavior but instead introduce more body dynamics. Lastly, the body undulation seen in the centipede (Figure 1.4A) resulting from leg pairs consisting of legs out of phase with each other, is not seen in millipedes as they are in phase (Figure 1.4B). On a robotic platform, this could be desirable as this means extra degrees of freedom that do not need to be accounted for achieving performance.

An example of a millipede-inspired robot platform can be seen in Figure 1.5B, developed by Kano et al. [27], [28]. The robot was designed for the purposes of investigating the decentralized control scheme of the legs in myriapod locomotion. With the focus of implementing feedback sensor control of ground reaction forces to determine the trajectory of the adjacent legs, the required computation power and actuator mechanisms require a larger scale robot, similar to the scale of the centipede robot designed by Koh et al. [19]. A miniature millipede-inspired design, the pillbot, took inspiration from pill millipedes [29]. This robot utilizes a similar mechanism as the whegs design described in Ref. [6].

1.2.4 General millipede biology

While the focus of this thesis will be on determining the physical mechanics that makes millipede locomotion effective for large thrust performance to handle situations such as burrowing, it is important to have some insight on millipede behavior, anatomy, physiology, and morphology that permit burrowing mechanics. There has been some extensive work on understanding the millipede biology [23], [30]–[32]. Both Hopkins et al. [33] and Minelli [25] provide a literature survey of millipede biology covering taxonomy, morphology, nervous systems etc. Wilson [34] has provided details on the millipede muscular anatomy, revealing while many aspects of the musculature are conserved, there exists some variations between different orders. Borrell [35] has studied the mechanical properties of the exoskeleton, which have importance in resisting loads due to burrowing, demonstrated that while there is variation between males and females, the mean fracture strength of the cuticle was 124MPa, with a Young's modulus of 17GPa, which both exceed what is found in insects. Liu et al. [36] have investigated the convergent evolution of morphological adaptations across various species indicating direct adaptation for the surrounding environment. Marek [24], [37] has studied the systematic evolution of millipedes and in the process discovered the species with most number of legs. Bowen [38] has investigated their burrowing patterns, revealing that variations in the burrow morphology can be attributed to its function, whether refuge or feeding . Francisco et al. [39] have studied the nervous system, showing that for a particular species, an additional cell layer exists for protection. .

Millipedes (myriapods of the class Diplopoda) family comprises of approximately 12,000 species, which can vary significantly in morphology as shown in Figure 1.6. Despite the variations in sizes they all possess the elongated segmented body, where most body segments possessing two leg pairs, and while some species may be more effective than others, they generally utilize their

morphology for burrowing applications. From the extensive work of Manton ([23], [30]–[32], Hopkins [33], Minelli [25], Wilson [34], Marek [24], [37], [40] and others, we can summarize the basic anatomy and morphology of millipedes, which lays the foundation of our study of their locomotion behavior.

General millipede musculoskeletal anatomy is provided in Figure 1.7. Such a physiology relates to the purposes of articulating body movements within high load burrowing environments. There are numerous muscles both within and between body segments, and while they may have slight variations across different species, the general anatomy is reasonably consistent. The complex muscular system is protected by a hard exoskeleton that possess numerous joints permitting a wide range of motion. Joints exist between body segments (resembling a ball-and-socket), as well as between segments along each individual leg (a combination of pivot and hinge joint structures). The head of millipedes is relatively large in comparison to a single body segment, and is usually used as the initial point of contact when performing burrowing actions.

There is significant details of other biological aspects on millipedes, relating to digestion, circulation, reproduction, sense organs, etc. Outside of the general morphology and physiology of the skeletomuscular system, another aspect of biological studies that is worth gaining insight for understanding their locomotion is the nervous system that is used to control and actuate movements. As seen in Figure 1.8 [41], the central nervous system consists of a brain that transmits signals to the rest of the body through a ventral nerve cord. Along the ventral nerve cord are nerve clusters called ganglia (two per body segment), which then transmit signals to the musculature in the respective body segment.

Figure 1.6: [fair use]
Display of various millipede morphologies across different species [40]: (A) *Apheloria virginiensis*, (B) *Platydesmid*, (C) *Hyleoglomeris*, (D) *Chaetaspis albus*, (E) *Narceus americanus*, and (F) *Illacme plenipes*

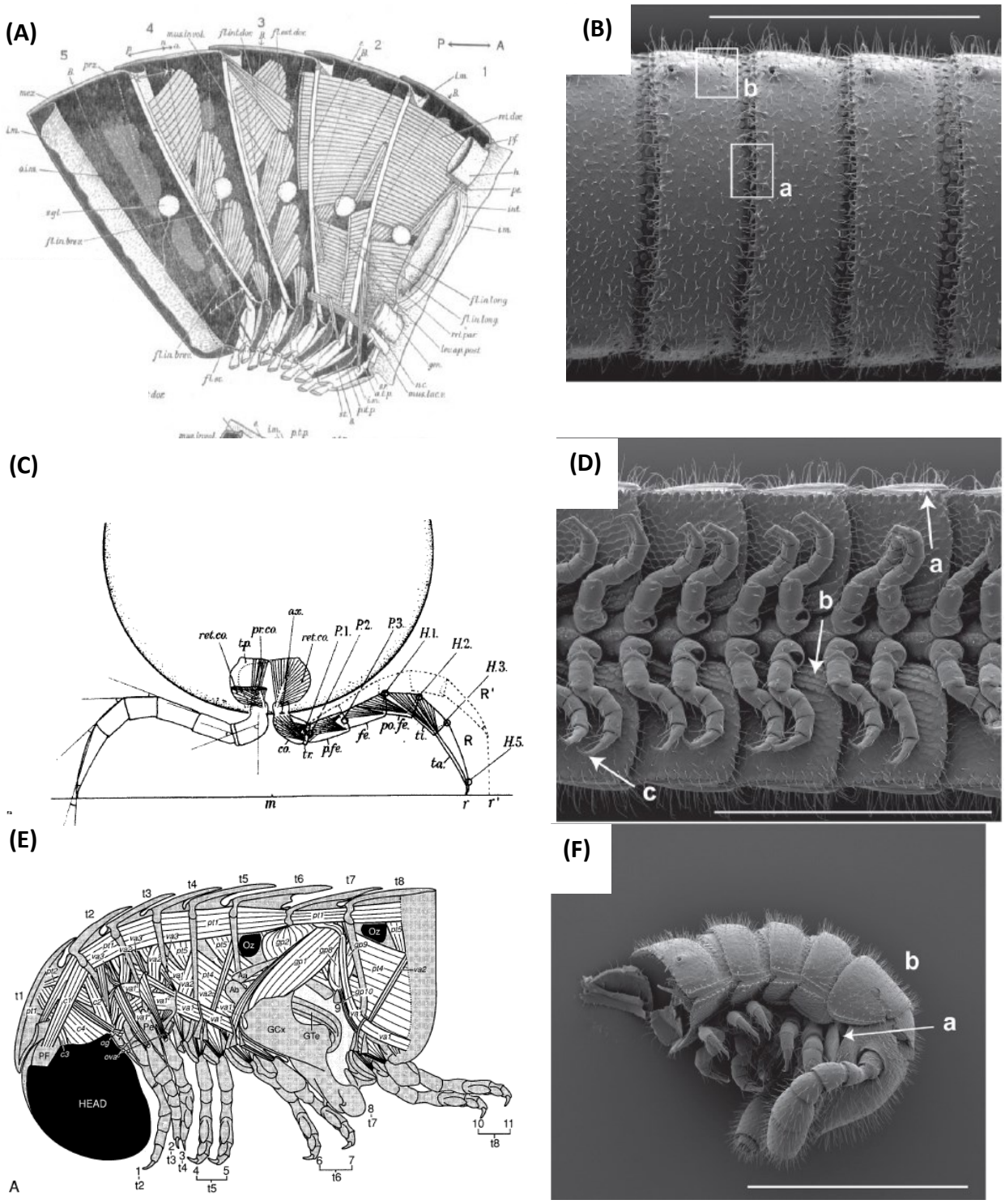

Figure 1.7: [public domain / used with permission]
Detailed general millipede physiology (A) Internal musculature of body segments [23] (B) Magnified photo of body segments [24] (C) Musculature of legs [23] (D) Magnified photo of legs [24] (E) Musculature of anterior segments and head [34] (F) Magnification of millipede head [24]

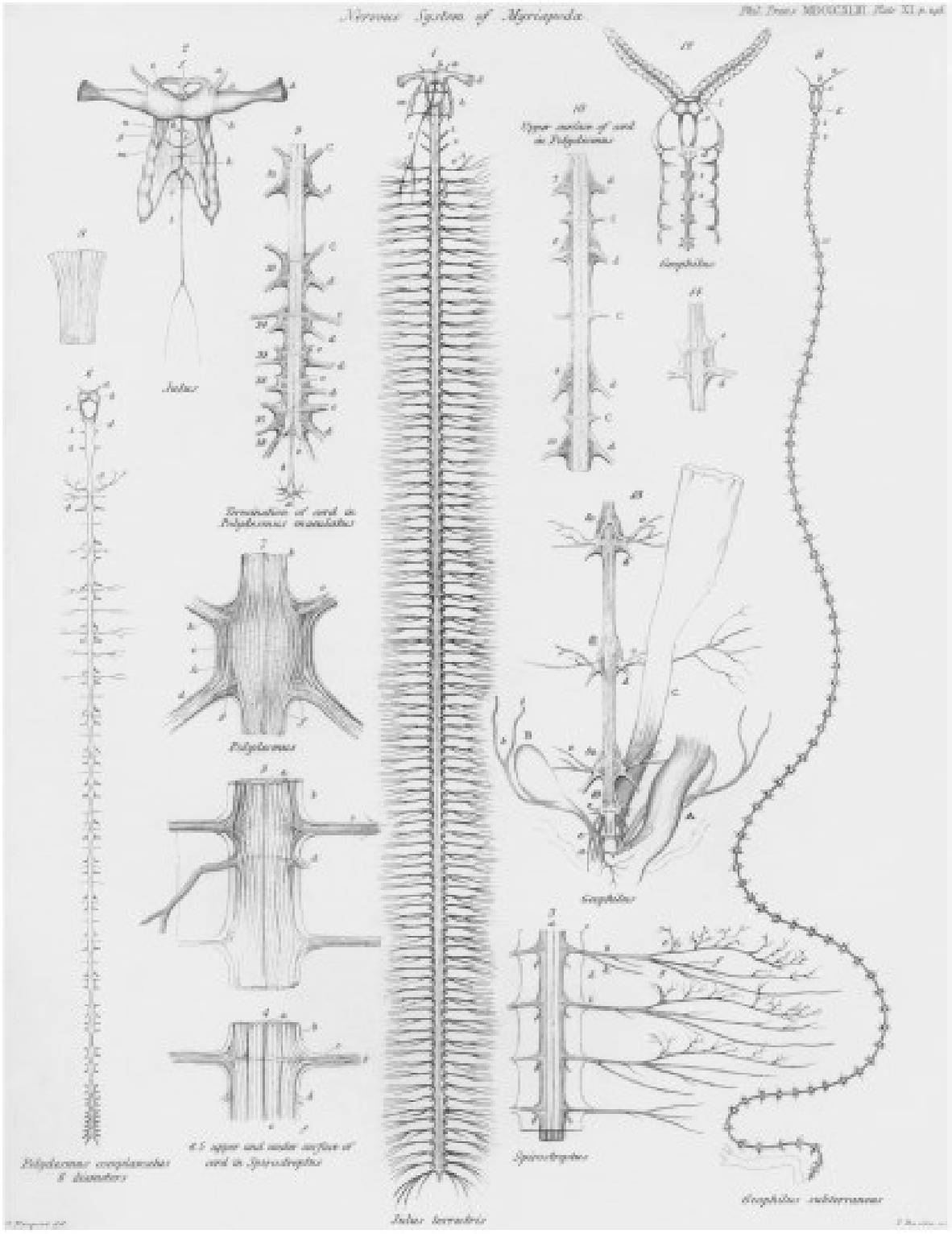

Figure 1.8: Millipede Central Nervous System (CNS) [41] [public domain]

1.2.5 Locomotion and anchoring devices for non-surface, submerged, or in-body applications

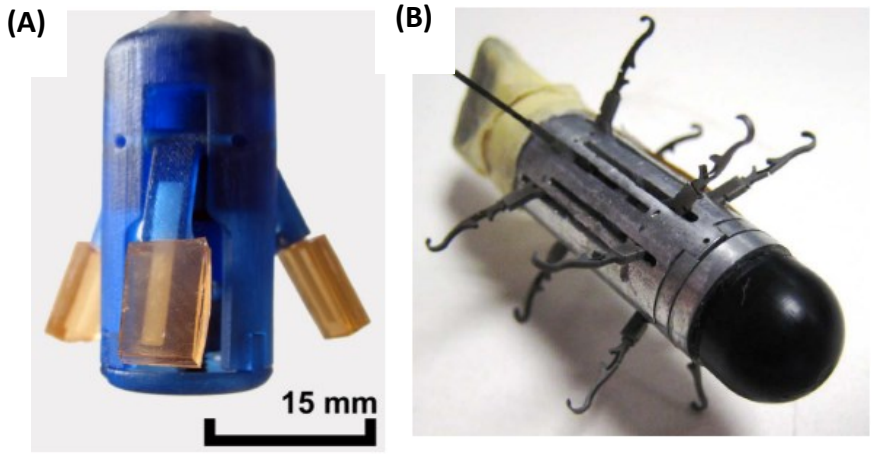

Figure 1.9: [used with permission]
Wireless Capsule Endoscopes (A) Micro-patterned adhesion for anchoring [41] (B) Appendages with hooks for anchoring and locomotion [46]

A detailed survey of existing miniature bio-inspired robotic platforms was conducted. It was found that most of these robots have been demonstrated to traverse on the surface, compared to operating inside a living body as required for a rumen ROV. Operation inside the body environment is the reason that makes millipedes burrowing technique of much interest. While there is no current locomotion mechanism explicitly used for a rumen ROV, there are mechanisms utilized on several existing devices for other internal body inspection applications. Such examples come from devices designed as endoscopes for inspection of the human GI tract. The techniques commonly used in these devices rely on either micropatterned adhesives to adhere to the gut walls (such as [42]–[46]), or use of appendages to anchor the devices to the wall surfaces (such as [47]–[49]). A couple others used conventional motors to drive screw-like locomotion ([50], [51]), A few examples of these devices are shown in Figure 1.9. It is worth noting while these endoscopes operate inside a living body, the environments are generally empty compliant tubular scenarios, while the rumen robot will be operating on viscous and dense substrate.

1.2.6 Conclusions

There is extensive literature on microrobotic locomotion platforms, mainly comprising of rigid body few legged systems and traveling wave/peristaltic/undulating bodies effective on surface or even compliant tubular environments. However, there appears to be a gap in implementation of the metachronal/wave locomotion technique in true burrowing applications. A device that could perform effectively in high resistance substrate situations would be ideal in developing an ROV locomotion mechanism required to explore the difficult rumen environment, as well as potentially other applications involving cluttered and complex surroundings. Millipede morphology and locomotion technique could potentially provide these features.

1.3 Dissertation Structure

The dissertation focuses on the development of the millipede-inspired locomotive capabilities required for traversing through the rumen environment. The organization of thesis is as following.

An in-depth study of bio-mechanics related to millipede locomotion is covered in chapter 2. The chapter discusses the experimental observations of how millipedes adjust their metachronal gait, effectively modulating the traveling wave, in different situations to generate the desired forward thrust. Furthermore, a dynamic model is developed to capture and simulate the variation in gaits and morphology.

In chapters 3-4 a millipede inspired robot is designed, built and tested. Chapter 3 describes the design process of the mechanisms and controls schemes developed to best capture the desired experimental locomotive behavior. The robot also served as a platform to test different parameters that cannot be explicitly monitored on the actual millipede specimens. Chapter 4 discusses how

the implementation of millipede gait on the robot performs in comparison to the actual animal, and further performs a parametric analysis for understanding the role of morphology and preferred gait behavior.

Chapters 5 translates our understanding of the millipedes' locomotion and utilizes it in design of an ROV locomotion mechanism. A millipede-inspired mechanism capable of handling the various substrates in the rumen environment is developed to be incorporated in the design of capsule device permitting sample collection and onboard sensors. Initial testing of the ROV locomotion is conducted in rumen-like environments to assess its performance capabilities.

Chapter 2 – Bio-mechanics and Modeling of Millipede Locomotion

2.1 Introduction

Millipedes are detritivores, typically found walking on the forest floor and burrowing into leaf litter, dead wood, and soil. They are some of the earliest terrestrial organisms and have evolved over ~420 million years to effectively traverse complex terrains and burrow into the soil matrix. While there are well over thousands of species of Diplopoda of varying morphologies and capabilities, two species of millipedes were used in thesis to perform bio-mechanical analysis. One of the species is *Apheloria virginiensis* (Figure 2.1A), which are considered flat-backed millipedes (Polydesmida) that grow to about 5cm in length. With such a body structure, they use a "wedging" method when burrowing. This involves inserting the anterior end into a crack or crevice, and then widen the gap by straightening their body and pushing upwards with their legs [23]. The other species investigated was *Narceus americanus* (Figure 2.1B), which have been found to grow up to 10 cm. This species has a nearly cylindrical body (as do all millipedes in the Juliformia: Julida, Spirobolida, and Spirostreptida) and employ a "bulldozing" burrowing technique, where the head is used as a surface ramming object [23]. Another burrowing mechanism seen in millipedes is "boring", exhibited by species (e.g., in the Polyzoniida) with a narrow anterior end followed by progressively wider body segments enabling further penetration. These species were not investigated in this study. The two specific species were selected because they are copious in

Virginia and demonstrate effective locomotion at scales that can be easily captured on camera and are of interest in potential robotic applications.

Before we can try to emulate locomotion capabilities on a millipede-inspired robot we need to understand the kinematics and dynamics of millipede gait under varying environment conditions. In this chapter, initial observations and characterization of millipede locomotory mechanisms (metachronal gait in combination with a segmented flexible body) is performed, providing a fundamental understanding of their general movements. This characterization will provide data needed to delve into an in depth study on modeling of millipede gait for various purposes.

2.2 Background and Initial Observations

2.2.1 Traveling wave generated by metachronal gait

When watching a millipede in motion, the most noticeable characteristic is the generated traveling wave across its many number of legs. As mentioned previously, this phenomenon is a result of their metachronal gait, with leg pairs operating in bilateral phase. The wave's characteristics (such as frequency, amplitude etc.) appear to vary depending on the species, number of legs, weight, size, substrate and desired thrust.

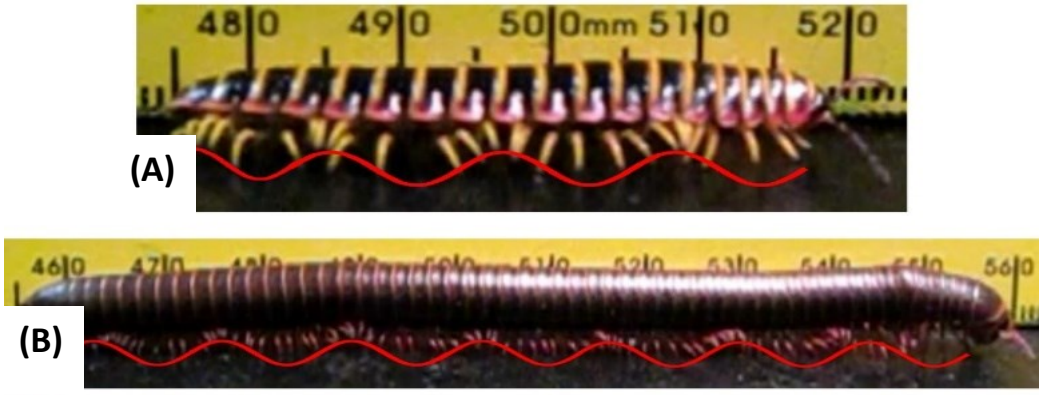

Figure 2.1: An illustration of the traveling wave locomotion created by the metachronal gait (A) *Apheloria virginiensis*, (B) *Narceus americanus*

The metachronal gait of millipedes has captured the attention of several studies [52][23]. Sathirapongsasuti et al. [52] developed a model for predicting the position of a millipedes individual leg based on the assumption that the leg trajectory traces a clipped circular path. A visual representation of this is shown in Figure 2.2A, where the solid blue line indicates the path traveled by the tip of an individual leg when crawling. With this assumption, the referenced circular path is disrupted by the ground and leads to the forward propulsion. The equations of motion derived for this model [52] are:

$$V_{wave} = \frac{\theta R}{t_T} \tag{2.1}$$

$$V_{millipede} = \frac{2R\sin\left(\frac{\theta}{2}\right)}{t_P} \tag{2.2}$$

$$T = t_T + t_p \tag{2.3}$$

$$H = R - R\cos\left(\frac{\theta}{2}\right) \tag{2.4}$$

$$\omega = \frac{\theta}{T - \frac{2R\sin\left(\frac{\theta}{2}\right)}{V_{millipede}}} \tag{2.5}$$

where V_{wave} is the velocity of the traveling wave, $V_{millipede}$ is the velocity of the millipede, t_T is the duration of the transfer period (leg in the air), t_P is the duration of the propulsion state (leg on the ground), H is the maximum height of the leg and w is the angular velocity of the leg tracing the circular reference path.

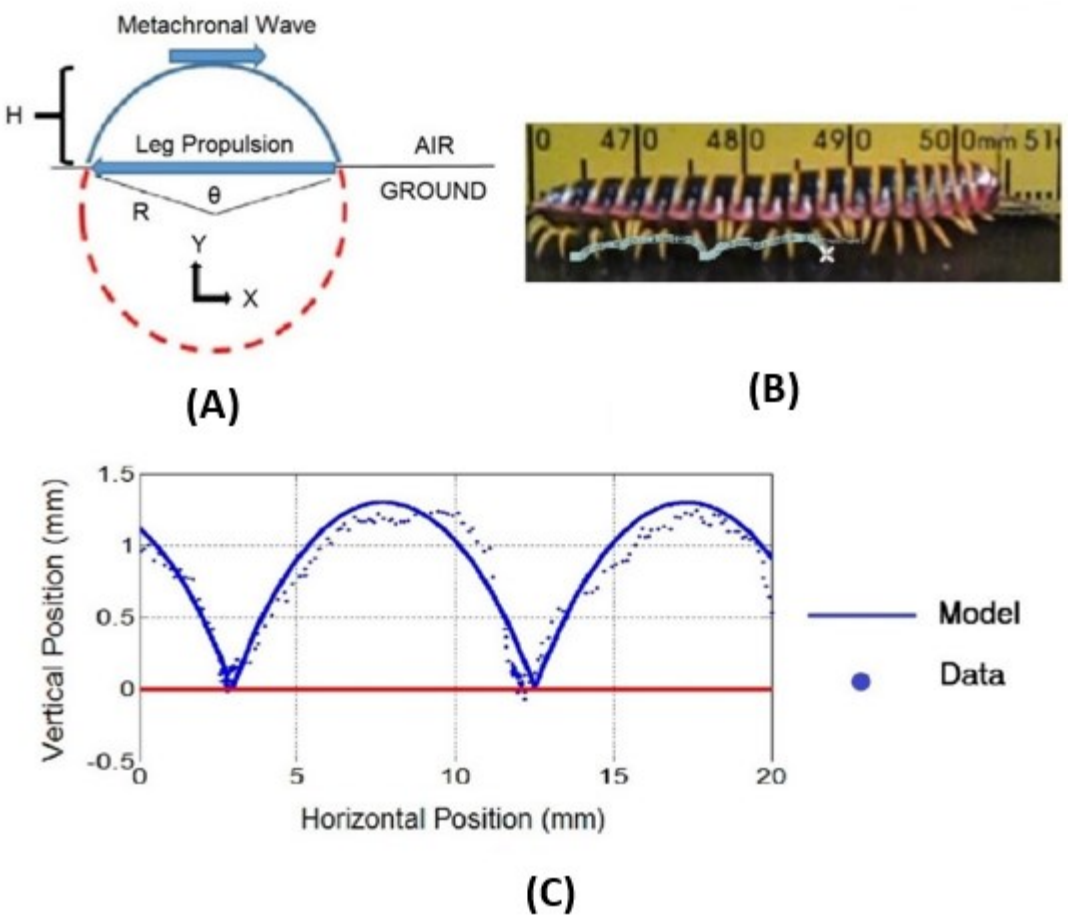

Figure 2.2: (A) Kinematic walking model using a circular path developed by Sathirapongsasuti et al. [50], (B) Image of video tracking process applied on footage of *A. virginiensis* using Adobe After Effects, (C) Plot comparison of the model determined trajectory with the collected video footage tracking of the end of the millipede leg.

Solving equations (2.1) to (2.4), R and θ can be determined. The position of the legs can then be tracked over time:

$$X(t) = \begin{cases} V_{millipede}(t - \emptyset_t) - R\sin\big(\omega(t - \emptyset_t)\big), & transfer \\ -V_{millipede}(t - \emptyset_t), & propel \end{cases} \tag{2.6}$$

$$Y(t) = \begin{cases} H - R - R\cos\big(\omega(t - \emptyset_t)\big), & transfer \\ 0, & propel \end{cases} \tag{2.7}$$

where the time phase $\emptyset_t$ between adjacent legs is found by $\frac{d}{V_{wave}}$ (d is the distance between pairs). This model of the millipede gait was compared to the actual leg motion observed for the *A. virginiensis*, using the video processing approach on Adobe After Effects, as shown in Figure 2.2B and C.

While tracking the motion of a single leg of a walking millipede, indicated that the model developed by Sathirapongsasuti et al. [52] captures the desired aggregate behavior, a more computationally efficient approach can be taken. Eliminating the dependence of the model [52] on two separately defined velocities, the position of the legs can be estimated using an elliptical model. Along with the assumption of a "constancy of forward strokes" as observed by Manton [23], this model was accomplished using equations:

$$X(\tau) = R\cos(\tau) \tag{2.8}$$

$$Y(\tau) = H - K(1 - \sin(\tau)) \tag{2.9}$$

where τ is the angle ranging from 0 to 2π. While R and K are calculated as:

$$\lambda = V_{wave}T \tag{2.10}$$

$$n_{wave} = \frac{\lambda}{d} \tag{2.11}$$

$$n_{elevated} = \frac{V_{wave}t_T}{d} \tag{2.12}$$

$$\emptyset_A = \frac{2\pi}{n_{wave}} \tag{2.13}$$

$$n_{elevated} = \frac{\emptyset_A n_{elevated}}{2} \tag{2.14}$$

$$r = \frac{V_{millipede} t_P}{2} \tag{2.15}$$

$$k = \frac{r}{\tan(\theta)} \tag{2.16}$$

$$K = H + k \tag{2.17}$$

$$R = \sqrt{\frac{r^2}{1 - \left(\frac{k^2}{K^2}\right)}} \tag{2.18}$$

where n_{wave} and $n_{elevated}$ are the number of legs per wave and the number of legs elevated in the forward strokes profile, respectively. Note that $\theta_{initial}$ for a circular case, but is then incrementally adjusted until the propelling leg velocity is within a desired tolerance of the body velocity and has the correct number of elevated legs.

This model is capable of capturing the aggregate behavior of the legs when walking as shown in Figure 2.3, and did so in 0.496 seconds in comparison to the model presented in [52] which took 112.9 seconds. In essence, the elliptical model improves computational efficiency by representing the temporal duty cycle geometrically and proved to still capture the aggregate traveling wave behavior.

Traveling Wave Modulation: The traveling wave created by the legs across the body has been observed to change depending on the magnitude of force exerted to traverse the varying environments, including walking, climbing, and burrowing. Manton [23] observed an effective traveling wave modulation when millipedes encountered forces resisting their desired motion. In Manton's experiments, millipedes were pulling on 'mini sleds' as well as had small weights placed

along their back. It was found that a millipede would increase the number of legs in contact with the ground ‘per wave’ to accommodate the loading.

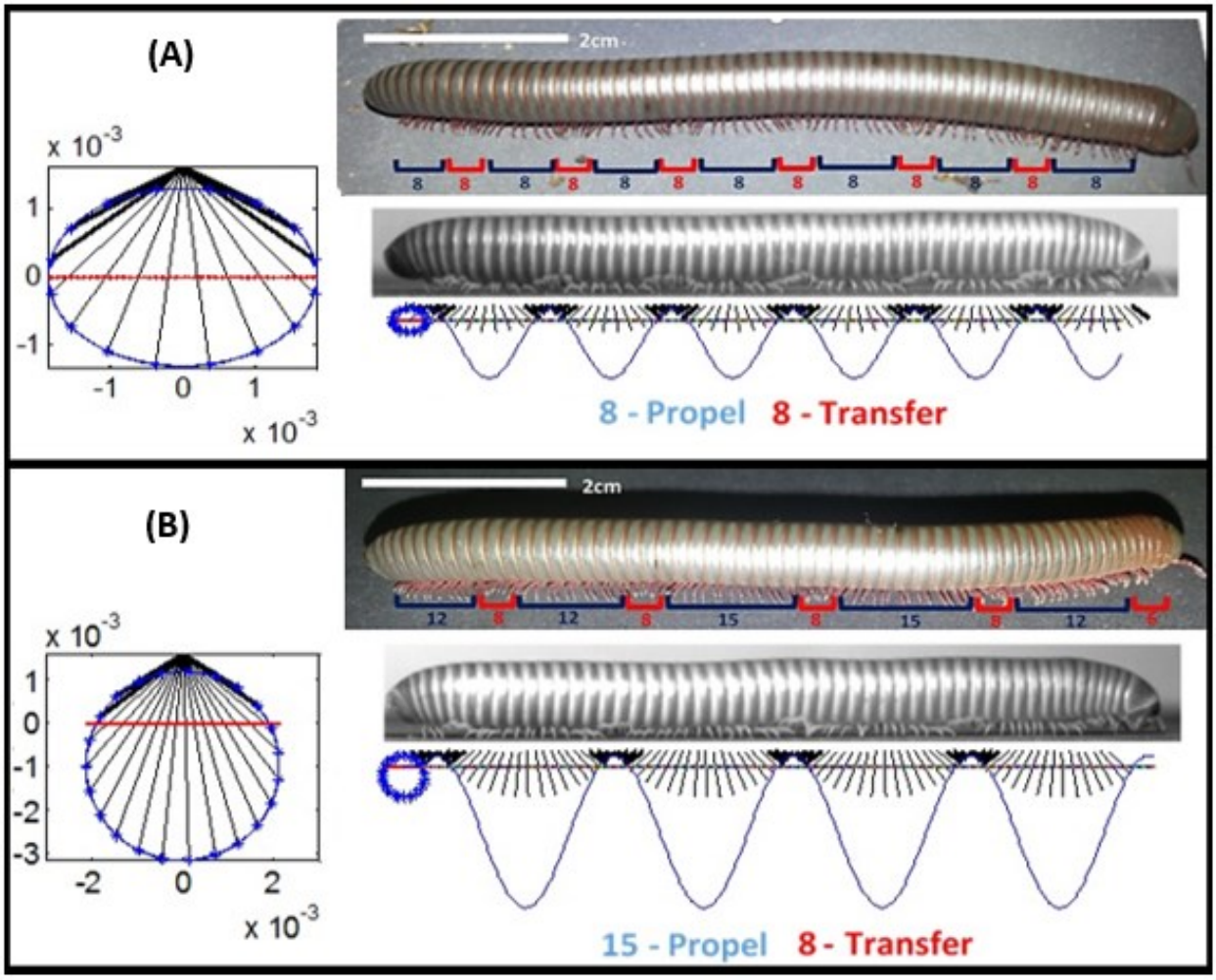

Figure 2.3: Using the elliptical model to efficiently capture the kinematics of aggregate behavior of all the legs that create the traveling wave for two different instances (A) no resistive load (flat surface) and (B) large resistive load (steep inclined surface)

The work later in this chapter here utilizes two different approaches to further investigate these wave modulations, the first varies a slope as a means to control the resistive force acting against the millipedes’ motion, over a wide range of angles to determine the relationships of the traveling wave modulations relative to the desired forward thrust. The second approach is use of a stage

developed to try emulate a burrowing environment providing loads both axially and radially on the body, but where their gait adjustments can be observed. The main parameters that define the motion of a single leg, which influences the aggregate behavior of a traveling wave across all the legs along the body, are the duty cycle and phase difference. Variations of these parameters result in modulating the wave velocity and length. By investigating how these gait parameters relate to propulsive thrust, we can begin to understand and model the dynamics involved that make the millipede locomotion effective for tasks such as burrowing or climbing.

2.2.2 Body movements

The flexible body motions that permit millipedes to conform to different surfaces are accomplished by articulation of a three-degree-of-freedom rotary joint between body segments similar to a ball and socket. This type of attachment at the joint permits the three body degrees of freedom—lateral motion, dorsoventral motion, and rotational motion [23][33] — while limiting any telescopic effects between segments when facing body axial loads. The anterior ends of each segment is tapered and inserted into the wider posterior end of the segment ahead of it. A complex musculature (Figure 1.7A), in combination with the structure, allows for the rigidity needed for burrowing. Even though there are variations between species, a visual example of Manton's general description [23] of the joints between body segments can be seen in Figure 2.4.

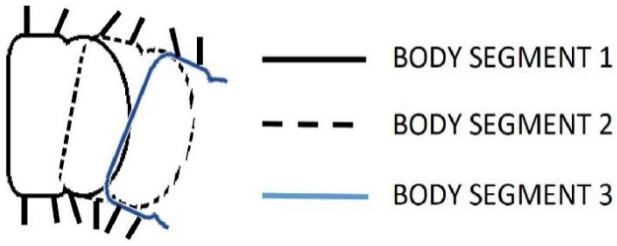

Figure 2.4: "Ball and socket"-like joints between body segments permitting three degree-of-freedom motion

Turning (lateral motion): To further understand how millipedes perform a turning motion, millipedes were placed in scenario with a large obstacle in their path. Footage was taken of both the *A. virginiensis* and *N. americanus* in similar situations, as shown in Figure 2.5A. The bodies of both species display a lateral bending while turning, in the manner where all the body segments tend to follow the path initially traversed by the first segment (head). To capture data that represents these movements, several points along the *A. virginiensis's* body were tracked. By tracking seven points, the position and angle of six sections could be determined. The points were selected so that each section represented three body segments. For the purposes of capturing the aggregate behavior, it was assumed that the angle of a given section was the summation of the angles between the internal segments. From the data collected from the key framing image process, the trajectories in Figure 2.5B and 2.5C were generated with smooth splines by using MATLAB's cftool function. Figure 2.5B displays the absolute angle of the body sections. From this data, a sequential behavior of the body sections changing angles over time, and of similarly followed trajectories, is evident. This is consistent with the motions expected from Manton's description and the "follow the leader" observation of the body segments. The relative lateral angular motion between sections during the turning period was determined and these trajectories are seen in Figure 2.5C. The maximum relative angular displacement between adjacent sections, during the turn by the *A. virginiensis* in Figure 2.5A, was 15°, which for three body segments is representative of approximately 5° per body segment. The particular turn captured was certainly conservative to its maximum capabilities, which Manton [23] determined to be up to 35° per segment depending on the species. Furthermore, across the different species of millipedes, some have eyes to help with sensing their environments, while others are completely blind. However, regardless of having vision or not, millipedes generally rely on the use of antennae to indicate direction of motion. As

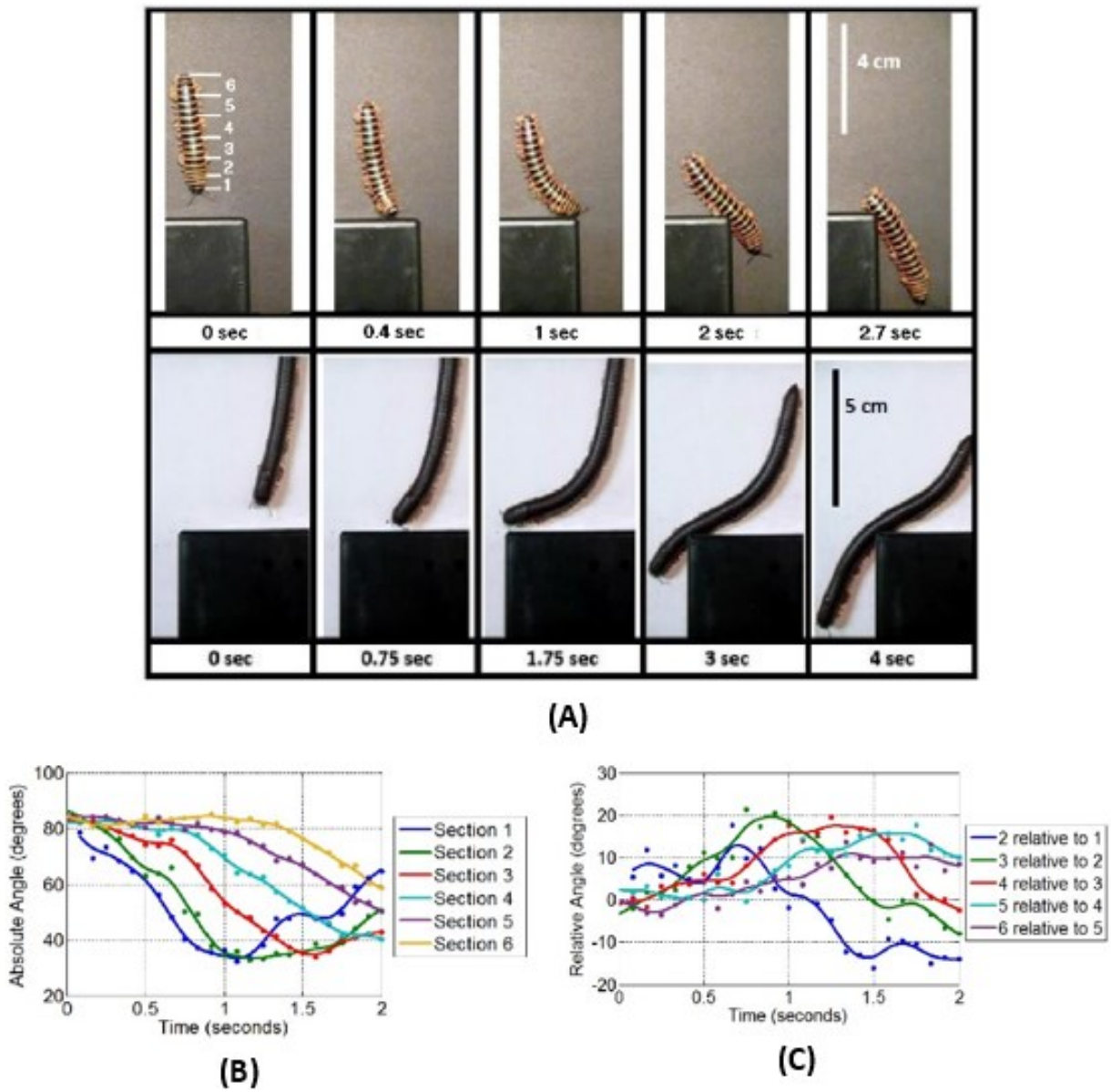

Figure 2.5: Tracking a millipedes turning motion. (A) *A. virginiensis* and *N.americanus* turning time instances, (B) Absolute body segment angles of *A. virginiensis*, (C) Relative body segment angles of *A. virginiensis*

seen in Figure 2.5A, both the blind *A. virginiensis* and *N. americanus* that has eyes, begin to turn once the antennae make contact with the obstacle, towards the path of least resistance. These observations provide an initial understanding of the turning locomotion, a sound basis for developing approaches and means to emulate turning for an elongated segmented bodied robot.

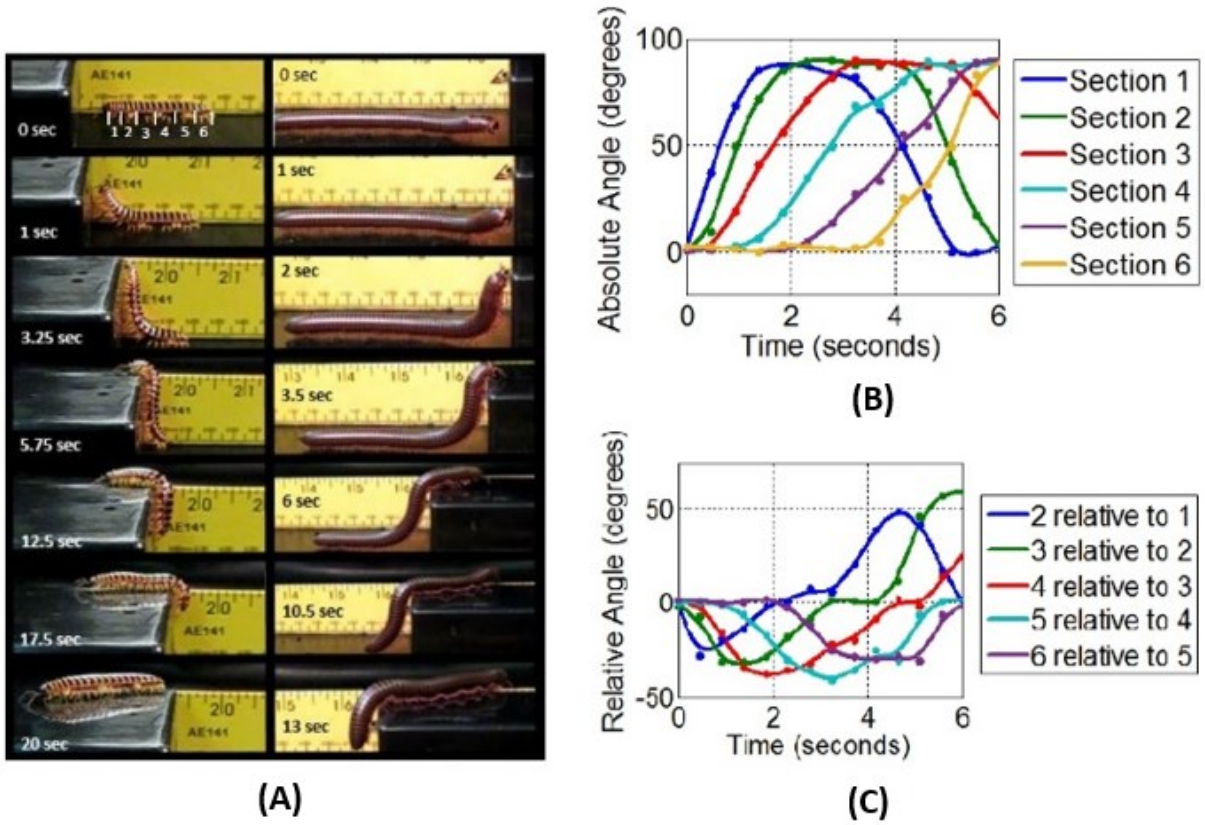

Figure 2.6: Tracking a millipedes climbing motion. (A) *A. virginiensis* and *N.americanus* climbing time instances, (B) Absolute body segment angles of *A. virginiensis*, (C) Relative body segment angles of *A. virginiensis*

Climbing (dorsoventral motion): One movement of interest introduced by myriapods is the ability to conform to uneven surfaces and climb. Adding this degree of freedom to the lateral motion allows the body to easily traverse 3-dimensional terrains. In particular, it allows the change from horizontal to vertical surfaces without much adjustment of its walking gait, by controlling its body position instead. This myriapod morphology becomes clearly advantageous over rigid bodied insects, which would require significant changes in gaits to accomplish the same task. Like the experiment conducted for capturing the turning locomotion, both millipedes were placed in situations that encouraged a climbing behavior. Figure 2.6A shows both performing the task in similar fashions. Again, data was collected from the footage of the *A. virginiensis*, tracking the

absolute and relative angles of the six sections consisting of three body segments each. Figure 2.6B clearly indicates a similar sequential angular motion of body segments as before but in the dorsoventral plane.

Observing the relative angular dorsoventral motion (Figure 2.6C), the degree of freedom allows motion in both directions in the plane. Also, that for *A. virginiensis* to achieve a 90° bend in the dorsoventral direction (reaching up to 50° between sections), corresponds to each segment bends a maximum of about 17°. Again, this motion captured is conservative relative to its maximum capabilities. The range of motion varies among different species of Diplopoda. For instance, juliform millipedes (e.g., *N. americanus*) are capable of a large range of dorsoventral motion, when curling up tightly into a spiral for defensive purposes.

While this degree of freedom is helpful in millipede climbing efforts, and several species demonstrate the ability to climb on rough surfaces reasonably well, millipedes are not the most effective climbers. The ability of millipedes to climb is dependent on their morphology of numerous legs providing many points of contact clamping on terrain for support and their flexible bodies to transition to crawling on steep surfaces with relative ease. Despite these desirable characteristics for effective climbing, they do not have adhesion techniques seen in other arthropods like ants, beetles and spiders. A few species of millipedes possess claw adaptations for climbing and living in caves, but not *A. virginiensis* or *N. americanus*.

Righting (rotational motion): One conspicuous movement exhibited by millipedes is the ability to rotate individual body segments relative to each other about the long axis of its body. Again, this motion is possible with the presence of the "ball and socket" like joint in between segments combined with strong musculature. Manton [23] described that such motion was not demonstrated in open surfaces, and postulated that its function was for burrowing purposes as species that burrow

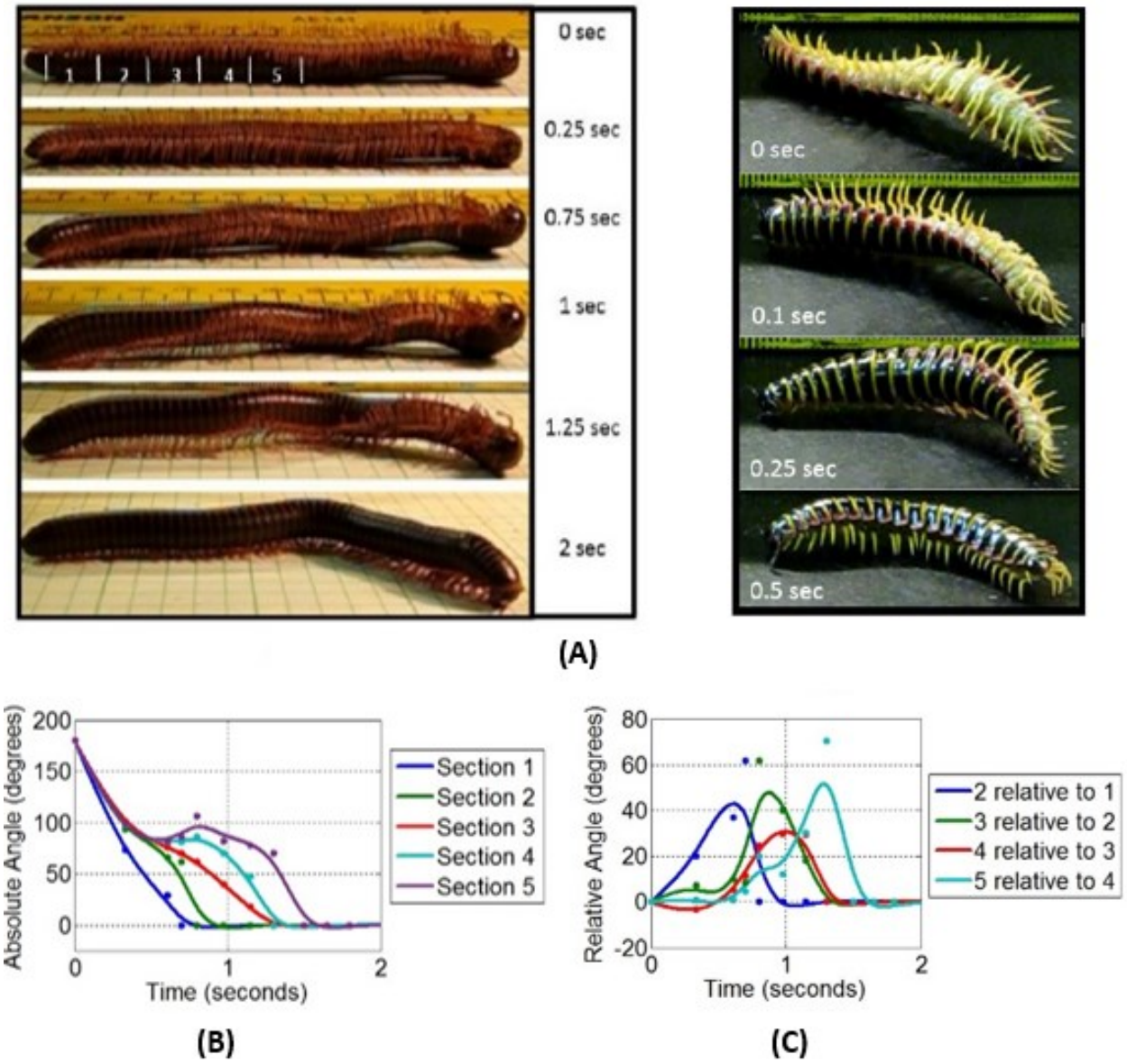

Figure 2.7: Tracking a millipedes righting motion. (A) *A. virginiensis* and *N.americanus* righting time instances, (B) Absolute body segment angles of *N.americanus*, (C) Relative body segment angles of *N.americanus*

more effectively, for example a juliform millipede could rotate more than surface active species like the flat-backed millipedes in the Polydesmida. During the experimental process of collecting video footage of the millipedes crawling, it was found that they would use the ability to rotate body segments to right itself back on its feet. Rigid body insects, such as beetles, would not be able to right themselves if fallen. The ability to perform this motion on a robotic platform would be

desirable, if traversing in dangerous and unknown terrains. Similar key framing techniques that were used in collecting data for the turning and climbing scenarios were performed for the twisting motion of the millipedes righting themselves. The movement displayed can be seen in Figure 2.7A. Data was collected from the *N. americanus*, because there was a larger region of its body that displayed only twisting of body segments without other lateral or ventrodorsal flexions, simplifying the key framing tracking process. Five sections of 1 cm intervals were tracked, each section consisting of six body segments. The angle was determined by tracking the position of the attachment point of the legs to the body relative to the rotational axis along the body (assumed to be halfway up the body from the side). The results of the absolute and relative angles of the body sections selected are seen in Figure 2.7B and 2.7C respectively. Looking at the absolute angles, again we see the sequential behavior of body segments rotating. However, it is interesting to note how the millipede gets back on its feet. At about 0.75s the fifth section begins to rotate back upwards. Watching the motion (as seen in Figure 2.7A) the *N. americanus* would rotate the anterior and posterior ends in opposite directions until one end plants its legs on the ground. The grounded legs then act as an anchor, while the adjacent body segments rotate sequentially until the other end is in the same configuration. Similar motion was observed for the *A. virginiensis*. The relative rotation of segments from the bottom plot of Figure 2.7C shows that the maximum relative angle between adjacent segments to complete this motion was approximately 9° (55°/ 6 body segments). This result appears to be relatively consistent to the maximum of 11° observed by Manton on another species of juliform millipede [23].

2.3 Traveling Wave Modulation Investigation Methods

Two experiments were performed on the millipede specimens to observe the adjustments in gait in the presence of resistive loads. The first experiment of a varying inclined slope was performed with six specimens across two different species of millipedes. Three of the test subjects were *Apheloria virginiensis*, the flat-back millipedes (Polydesmida) that use the "wedging" burrowing technique. The other three specimens used in this investigation were *Narceus americanus,* which use the "bulldozing" burrowing technique mentioned earlier.

To characterize how the traveling wave gait implemented by millipedes is modulated with respect to variations in thrust force demand, all six specimens were placed on a ramp, at randomly selected slopes ranging from 0° to 50°, at 5° increments with 15-minute rest intervals. Each case was captured with a high-speed camera operating at 250 fps (Photron FastCam SA4). The ramp stage was actuated with a stepper motor to ensure repeatability of the randomly selected angles. The angles were accurate to within 0.0002°, and the zero-degree position was calibrated with a digital limit switch before each angle adjustment. Sand paper of 400 grit was placed on the acrylic ramp to allow traction for the millipedes to climb a broad range of angles (Figure 2.8A).

Using the slope as a means to provide a consistently controlled gravitational force in the direction against the desired motion, we can quantify the magnitude of the applied force. To do this, we determined the resisting force caused by gravity with knowledge of the slope angle. However, we need to take into account the mechanical and behavioral response due to loss of traction resulting from large incline angles. The effective resistance force to motion was determined using the traction on a perfectly horizontal case as a baseline, as shown in (2.19).

$$F_R = F_o - (\mu F_N - \mu F_N{}^{0^\circ}) \tag{2.19}$$

where μ is the coefficient of friction and $F_N^{0^\circ}$ is the normal force on the horizontal case.

The second experimental setup utilized a developed stage that provided both axially horizontal loads as well as radially vertical loads. Four specimens were used for this experiment, two *Narceus americanus* and two *Apheloria virginiensis*. This was done with the purpose of imitating real life environments of burrowing where it is believed their powerful metachronal gait is of great value. Furthermore, with the different burrowing techniques described earlier between the two species, it is of interest to see their preferences of how they engage with the surrounding environment regarding resistive loads present from different directions. The built stage was 3D printed (Objet), and used 8-32 screw nuts as weights to incrementally increase the loads in both directions, this can be seen in Figure 2.8B The same resting time increments were used as the slope experiment, and also filmed using the same camera settings.

The collected footage was then processed using the open source program DLTdv5 (Direct Linear Transformation digitizing environment) in conjunction with MATLAB to track points of interest. The extracted data was assessed and manipulated in MATLAB to investigate trends and characterize the traveling wave gait.

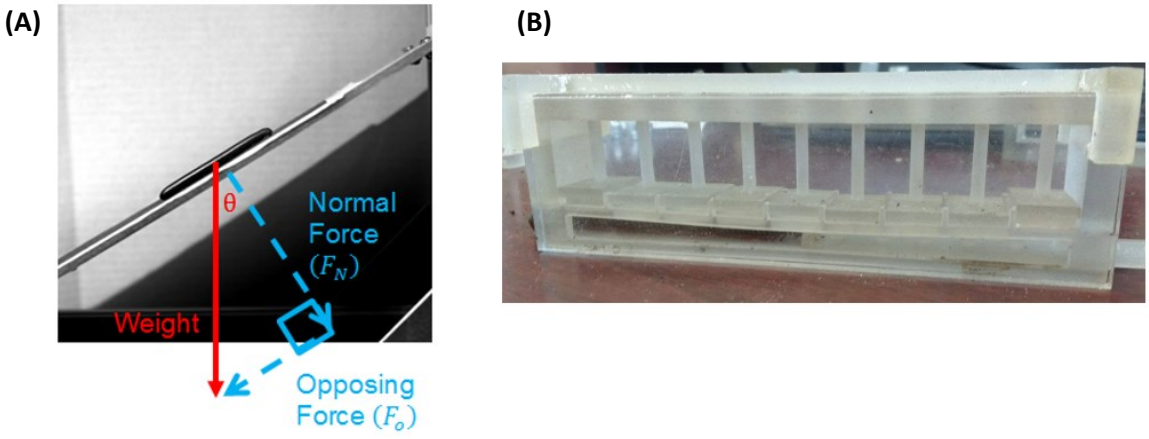

Figure 2.8: (A) Climbing incline slope experimental setup and depiction of forces, (B) Burrowing stage experimental platform

2.4 Traveling Wave Modulation Observations and Results

By tracking the millipede's leg movements from video footage, the gait parameters and wave characteristics described earlier were determined for each specimen for the range of incline angles and range of weighted burrowing resistances tested.

2.4.1 Traveling wave gait observations (Slope experiment)

Wavelength – As expected from previous findings [23], there is a clear increase in wavelength with increased propulsive force demand as shown in Figure 2.9A and B. The dimensionless force is the resistive force as a ratio of the specimens' body weight. The dimensionless wavelength (λ_{DL}) was calculated as shown in equation (2.20):

$$\lambda_{DL} = \left(\frac{\lambda}{L}\right)\left(\frac{DN}{L}\right) \tag{2.20}$$

where λ is the actual wavelength, L is the body length of the millipede specimen, D is the body diameter (shown in Figure 2.9E and F), and N is the number of leg pairs. The first component captures the length ratio of the generated traveling wave with the length of the specimens' body. However, this alone does not make this characteristic comparable between millipede species given the wide variation in morphologies. The multiplied factor captures these different features essentially by an aspect ratio of the body and the number of legs. These parameters were chosen as Manton [23] had indicated that the force output by the millipedes' muscles is proportional to its body segment or ring volume, which allows us to draw comparisons in wave modulation across the two different species tested despite the differences in size and morphology. As seen in Figure 2.9A and B, there is a distinct increasing trend in dimensionless wavelength for both species climbing more inclined surfaces (increasing the perceived resistive load as a result of reduced traction). It is worth noting that all specimens did not want to climb on the given surface at the

angle that encouraged a behavioral response that emulates a resistive force just over twice their weight. An increase in wavelength is a result of adjusting the number of legs per wave, but doing so while maintaining a "constancy in forward strokes" [23] this results in a higher ratio of legs in the propulsive backward stroke phase to the swinging forward stroke phase per wave.

Based on the assumption that all the legs are performing identical motions, this indicates an increase in duty cycle with increasing resistive force (the quotient of stance duration and stride duration, also commonly referred to as duty factor).

Wave Velocity – While it was observed that the wavelength was not significantly adjusted by variations in body speed, the wave velocity was certainly influenced as it directly relates to the motion of the legs. To compare across the different specimens at different slopes and moving at varying velocities, the effective Strouhal number was determined for each case. While typically used for fluid dynamic applications, the Strouhal number is the ratio of the wave velocity to the body velocity, which provides a dimensionless value to compare the different cases. A distinct increasing correlation of the Strouhal number with increased dimensionless force was observed for both species shown in Figure 2.9C and D. This is expected as the wave velocity (thus Strouhal) number is directly related to the duty cycle, which increased to create the change in wavelength.

2.4.2 Traveling wave gait observations (Burrowing experiment)

While the incline slope experiment allowed us to observe the traveling wave modulations at very controlled resistive loads in the direction of motion, these gait adjustments were actually only behavioral responses created by the loss of traction on the increasing incline attempting to replicate the situation of increased loading. Further experiments are needed to confirm whether such gait variations translate from the behavioral response from climbing, encountering a perceived resistance, to burrowing activity where actual loads are present. In Manton's experiments [23],

specimens were made to pull on weighted sledges as well as carry weighted loads on their back, which captures both axial and radial loading. However, while the load capacities were tracked in observing the millipedes' capabilities of handling resistive loads, and associated gait patterns', there were no mathematical models to capture the observed trends. To try capture the gait responses, a novel burrowing stage was developed. The setup allowed increased incremental loading in both the horizontal (axial) and vertical (radial) directions in attempts to emulate a burrowing situation (Figure 2.9G and H).

Wavelength – In order determine if the behavioral response of the millipedes during the climbing incline experiments translates to burrowing applications, the initial tests were performed with only a horizontal (axial) resistance present in the burrowing stage. It can be seen in Figure 2.9A and B that the wavelength adjustments made by both species in cases of only horizontal (axial) resistances follow the trend that the millipedes exhibited in the climbing incline experiment, up to the resistance (created by large incline angle corresponding to about twice their body weight) which the millipedes no longer desired to climb. Beyond that point, it is important to note that the millipedes still exhibited capabilities of burrowing, however, the adjustments in gait behavior shift and appear to become sporadic. Further tests were performed introducing combinations of horizontal (axial) with vertical (radial) loads, and while the changes in gait are certainly more sporadic, there still exists an overarching trend of increasing the wavelength, as seen in Figure 2.10. Note that the load increments on the burrowing stage were the same for both species, so while the *N. americanus* was willing to burrow through all combinations of axial and radial resistive loads, the *A. virginiensis* which is considerably smaller (about half the length and weight)

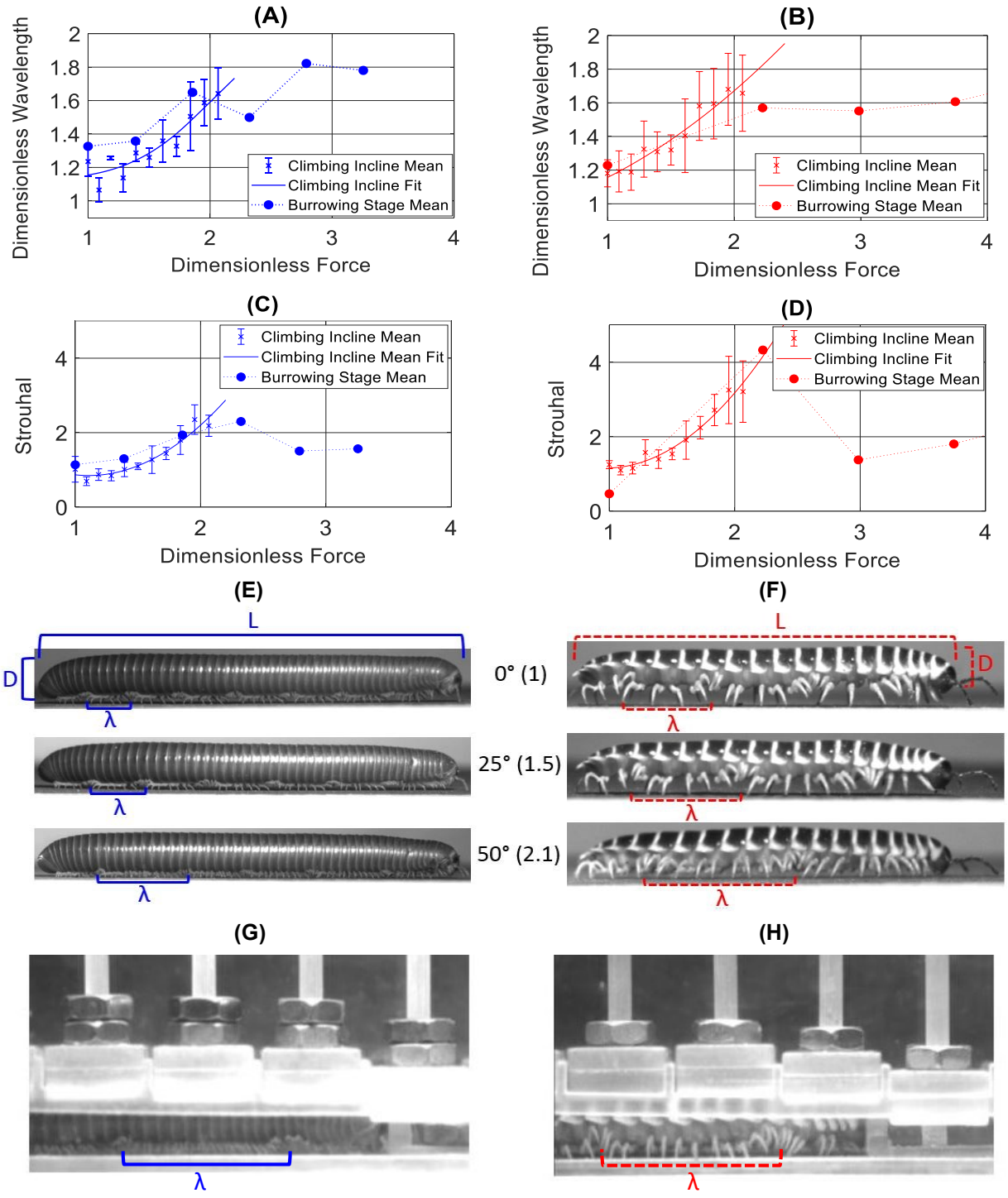

Figure 2.9: (A) *N. americanus* dimensionless wavelength versus dimensionless force (climbing and burrowing) (B) *A. virginiensis* dimensionless wavelength versus dimensionless force (climbing and burrowing) (C) *N. americanus* strouhal versus dimensionless force (climbing and burrowing) (D) *A. virginiensis* strouhal versus dimensionless force (climbing and burrowing) (E) *N. americanus* climbing image frames (F) *A. virginiensis* climbing image frames (G) *N. americanus* crawling in burrowing stage (H) *A. virginiensis* crawling in burrowing stage

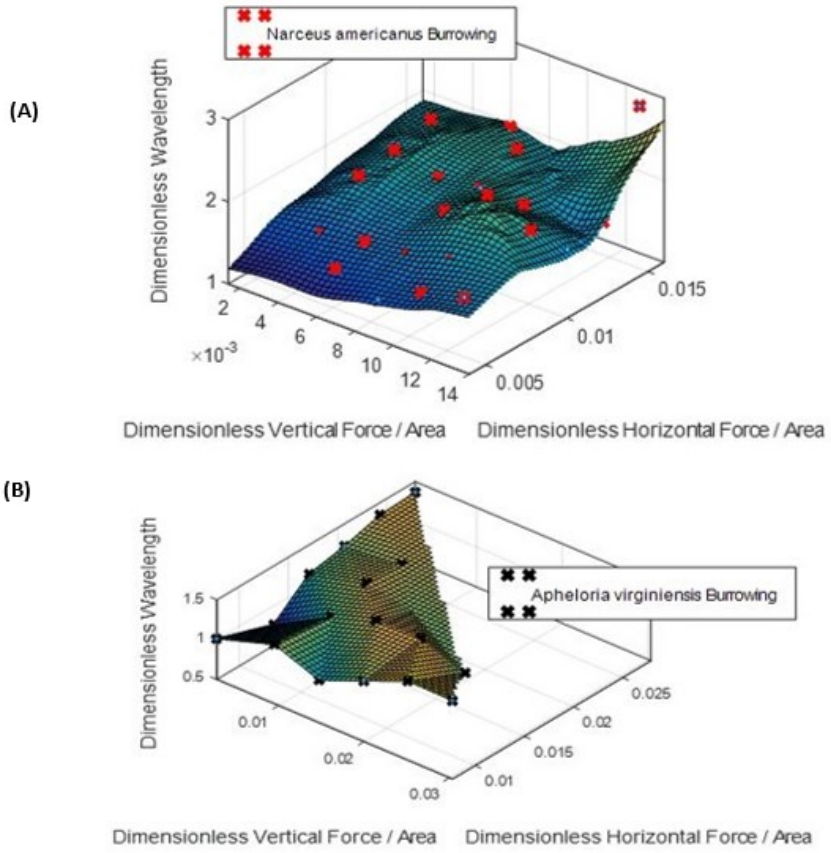

Figure 2.10: (A) Surface plot of *N. americanus* dimensionless wavelength against horizontal and vertical load combinations, (B) Surface plot of *A. virginiensis* dimensionless wavelength against horizontal and vertical load combinations

would not willingly engage in the higher load burrowing situations. This likely is not indicative of their performance capabilities because while the setup of the burrowing stage (that allows observation and variable control) attempts to emulate and encourage such behavior, it is very different to the substrate and environments millipedes typically would desire to burrow through.

Wave Velocity – Similarly, the wave velocity created by the metachronal gait while in the burrowing stage against only horizontal (axial) loads, follows the same trend displayed in the incline experiment, up to about twice their body weight (the limit observed in the incline experiment), as shown in Figure 2.9C and D. Beyond this load limit, and introducing of vertical (radial) loads, the adjustment in wave velocity, like with wavelength, becomes somewhat sporadic.

(visuals of the complete wavelength variations of all specimens can be found in Figure 2.17 and Figure 2.18).

From the results of these two experiments, we can see that the incline climb experiment does capture the behavioral gait adjustment response with regards to horizontal (axial) loading. This allows us to utilize the fine incremental control of the incline experiments to understand the changes in millipede locomotion dynamics when encountering loads against the desired direction of motion. While the cases in the burrowing stage beyond the gait behavior exhibited in the incline experiment (horizontal/axial loads), clearly indicate impressive capabilities of the millipedes to burrow against larger and vertical/radial loads, more experiments with finer increments of the burrowing stage loading are required in order to illustrate the more sporadic gait behavior.

2.5 Gait Dynamic Model

In order to understand the fundamental mechanics of millipede locomotion, with interest in their ability to propel their bodies against large resistive loads in the desired direction of motion when burrowing, we primarily look to understand and model the gait behavior when handling body axial loads.

Until now we have only observed the trends of the traveling wave modulations in relation to adjusting thrust performance, however, to understand this locomotion technique we need to study the mechatnics of each individual leg to reveal why such wave adjustments need to occur.

Kinematic studies have been done on determining the position and motion of millipede legs to create a traveling wave [52], [53]; however, these models did not involve the dynamics of the gait.

Siddall [54] explored the basic forces involved in a metachronal gait system, taking a quasi-static approach (static + propelling forces) (Equations 2.21-2.24). The model assumed a many legged robot body with pneumatic cylinder legs that could autonomously adjust in length, with forces transmitted by a single rotating degree of freedom at the hip. The resulting forces were calculated with trigonometric functions calculated with the angle of the leg at a given instance. Another kinematic/dynamic model [55] developed by Fang, used elastic mesh deformation to determine ground reaction forces, while governing the leg motions with different leg states with implementation of a decentralized controller. Kano et al. in their work [27], [28] used a legs with a circular trajectory, but with compliant behavior when in encountering ground reaction forces used as local feedback in their work on decentralized control. One interesting approach treats the traveling wave like peristaltic locomotion. In the modeling techniques used by [56]–[58] (Tanaka et al. and Spinello et al.), a Timoshenko beam coupled with a substrate generates locomotion by shape morphing in a fashion that replicates sparse and dense regions recognized in peristaltic movements, relating this to the aggregate behavior of metachronal motion of myriapods. The model details the nature of how the generated wave anchors with the substrate (whether within the sparse or dense region of the mechanism) which dictates the direction of the wave motion relative to the direction of the locomotive body. However, this model does not capture the mechanically clipped and modulating nature of the wave, which would correspond to adjusting the anchoring contact point of the wave to beyond a single point. This aspect of the wave adjustment appears to be crucial in adjusting thrust force ability.

To keep the modeling approach simple and allow flexibility of further adjustments, the kinematic and dynamic models of [52]–[54] were built upon, to develop a simulation model to capture the dynamic thrust performance of millipedes. In making this model there were many variables that

needed to be considered, both morphological and behavioral. Morphological parameters include the body length, number of body segments, number of leg pairs, body diameter, leg length, musculature strength, etc., while behavioral gait variables include duty cycle, stride length, leg thrust force, velocity, phase difference, etc.

The initial model determined the leg positions using the approached discussed earlier [52]. Once the positions and angles of each the legs were determined, the quasi-static approach used by Siddall [54] was used to determine the forces involved with the metachronal gait (equations 2.21 – 2.24), illustrated in Figure 2.11.

Static Analysis (Figure 2.11A):

$$F_{Static\_Tangent\_i} = -F_{ST}\sin(\varphi_i) \quad \rightarrow \quad \sum F_{Static\_Tangent\_i} = 0 \tag{2.21}$$

$$F_{Static\_Normal\_i} = F_{SN}cos(\varphi_i) \quad \rightarrow \quad \sum F_{Static\_Normal\_i} = Weight \tag{2.22}$$

Propulsion Analysis (Figure 2.11B):

$$F_{Propel\_Tangent\_i} = F_{PT}cos\,(\varphi_i) \quad \rightarrow \quad \sum F_{Propel\_Tangent\_i} = F_R \tag{2.23}$$

$$F_{Propel\_Normal\_i} = -F_{PN}sin(\varphi_i)$$
$$* \boldsymbol{F_{Propel\_Normal\_i} = F_{PN}(sin(\varphi_i) + cos(\varphi_i))} \quad \rightarrow \quad \sum F_{Propel\_Normal\_i} = F_V \tag{2.24}$$

Dynamic Analysis (Figure 2.11C): Static + Propulsion Forces

where F_V is the sum of residual vertical forces acting on the body from the assumed leg propulsion motion, that would result in small oscillatory dorsoventral deflections along the body when walking. Such deflections are not large, but become noticeable at high speeds.

In the initial modeling process, approximated average values of morphological features were selected for both species, shown in Table 2.1 and 2.2. The morphology in the model was assumed each body segment consisted of two leg pairs, the weight was equally distributed between body segments, and the body possessed a number of legless segments (representative of the relative size of anterior and posterior of the given species) at both ends of the body.

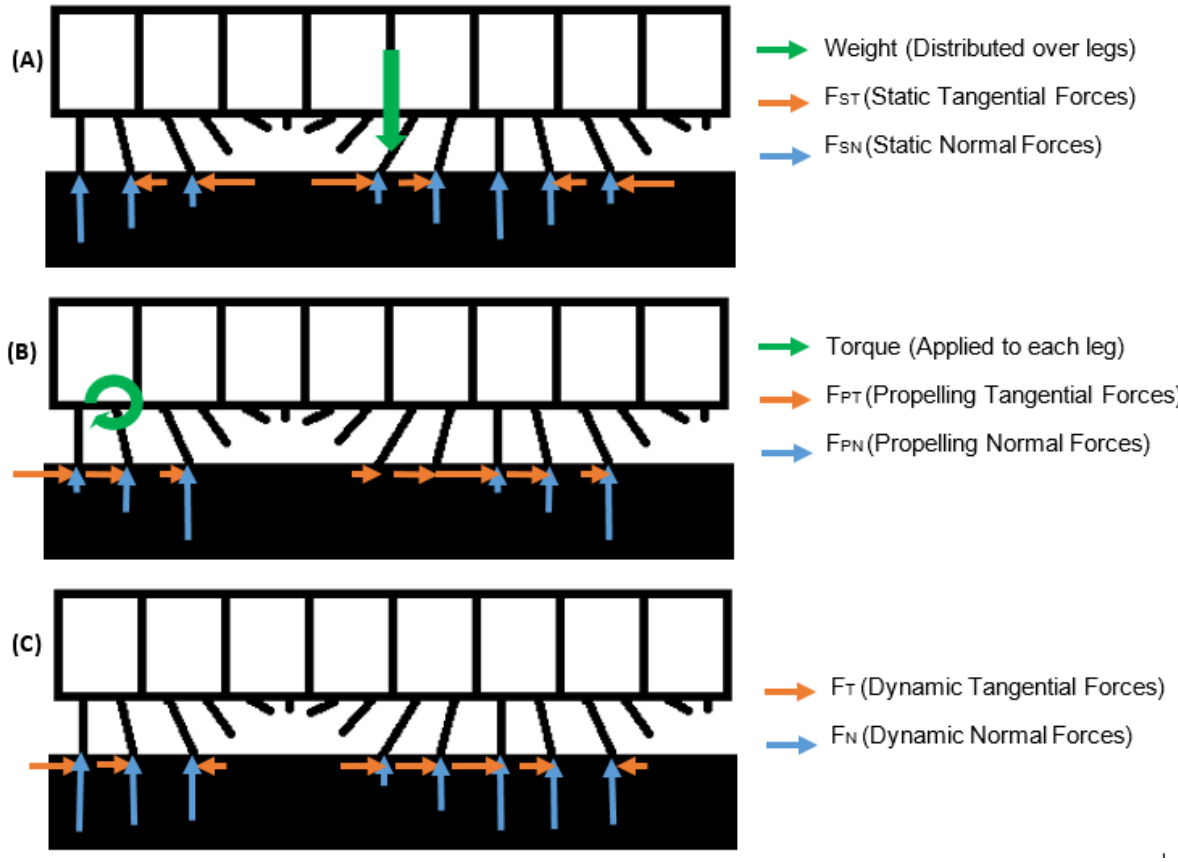

Figure 2.11: (A) Static leg ground reaction forces (B) Ground reaction forces resulting from leg swinging motion (C) Quasi-static/Dynamic Ground reaction forces of walking millipede

Like the morphological parameters were determined from experimental measurements and observations, the behavioral gait variables (duty cycle, stride length, phase difference, individual leg thrust force) were measured from the incline experiment for both species. This would then

allow us to begin determining the trends or relationships of each of these variables with the overall output thrust force of the gait propelling the body.

From these results, the clearest observation was the change in duty cycle, as expected. The duty cycle would range between 0.3 and 0.7 for both species (Figure 2.16C). The other gait variables that could be explicitly determined were the stride length and the leg phase of each pair creating

Table 2.1: *N. americanus* parameters

Narceus americanus					
Specimen	Body Length (cm)	Height (cm)	Width (cm)	Weight (g)	Number of Leg Pairs
1 (Climbing)	8.8	0.91	0.89	5.25	86
2 (Climbing)	8.4	0.91	0.77	3.91	91
3 (Climbing)	8.1	0.76	0.74	3.12	85
4 (Burrowing)	8.9	0.81	0.77	5.09	89
5 (Burrowing)	10.7	0.79	0.74	4.68	96
Model	**10.0**	**0.8**	**0.8**	**4.50**	**90**

Table 2.2: *A. virginiensis* parameters

Apheloria virginiensis					
Specimen	Body Length (cm)	Height (cm)	Width (cm)	Weight (g)	Number of Leg Pairs
1 (Climbing)	5.1	0.67	0.99	1.84	30
2 (Climbing)	5.4	0.61	0.99	1.51	30
3 (Climbing)	4.5	0.56	0.79	0.96	30
4 (Burrowing)	4.9	0.47	0.75	1.56	30
5 (Burrowing)	5.6	0.64	0.95	2.54	30
Model	**5.0**	**0.6**	**0.8**	**2.00**	**30**

the traveling wave. The stride length appeared to slightly decline with increased with total thrust force (Figure 2.16E). Regarding the metachronal gait leg behavior, what Manton [23] described as a “constancy in forward strokes” (number of legs elevated per wave) actually appears to also slightly decrease as well (Figure 2.16F).

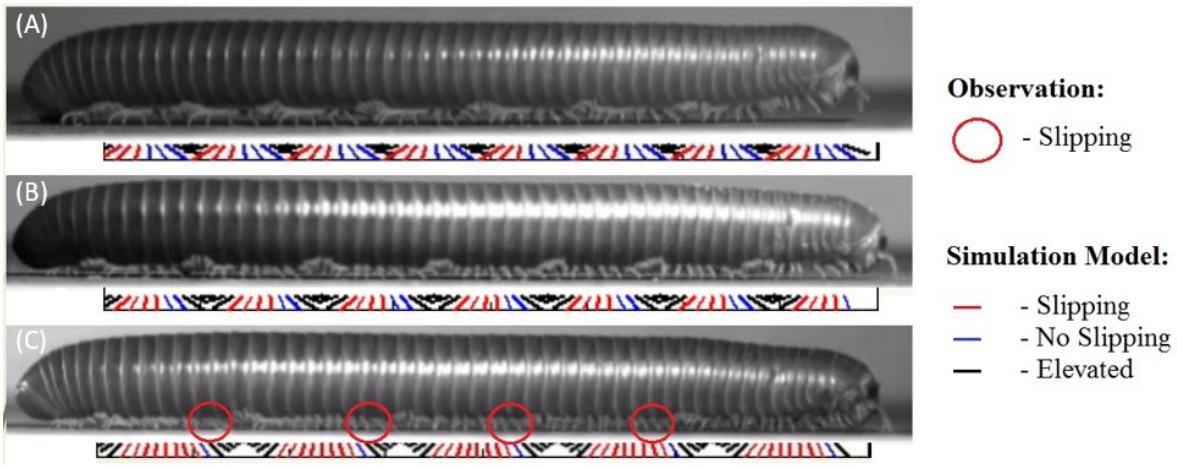

Figure 2.12: A comparison of locomotion observation with dynamic model at different ramp inclines of (A) 5° (B) 30° and (C) 50°

The last variable of interest was the force output of an individual leg, in relation to the total thrust of the gait. To do this, the other behavioral variables experimentally measured from the video footage for each specimen were used to generate kinematic simulations of each case, determining the leg positions through time. From knowledge of the leg positions/angles, the force values of each leg were back calculated using a quasi-static approach described earlier in equations 2.21-2.24 and Figure 2.11. However, this approach appeared inconsistent when comparing the simulation with observation, as there was discrepancy with expected slipping behavior (Figure 2.12). The model determined slipping would occur on legs during the latter half of the propulsion stance, just prior to elevating the leg. On the other hand, observation of the actual specimens suggested that the contrary was true, such that majority of the slipping occurred during the initial half of the propulsion stance just after landing. Given that the friction force tangential to the surface determines if a leg experiences slipping, the magnitude of the normal ground reaction forces become the governing factor (assuming a constant coefficient of friction).

In the simulation, these forces were calculated based on the assumption that the force driving the leg consisted of only a single degree of freedom resembling torque applied to a pendulum. In

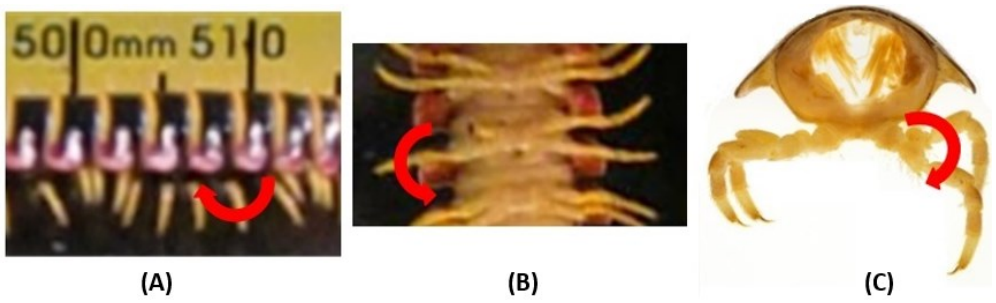

Figure 2.13: Main degrees of freedom of a millipede leg. (A) horizontal body line normal rotary axis (B) rotation about vertical axis at the leg attachment point (C) rotation about axis parallel to body line at leg attachment point

reality each millipede leg has multiple degrees of freedom that can influence the ground reaction forces during the propulsive stage or backstroke. Further model development required taking into account these other degrees of freedom, but without accounting for redundant complexities. Walking legs in general displayed three main degrees of freedom. The first motion is about the horizontal (body line normal) rotary axis (Figure 2.13A). The second motion is rotation about the vertical axis at the leg attachment point to the body, which results in a swinging the end of the leg with an outward curvature (Figure 2.16B). Lastly, each leg can rotate at the attachment point about the axis parallel to the body axis that permits the leg lifting motion (Figure 2.16C). It is the last degee of freedom which allows the lifting leg motion that can influence the normal ground reaction forces when walking, thus changing the general slipping behavior.

Anatomically, millipedes have a set of extrinsic muscles (two for *N. americanus* and four for *A. virginiensis* [25]) that provide motion in the horizontal plane only (Figure 2.16A and B), which leaves the vertical motion conducted by intrinsic muscles along the legs distal segments (Figure 2.16C). With this understanding we made the assumption that millipedes can control vertical motion of their legs independently such that limited vertical force is applied initially after landing, then gradually increases until mid-stance, and afterward provides relatively large forces pushing the body forward until the leg is elevated for the forward stroke. Millipedes can accomplish this

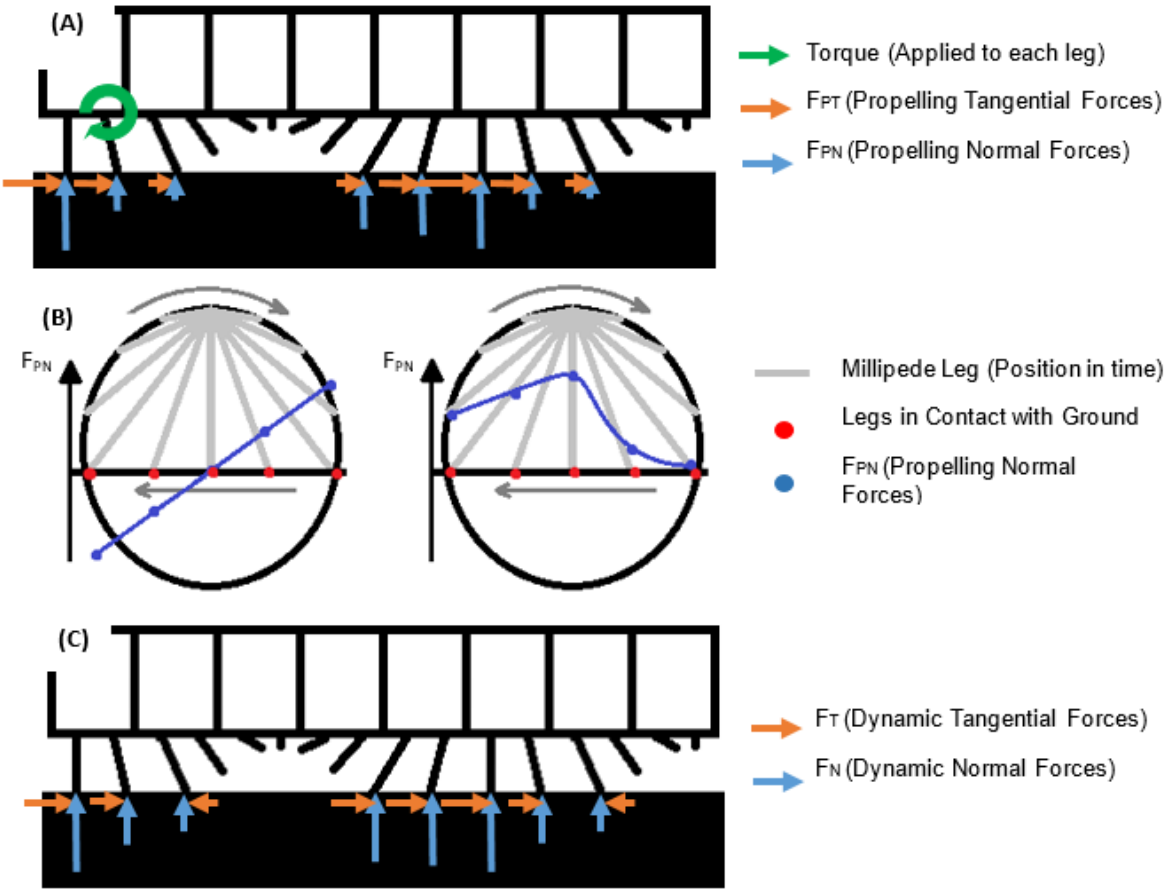

Figure 2.14: (A) Modified ground reaction forces from swinging propulsion motion (B) Visual comparison of the original and modified ground reaction force patterns (C) Modified resulting quasi-static/dynamic force model

by their control of a complex musculoskeletal system and central nervous system (a glimpse of the generic millipede anatomy can be seen in Figure 3.10A).

To reflect such change in the model, a change of the trigonometric functions defining the vertical motion forces was made from the single degree of freedom of "$-F_{PN}\sin\theta$" to a combination of "$F_{PN}(\sin\theta + \cos\theta)$". A visual comparison of the implemented change to the dynamic model of the propulsive force is shown in Figure 2.14B. This adjustment to the simulation captures the slipping behavior observed (Figure 2.16G and H). Furthermore, more importantly, the model indicated that the maximum force an individual leg performed stayed relatively constant regardless of the overall

thrust force demand for the body, which indicates that ability to improve thrust force is not dependent on the increasing effort of the legs, but primary response is the gait pattern used (Figure 2.16D).

Table 2.3: Modeling variables

Circle Path Radius (R)	2-4.5mm
Elevation of leg height (H)	1.5mm
Stride	$2\sqrt{R^2 - H^2}$
Time transfer stage/forward stroke (T_T)	0.5
Θ	$2\cos^{-1}(1 - (H/R))$
Ω	θ/T_T
Wave Velocity	ωR
Time propel stage/backward stroke (T_P)	$T_T(Duty\ Cycle)/(1 - Duty\ Cycle)$
Body Velocity	Stride/T_P

It can be seen that variation in effort by an individual leg varies more in the *A. virginiensis* compared to the *N. americanus*, which could likely be related to the fact that the *N. americanus* has significantly more legs, permitting finer control over the traveling wave gait modulations and less dependency on individual leg performance. Despite this slight variation seen in the *A. virginiensis*, the overall forward thrust of the individual leg does not vary significantly, staying relatively constant, which would support the assumption that each leg performs identical maximum thrust performance regardless of the desired total output thrust. With this data, the initial model framework given the average morphologies of each species, the input of an increasing duty cycle, and assumption of constant performance regarding force output of individual legs, the gait parameters yet to be modeled are the stride length and number of legs elevated per wave. Sweeps were performed for varying (physically realistic limited by maximum leg length) values for each the stride length and number of legs elevated, while holding the other variable constant. The variations in stride length revealed small changes in total thrust force of the gait, almost negligible

relative to the change in total force created by adjustments in duty cycle. More interestingly, the changes made in number of legs elevated per wave, did not change the overall thrust force of the gait. While a "constancy in forward strokes" (Manton [23]) results in more legs in contact with the ground per wave, changing the number of legs elevated per wave (which is a change in the temporal phase difference between leg pairs) does not change the ratio of number of legs in contact with ground across the entire body (thus does not change thrust force when varied independently), which is governed by duty cycle. This raises the question "what dictates the number of legs elevated per wave?".

To answer this question, the main issues that arise relating the number of elevated legs are (similar observations found in Mantons [23]): (i) If there are too many legs elevated per wave, this results in a large region of the body without vertical support, forcing dependence on the musculature between body segments to hold adjacent segments off the ground (Figure 2.15A). (ii) If there are too many legs elevated (for a given duty cycle) the phase difference between leg pairs decreases, resulting in an exponentially increasing wavelength. Too large of a wavelength would result in upright instability (Figure 2.15B). (iii) If there are too few legs elevated off the ground, this would lead to overcrowding between leg pairs in the propulsive stance (Figure 2.15C).

Given these issues, intuition would indicate that it is desirable to minimize the number of legs elevated, and maximize the number of legs in contact with the ground for both support and propulsive purposes. With this premise, we are left with minimizing the number of legs elevated,

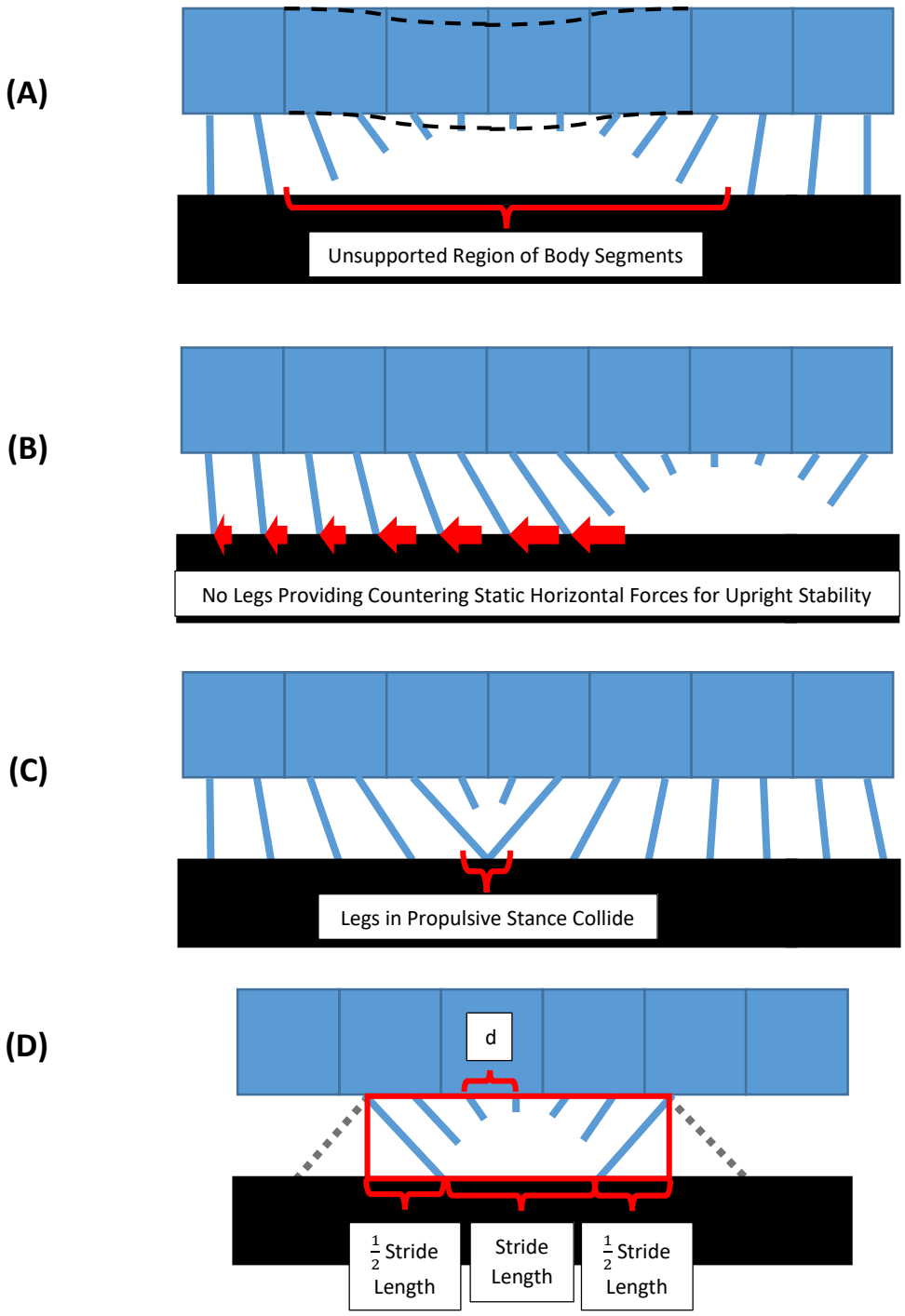

Figure 2.15: (A) Too many legs elevated per wavelength results in a large region of body segments without vertical support (B) Too long a wavelength (or too small a phase difference) results in upright instability (C) Too few legs elevated per wavelength could result in collision be legs in stance phase (D) Schematic of how legs elevated (temporal phase) is determined based on the morphological parameters

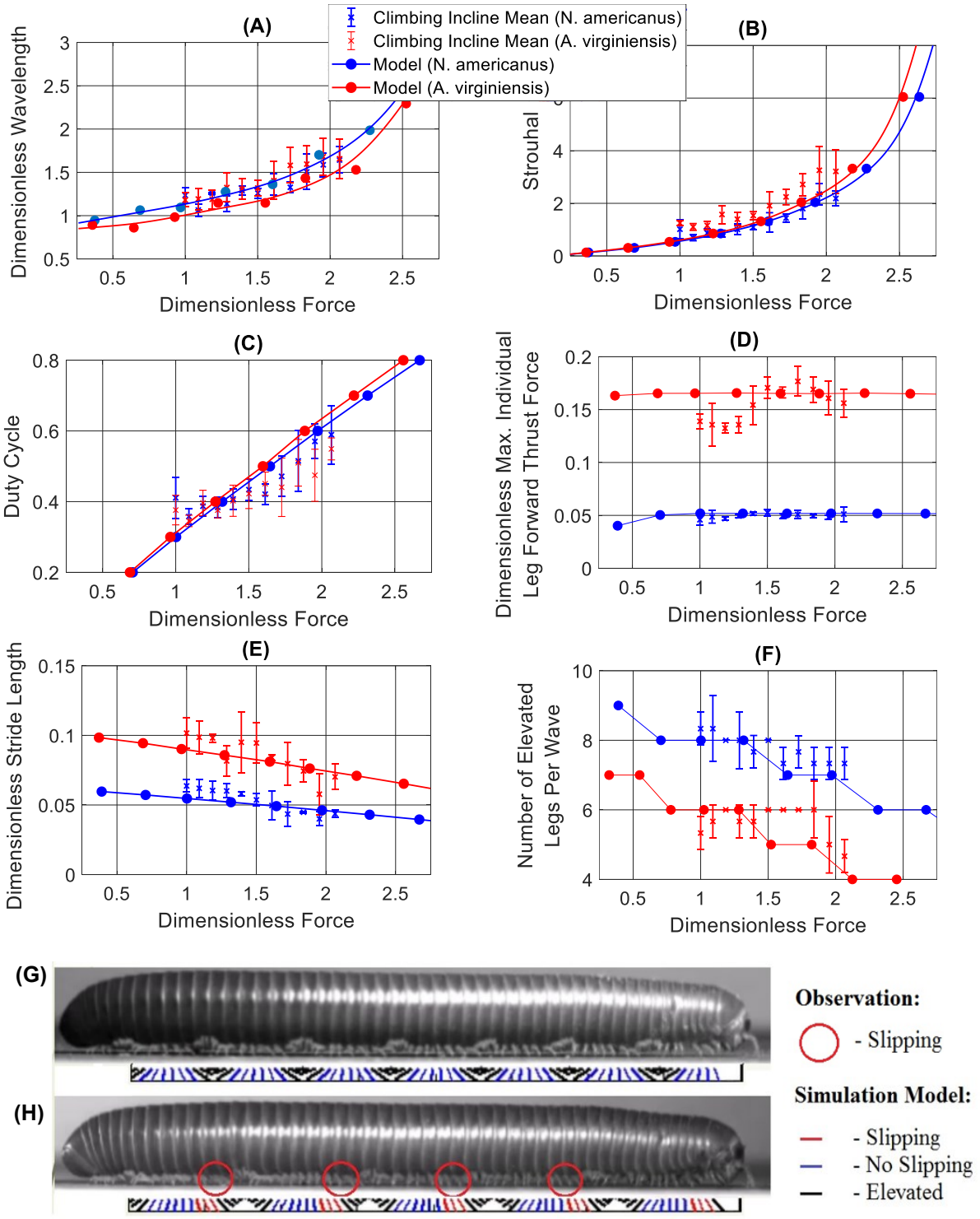

Figure 2.16: (A) Dimensionless wavelength versus dimensionless force (B) Strouhal versus dimensionless force (C) Duty cycle versus dimensionless force (D) Leg thrust force versus dimensionless force (E) Dimensionless stride length versus dimensionless force (F) Legs elevated versus dimensionless force (G) Experimental observation compared to model with no slipping (H) Experimental observation compared to model with slipping

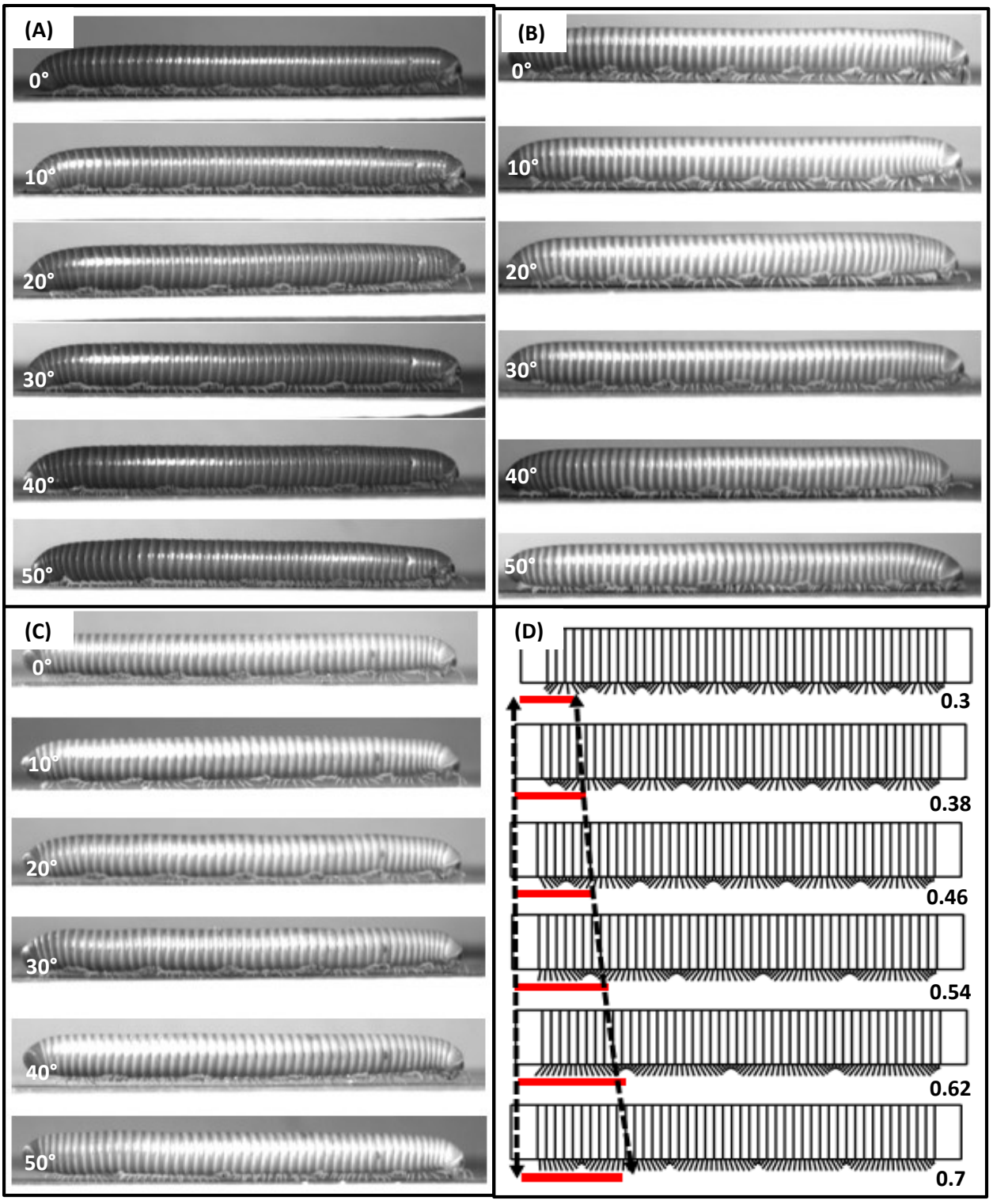

Figure 2.17: *Narceus americanus* specimens climbing on increasing inclines, demonstrating the variation in their gaits wavelength (A) Specimen 1 with incline angles, (B) Specimen 2 with incline angles, (C) Specimen 3 with incline angles, (D) Model (Red lines indicates the average wavelength) with input duty cycle to achieved desired forward thrust

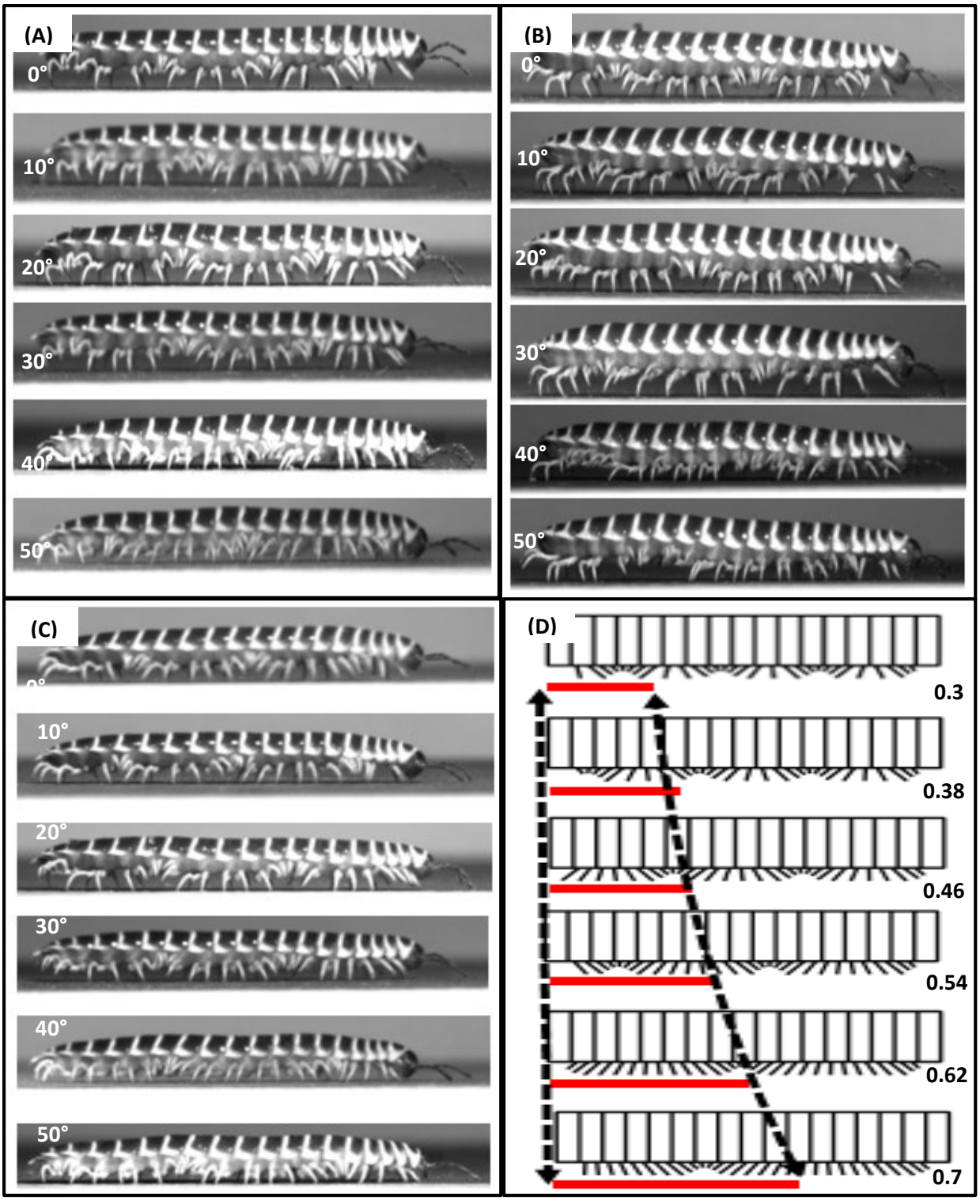

Figure 2.18: *A. virginiensis* specimens climbing on increasing inclines, demonstrating the variation in their gaits wavelength specimens climbing on increasing inclines, demonstrating the variation in their gaits wavelength (A) Specimen 1 with incline angles, (B) Specimen 2 with incline angles, (C) Specimen 3 with incline angles, (D) Model (Red lines indicates the average wavelength) with input duty cycle to achieved desired forward thrust

but avoid overcrowding of legs in the propulsive stance. Noting that the stride length also shows an inverse trend, the following relationship was generated:

$$N_{LegsElevated} = \left(\frac{2S}{d}\right) \tag{2.25}$$

where $N_{LegsElevated}$ is the number of legs elevated per wave, S is the stride length, and d is the distance between leg pairs. A schematic of what this equation illustrates can be found in Figure 2.15D. The if the numerator in equation (2.25) was just a single stride length, this would mean that there would be a collision between leg pairs in contact with the ground (the leg just prior to elevating and the leg that just landed), meaning any amount of slip on the surface could potentially cause one leg tripping another causing instability. Furthermore, if there was an instantaneous demand for vertical support of the body segments with elevated legs, there would be no space in between the legs performing strides for the elevated legs to come down. A gap of another stride length keeps the gap where legs are elevated minimal, but provides enough space to avoid collisions due to overcrowding. Using this relationship, we find that the model matches the observation with regards to the number of legs elevated per wave (Figure 2.16F).

From the experimental observations to determine the trends of the gait parameters, we now have a simulation model, which given the morphology of the millipede specimen, can determine the mechanics of the metachronal gait as well as the traveling wave locomotion characteristics of wavelength and wave velocity (Figure 2.16A and B) with the corresponding output thrust force.

2.5.1 Parameter Study

We have been able to model the millipedes' initial response and primary means of gait adjustment to handle increased resistive loads, which appears to range from its own body weight to just over twice its weight (while certainly capable of handling larger loads, this is the first steps of

understanding the mechanisms that make their powerful gait effective). In developing the model, we tested the behavioral parameters like duty cycle, stride length, phase difference, and their effects on the overall performance regarding thrust force. Now understanding that the individual leg force effort stays constant (at least within the desirable behavior exhibited from the incline experiments), comparing the remaining behavioral parameters, it appears that the duty cycle is the most sensitive in relation to the total thrust force, compared to the stride length or the number of elevated legs (phase difference). This suggests that the duty cycle is the primary factor in changing forward thrust. Regarding the wave characteristics, it appears to be desirable to keep the wavelength as short as possible to avoid instability, with 'legs elevated profile' also as small as possible to maintain upright support across body segments.

Up to this point we have addressed how the behavioral gait variables are determined, by comparing the model with the experimental observations, however the model has so far only used the morphological parameters of the observed species. With the model we can now perform a parametric study, where the most intriguing question is why do the millipedes have so many legs? And why do they differ between species?

To answer this question, a parameter sweep from 5 body segments to 90 body segments was performed, against sweeps of the gait variables (duty cycle, stride length, and legs elevated) to see if their influence on the resulting output thrust force was sensitive to the change in the morphological parameter of number of body segments. The surface plots on Figure 2.19 show the results of the sweep using the average segment size of the *N. americanus.* Similar sweeps were also done with the average segment parameters of the *A. virginiensis* (Figure 2.20), as well as arbitrary segments sizes by dividing across a fixed body length. Each of these revealed similar trends.

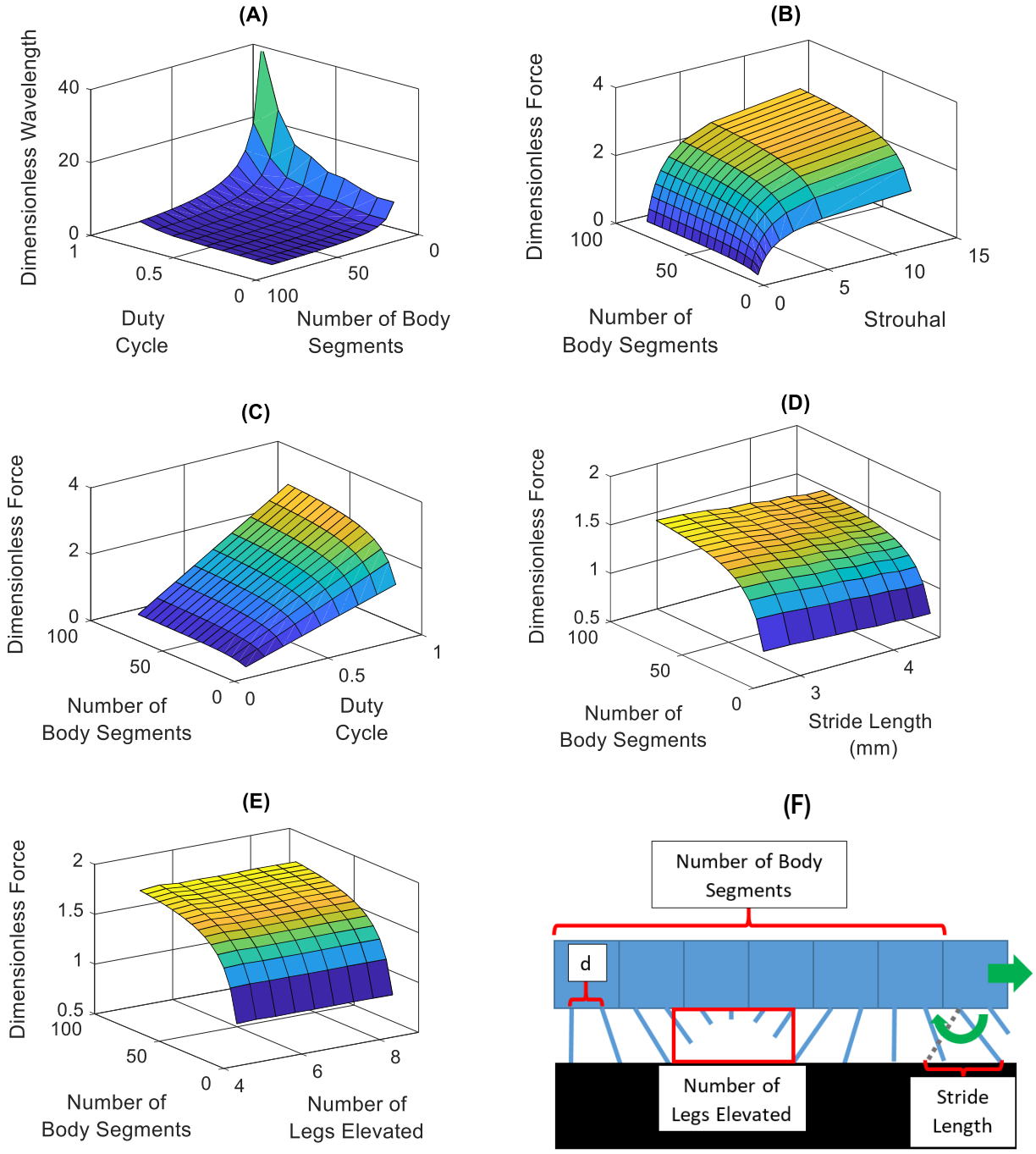

Figure 2.19: *N. americanus* segment parameters (A) Dimensionless wavelength vs duty cycle vs number of segments (B) Dimensionless force vs strouhal vs number of segments (C) Dimensionless force vs duty cycle vs number of segments (fixed number of legs elevated and stride length) (D) Dimensionless force vs stride length vs number of segments (fixed duty cycle and number of legs elevated) (E) Dimensionless force vs number of legs elevated vs number of segments (fixed duty cycle and stride length) (F) Schematic of parameters being analyzed

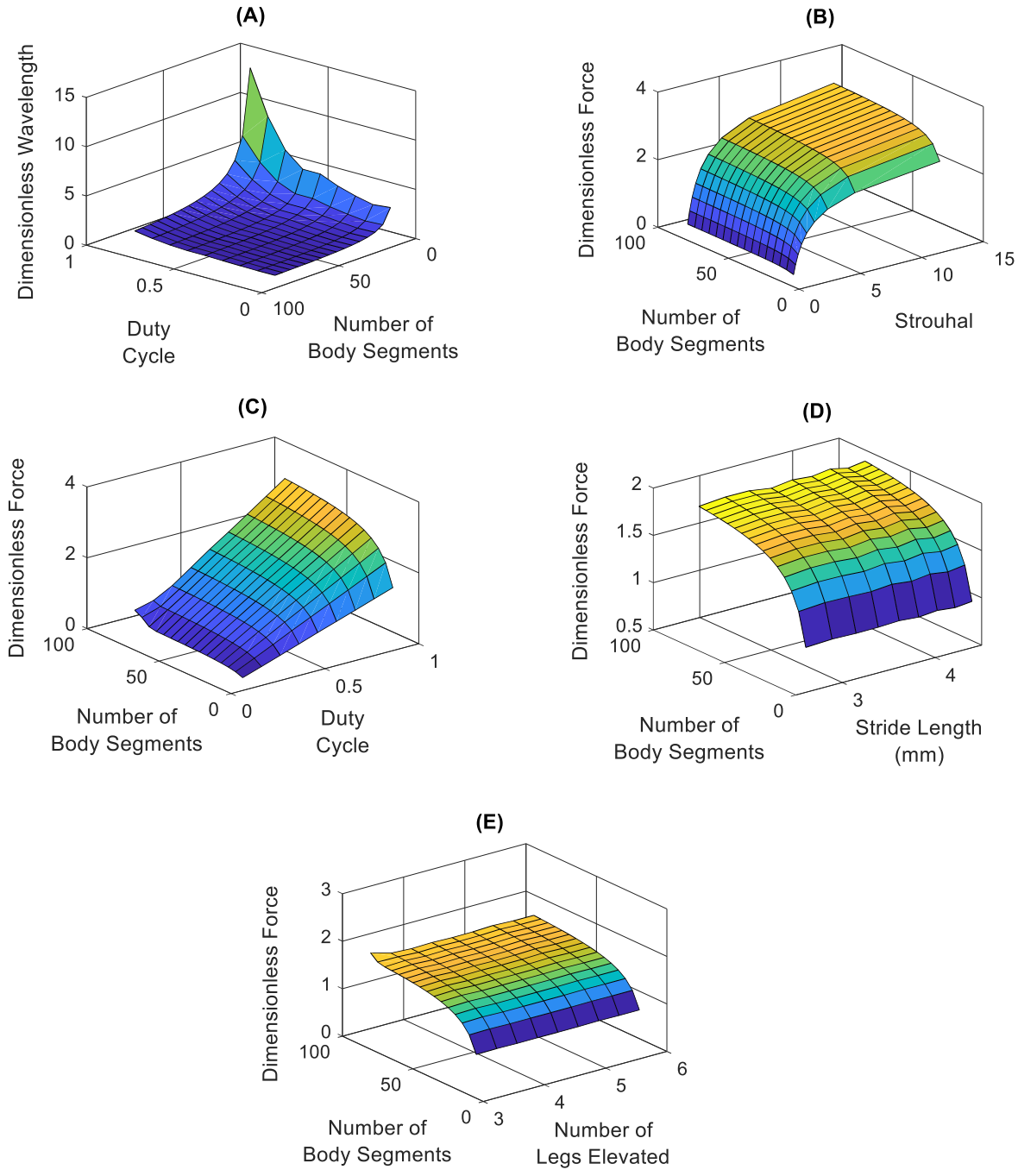

Figure 2.20: *A. virginiensis* segment parameters (A) Dimensionless wavelength vs duty cycle vs number of segments (B) Dimensionless force vs strouhal vs number of segments (C) Dimensionless force vs duty cycle vs number of segments (fixed number of legs elevated and stride length) (D) Dimensionless force vs stride length vs number of segments (fixed duty cycle and number of legs elevated) (E) Dimensionless force vs number of legs elevated vs number of segments (fixed duty cycle and stride length)

2.6 Discussion

Looking at Figure 2.19A and B we see the relationships of the wave characteristics of wavelength and strouhal number with changes in number of body segments/legs. While the strouhal is not influenced by the number of body segments (as expected), the dimensionless wavelength certainly is. By changing the number of body segments, this directly changes the body length, and thus the dimensionless wavelength (equation 2.20). Figure 2.19A indicates that reducing the number of body segments results in exponentially increasing the dimensionless wavelength outside of the desired region of operation, which could lead to stability issues. This may suggest the morphology of body length dictates the behavioral gait limits. While these wave modulations are interesting, understanding the behavioral gait variables that dictate the traveling wave modulations are also

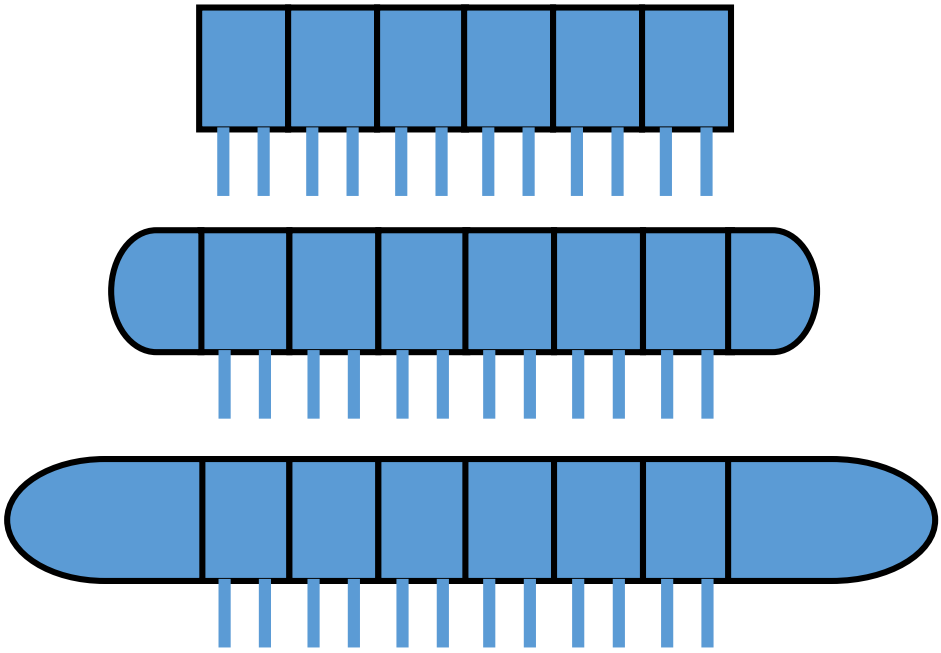

Figure 2.21: Variation portion of body without legs (A) Body only possesses body segments with leg pairs (B) *A. virginiensis* model consists of a body with an anterior and posterior end weights without legs the same size as the average body segment (C) *N.americanus* model consists of a body with an anterior and posterior end weights without legs almost triple the size of the average body segment

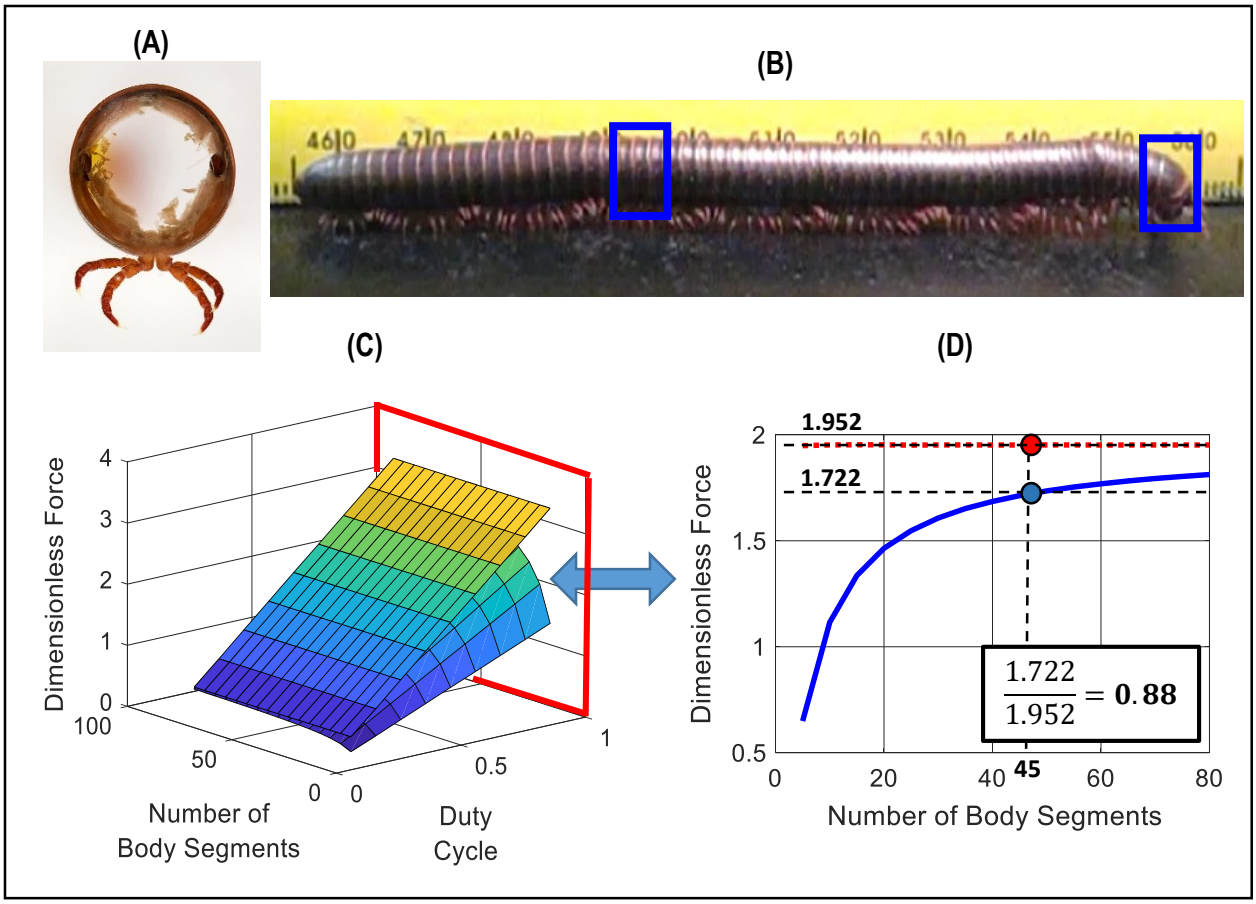

Figure 2.22: *N. americanus* (A) Single body segment (B) Full body length (C) Surface plot of dimensionless force vs number of segments vs duty cycle (D) Plot of dimensionless force vs number of segments at a duty cycle of 0.5

key in understanding the millipede locomotion dynamics. In Figure 2.19C we can see an increasing total output thrust force with increased number of body segments, however with eventually diminishing returns regardless of the duty cycle. Similarly, for plots Figure 2.19D and E, we can see the asymptotic behavior with increased number of body segments with stride length and legs elevated per wave (phase difference). Furthermore, these plots confirm the limited influence stride length and phase difference have on the total output thrust force compared to the duty cycle.

From the developed model and parameter analysis, it appears that the primary factors that govern the thrust force capabilities of millipedes is number of body segments (morphology) and the duty

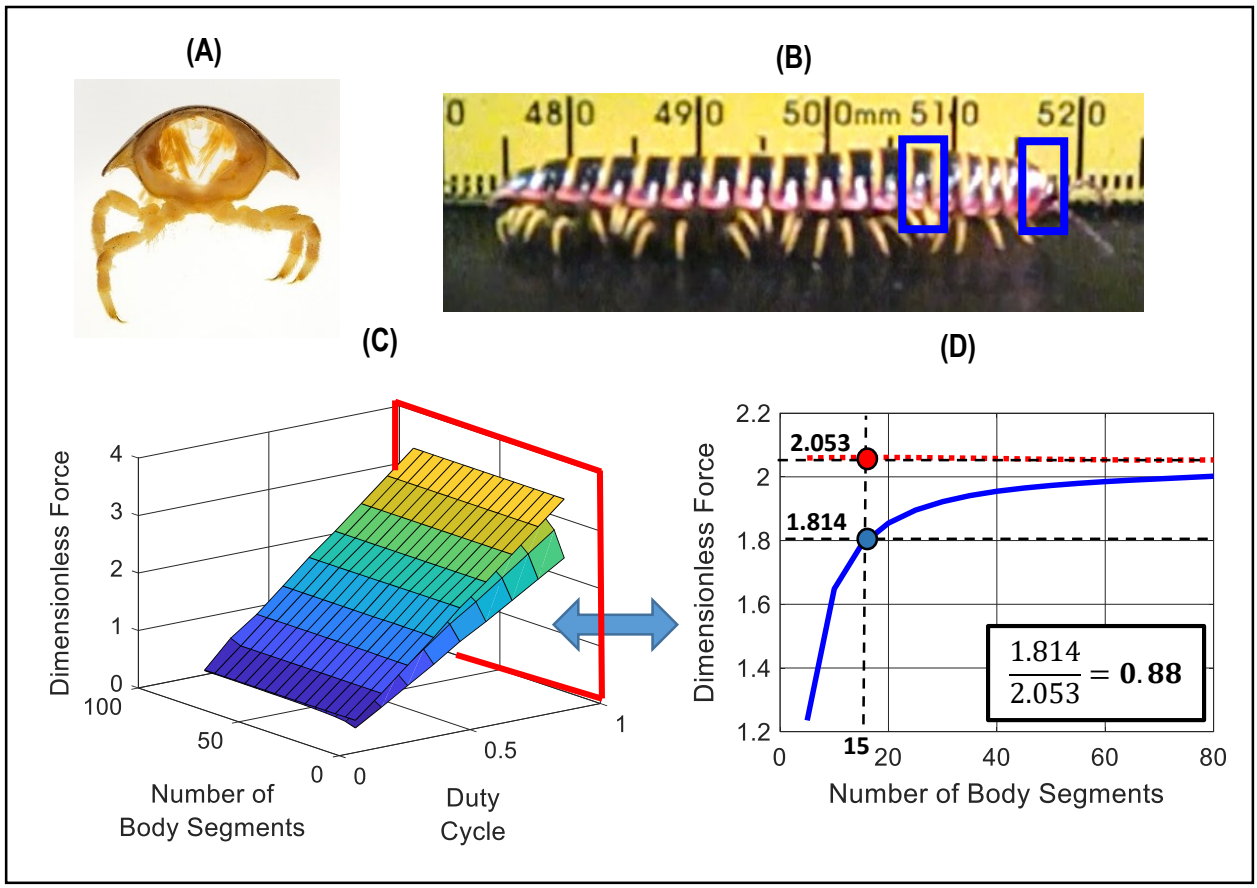

Figure 2.23: *A. virginiensis* (A) Single body segment (B) Full body length (C) Surface plot of dimensionless force vs number of segments vs duty cycle (D) Plot of dimensionless force vs number of segments at a duty cycle of 0.5

cycle (behavior). While the specimen can dictate their duty cycle (and thus wavelength), the question regarding their morphology of number of body segments has yet to be determined. From Figure 2.22C we can see the asymptotic behavior of the diminishing returns of thrust force per added body segment. Given that the weight of each segment stays constant and the thrust force efforts of each leg is also constant, it is surprising that the relationship between thrust output and the number of body segments is not linear. What causes this asymptotic relationship is the weight of the anterior and posterior ends of the body that do not possess legs to assist with thrust performance. Disregarding the weight of the head and posterior results in a linear relationship between number of segments and thrust output (constant with dimensionless force) which the

actual performance asymptotically approach as shown in Figure 2.22C and Figure 2.23C (*N. americanus* and *A. virginiensis*, respectively). The magnitude of the extra weight governs the rate of the increase in thrust force provided per added body segment. It is worth noting that for the *N. americanus* the anterior and posterior ends of the body are relatively large compared to a single body segment Figure 2.22B, equivalent to approximately 3 body segments each. Comparing this morphology with the *A. virginiensis*, where the anterior and posterior ends are about equivalent to the size of a single segment (Figure 2.23B).

To investigate the questions relating to the millipedes' number of legs/segments and variation species, we looked at the of the return (thrust force per added segment) of each species. At first the rate of change of dimensionless force with the number of body segments was determined (at the points that corresponding with each species on their respective plots), however these values did not match or reveal any pattern. While the rate of change was not indicative of the species body segment morphology, that ratio of the dimensionless force value with the asymptotic value appears to reveal a desired minimum number of body segments. For both species, the number of active (with legs) body segments stop at approximately 0.88 ($\approx 90\%$) of the asymptotic value. What dictates this cap of about 90% may not be explicitly known, but while certainly being longer provides more forward thrust capabilities, the overall system experiences significant diminishing returns for the added segments, particularly beyond the 90% threshold. Furthermore, the price of growing too large may not be biologically advantageous in terms of surviving and escaping predators.

From this analysis, it has been revealed how the morphological parameter of the number of body segments influences thrust force capabilities, as well as its effect on the metachronal gaits wavelength, which if too large would lead issues of stability (Figure 2.15B). However, it has yet

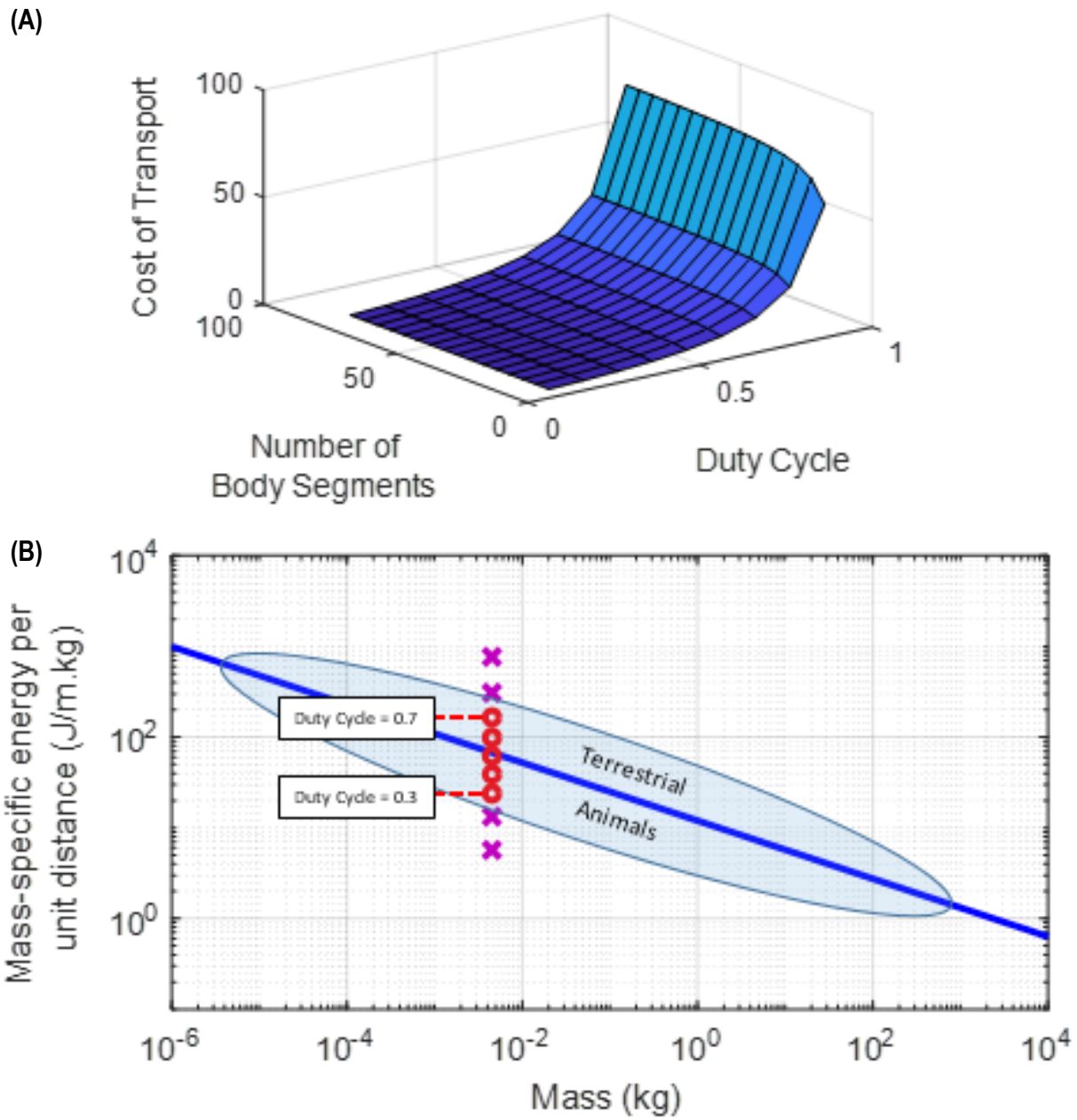

Figure 2.24: (A) Cost of transport (COT) vs Duty cycle vs Number of body segments (B) COT vs Animal mass

to determined why the millipedes' behavioral variable, duty cycle, that influences the thrust force operates in the space of 0.3 and 0.7. Regarding the thrust force capabilities, the larger the duty cycle is preferred. While utilizing a duty cycle greater than 0.7 would also increase the dimensionless wavelength exponentially leading to stability issues (Figure 2.15B), another

resulting factor would be the decrease in body velocity. Given the limits of the stride length and the set temporal phase (dictated by the number of legs elevated per wave), the cost of a high force duty cycle is the decrease velocity of the leg during the stance phase propelling the body forward. This can be demonstrated by determining the cost of transport (COT), determined in equation 2.26:

$$COT = \frac{P_{input}}{WV_{body}} \tag{2.26}$$

Where P_{input} is the input power provided by the millipede, W is the weight, and V_{body} is the resulting velocity of the millipedes' body. As seen in equation 2.26, the COT increases with decrease velocity, which is a result increasing thrust force by duty cycle. A sweep was performed using the *N. americanus* segment parameters to explicitly determine the relationship of duty cycle with COT (a sweep against number of body segments was also performed to see if it had any effects). The P_{input} was determined by back calculating the COT value of a myriapod, of same mass as the *N. americanus*, found in [59]. Figure 2.24B shows that this behavior of walking with the duty cycle between 0.3 and 0.7, operates in the region COT consistent with other terrestrial animals. Walking below a duty cycle of 0.3 would likely require larger thrust forces than desired by an individual leg to propel the body forward. Lastly, growing larger and increasing the body mass, does not significantly influence the cost of transport but would make the millipede deviate from the mass-specific energy per unit distance found commonly in terrestrial animals.

The locomotion mechanisms used by millipedes, as a result of their gait and morphology, has been studied and modeled with regards their initial responses to increased axial loading. However, when they have reached the limit of utilizing a duty cycle (with individual legs working at the desired effort) which results in too large a COT, the other gait variables are adjusted. The remaining gait variables include the stride length, phase difference (legs elevated), and leg effort. While the stride

length and phase difference vary slightly, they both do not have a significant effect on the forward thrust force while operating within realistic space of the millipede morphology. Stride length would be limited by leg length, and phase difference is limited by the vertical support of the body and potential collision between legs. One adjustment occasionally observed at the higher resistive loads was the abandoning of relationship determined in equation 2.25. Reducing the numerator, increasing the number of legs in contact with the ground while decreasing the number of legs elevated over the same wavelength, which essentially results in increasing duty cycle. Even with such adjustments, the overall effect on thrust force is limited. The most effective means to increase the thrust force of the millipedes' body, after maximizing duty cycle, is the change in leg effort. The effect of increasing the leg effort is trivial, as the thrust force of the body summation of legs performing the propulsive stroke.

From experimental observation, it appears that the action implemented by millipedes to increase thrust force occurs in three stages: 1) Increase duty cycle using desired/optimal leg effort and phase difference, 2) when at maximum threshold of COT, adjust 'elevated legs profile' (relating to stride length and phase difference) to effectively increase legs in propulsion stance per wave, 3) increase individual leg effort. To examine this hypothesis (Figure 2.25C), a *N. americanus* performance in the horizontal burrowing stage (Figure 2.9A of dimensionless force 3.25) was simulated in the model. First the number of elevated legs per wave was observed from the video footage to determine the phase difference. Then the duty cycle was adjusted to match the wavelength observed. Kinematically, these variables were able to match the millipede, but the resulting overall thrust force of the millipede when implementing the same leg effort previously fell short of the desired 3.25 dimensionless force observed. To tune the model to fit the observed performance, the individual leg effort needed to be increased by approximately 20%. However, while this appears

to be the general approach, the observed behavior of the actual millipedes beyond the initial changes in duty cycle are too sporadic to draw any evident conclusions.

From this work we have developed a simulation model that captures the fundamental mechanics of millipede locomotion to handle increasing axial loads. Furthermore, with such a model we can begin to understand why millipedes have evolved to possess such morphology and gait behavior to effectively burrow, which could help with the design of locomotion techniques for miniature devices.

2.7 Conclusion

The objective of understanding the fundamental mechanisms in millipede locomotion is to potentially reveal an untapped design space with regards to miniature locomotion techniques when encountering large resistive forces. From the experiments we see their capabilities, both on the inclines and burrowing stage, that with handling resistive loads the same technique is applied. This work has investigated the locomotion techniques utilized by millipedes to effectively traverse in environments that provide resistive forces such as climbing and burrowing. For the two species observed (*Narceus americanus* and *Apheloria virginiensis*) it was found that in combination to their flexible segmented body permitting complex motion in three dimensions (via lateral, dorsoventral, and rotational degrees of freedom) a traveling wave form of locomotion is utilized as a result of a metachronal gait. The traveling wave was observed to modulate its wavelength and velocity in relation to changes in load resistance in the axial (horizontal) direction of motion as well as radially (vertical specifically). From these observations, a dynamic model was built, which allowed us to investigate their gait variations. The simulations demonstrated that there was a desired operating region of the traveling wave modulations. With adjustments to in a millipedes' duty cycle, regardless of its morphology of body length, number of legs, etc., the traveling wave

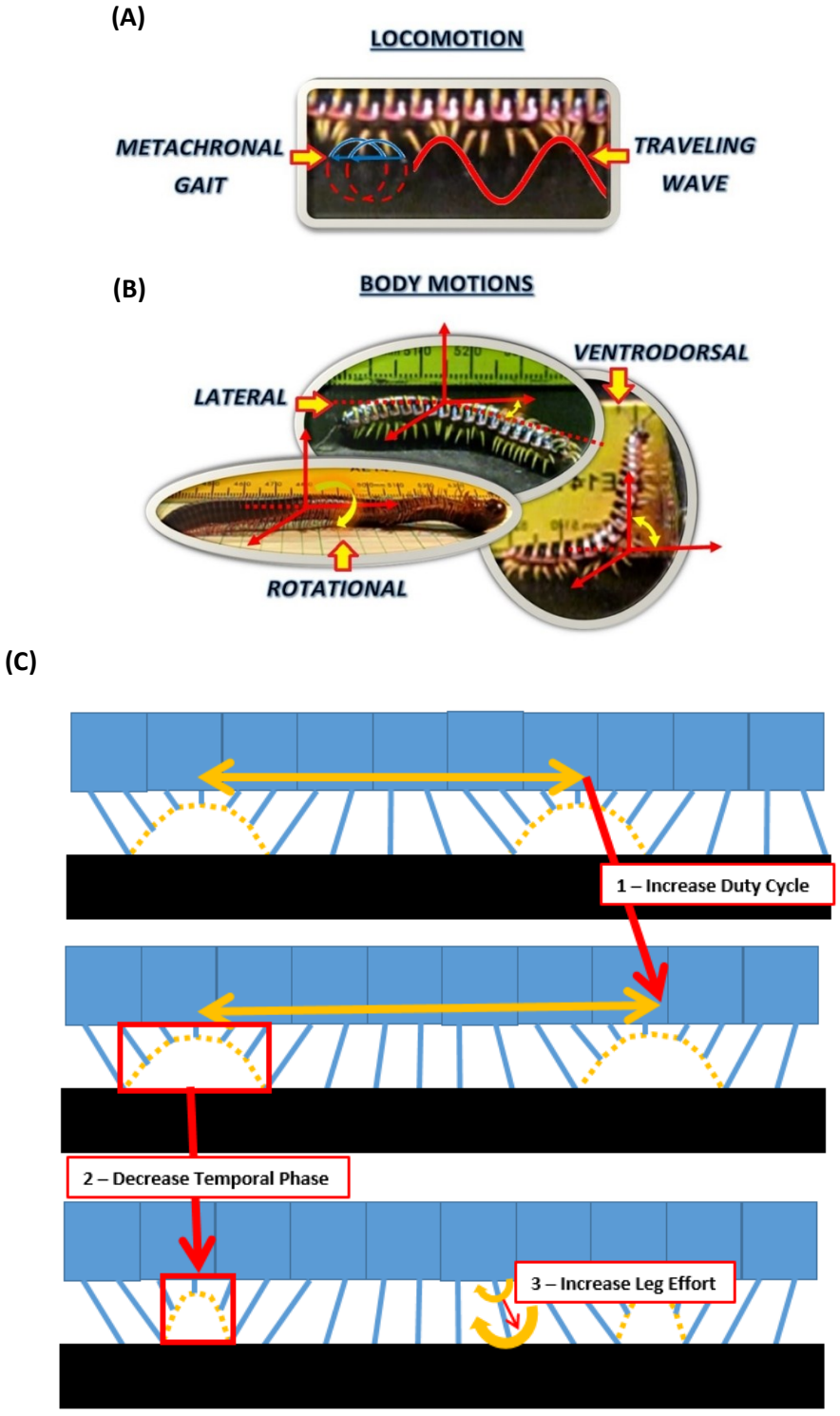

Figure 2.25: (A) A depiction of the created traveling wave from the metachronal gait of a millipede. (B) An illustration of the diversity of motions (lateral, dorsoventral, and rotational) from a millipedes' flexible segmented body utilizing ball and socket like joints. (C) Hypothetical millipede approach to increase forward thrust force

characteristics would start to increase exponentially which would be detrimental to their locomotion capabilities. For instance, with wavelengths that quickly increase to longer than its body length, the millipede will quickly encounter stability issues to remain upright. From the developed model it was also determined why millipedes of different species grow to different lengths, growing up to about 90% of the asymptotic value (ideal case of every segment contributing to body propulsion) of dimensionless force which is representative of return of thrust force per added body segment.

Future work would delve into a better understanding on the radial loading, and while we have explored the wave modulations millipedes initially exhibit to handle increased loads, the changes in gait for extreme loads (loads exceeding the desired leg effort and behavior) would also be of interest. Furthermore, while we have investigated the species *N. americanus* and *A. virginiensis*, which are millipedes that possess the general structure of a rigid body segments, there are a few species that possess body segments that exhibit varying degrees of freedom [23]. Such degrees of freedom come from the free movement of sternites that are able to move forward and backward assisting in burrowing activity of the legs. These body segments also permit flexibility radially such that the legs can be retracted into the body. While these species are generally smaller, they appear to be the most effective in large depth burrowing, and are less surface active. Such movements of flexibility may actually be the evolution permitting really deep burrowing utilizing similar leg-less peristaltic techniques used by worms. Such degrees of freedom could also be worth observing and modeling in the future as well.

Chapter 3 – Design, Manufacture, and Control of Bio-mimicking Millipede Robot

3.1 Introduction

As previously discussed, our interest is to develop a remotely operated vehicle (ROV) capable of traversing within the viscous and cluttered environments, allowing continuous and active monitoring of the cow rumen in order to improve our understanding of its biology and potentially develop engineering solutions for precision animal agriculture.

In the last chapter the bio-mechanics of millipede locomotion, with particular interest in their capabilities of using a powerful gait to handle large resistive loads, was investigated to utilize in the development of such a device. Chapter 2 provided qualitative observation, experimental measurements, and developed a simulation model of the millipede metachronal gait generating a traveling wave. It was found that the traveling waves modulations that occurred with increasing forward thrust were increased wavelength and strouhal number. The effective traveling wave, which is a result of the metachronal gait of many legs, was observed to be modulated primarily by the adjusting the duty cycle.

In this chapter a millipede bio-mimicking robotic platform is developed in order to see if we can replicate biological locomotion for controlling thrust force capability. Furthermore, such a robot would permit us to eventually test the other variety of gait parameters that cannot be directly governed on the actual biological specimens, which will allow us to better understand why millipedes adjust their gait in the fashion they choose to, that result in the effective wave

modulation compared to using another approach. While a dynamic simulation model can begin to reveal such trends, an actual robot platform will not only further verify the model, but indicate whether we can successfully emulate the effective traveling wave used by millipedes for burrowing.

Though there already exists a few millipede-inspired robots [11], [27], and an even more extensive existing body of insect/arachnid/myriapod-inspired robots ([1]–[6], [8]–[11], [18], [19], [21], [28], [60]–[62]) we need to develop a robot that will allow us to specifically test and capture the gait dynamic adjustments made that modulate the traveling wave to increase the thrust force against large loads.

3.2 Bio-mimicking Characteristics

In bio-mimicking design, while ideally one wants to capture every characteristic observed in order to best emulate the living organism, it is important to identify and highlight the key distinguishing features of interest, in order to best demonstrate the desired performance. For the purposes of this robot, while it would be desirable to be able to build a device that matches a real millipede's complex musculature and level of control of a central nervous system to articulate body and leg movements, there are limitations with existing controls, mechanisms, and actuator technology. Therefore, with the primary objective of this dissertation being to develop a ROV capable of traversing through the difficult rumen environment, in a bio-mimicking sense, the powerful locomotive gait of the millipede is of greatest interest. Based on the millipede locomotion observation, experiments, and modeling in the previous chapter, we can break down the main biological elements to prioritize when designing this millipede robotic platform.

3.2.1 Leg mechanics

With our focus being on the millipede's powerful locomotion gait, it is natural that trying to emulate the mechanics of the legs motions is a primary characteristic. As mentioned in the previous chapter, there are clearly two distinctive phases of the leg motion when walking, being the instance propulsive backward stroke or the elevated stepping forward stroke. When the leg is in contact with the ground, it is assumed to remain in contact with the ground at all times, performing a perfectly straight line motion (assumed to be on a flat terrain) while propelling the body forward. In a simulation mathematical model this is very easy to accomplish, translating this desired motion to an effective robot becomes challenging.

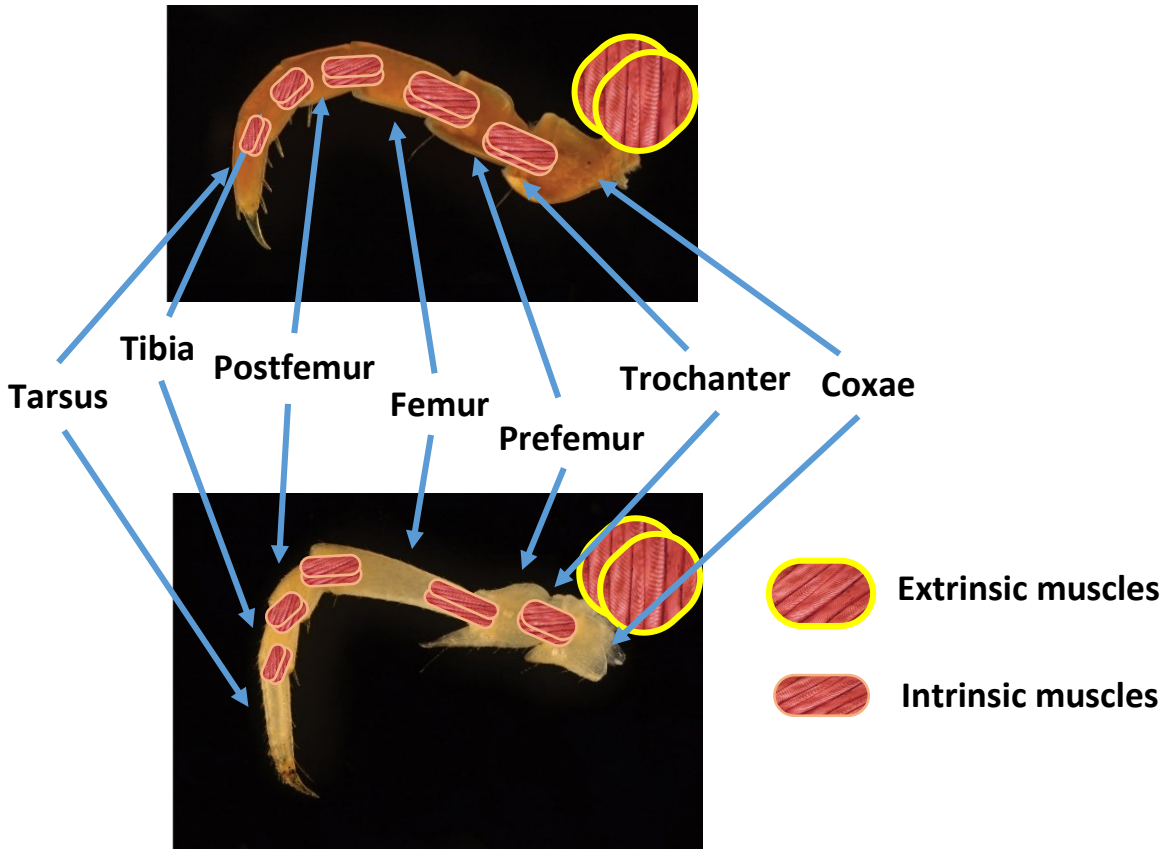

Figure 3.1: High resolution photographs of millipede species legs with labelled segments with generic schematic of extrinsic and intrinsic muscles. (Top) *N. americanus* Leg. (Bottom) *A. virginiensis* Leg

Furthermore, while in the previous chapter we reduced the number of degrees of freedom of a single leg to three main governing motions (Figure 2.13), in actuality a single millipede leg is articulated by several extrinsic and intrinsic muscles. Larger extrinsic muscles at the hip provide (two for *N. americanus* and four for *A. virginiensis*) motions making the legs drive the body forward on the horizontal plane, while many finer intrinsic muscles along the legs distal segments actuate motion in the vertical direction [23]. A schematic summarizing a generalized musculature of an individual leg is seen in Figure 3.1. From the observations and modeling performed in chapter 2, the legs muscles perform in a fashion that eliminates the notion of a simple pendulum motion, but instead create ground reaction forces that are minimized at initial leg contact, and relatively larger just prior to take off.

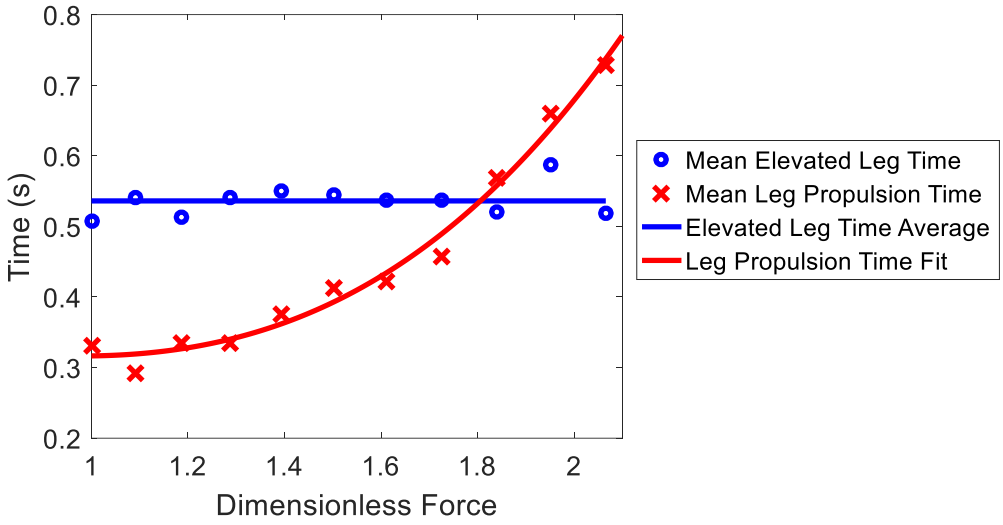

Figure 3.2: Plot of elevated time (Tt) and propulsion time (Tp) of an individual leg against dimensionless force

Drawing from these findings, in designing a mechanism for a millipede-mimicking robot, capturing the two degrees of freedom (vertical and horizontal) are essential in order to capture the elevation and propulsion stages of the walking gait. Furthermore, with the interest of replicating

the biological behavior observed in chapter 2, an explicit means to govern the duty cycle is necessary for modulating the effective traveling wave locomotion for improved forward thrust.

The control of the individual leg motions needs to be able to capture the variation in duty cycle previously mentioned. In addition to being able to mechanically accomplish the two stages of elevated forward stroke and propulsive backward stroke, to effectively capture the millipede traveling wave gait modulations, the time periods of both phase actuations need to be explicitly controlled. While Figure 2.16C indicates the relationship of the duty cycle with increase thrust force, Figure 3.2 shows the actual time periods of each phase of the strides, which indicates how exactly the millipedes are adjusting their duty cycle. It is interesting to see that there change in time duration occurs during the propulsion stage when the leg is in contact with the ground, while the duration of the transfer/elevation period remains relatively constant. This observed trend in duty cycle, reinforces our knowledge that the individual legs perform at a constant effort regardless of total thrust output, because the phase of the stride cycle that remains constant is when there is no effective resistive load. Operating the legs in such a fashion minimizes the work effort and simplifies the control schemes of the biological creature because if the time duration was kept constant during the propulsive stance, the individual leg would need to move faster, exerting more effort in the elevated phase when it is not providing thrust. Being able to replicate this is important as it correlates with the aggregate traveling wave behavior.

Lastly, it is worth noting scale of leg motion relative to the body and the dependency of the locomotion on stride length versus the frequency. In designing the robot, while there will be restrictions with regards to actuator size and performance in addition on board space for microcontrollers/drivers and power supplies, it would be desirable to keep these scales comparable in order to not deviate too far from the biological specimen's system dynamics.

3.2.2 Decentralized gait control

The second biological feature that is integral to its powerful gait performance is the metachronal gait locomotion control. In millipedes, it's intriguing how such fine control is achieved, as it requires command for coordinating, from the least, 22 legs, up to about 750 legs, depending on the species. As mentioned previously, it is understood that millipedes have central nervous system, that consists of a ventral nerve cord stemming down the body from the brain. Along the ventral cord ganglia (nerve clusters) are present at each pair of legs, resulting in two ganglia per body segment [25]. Such morphology indicates a decentralized level of control, where the ganglia act as neural networks interpreting the CNS signal and converts it into the specific movements of the local leg pair. Furthermore, in a recent study [27] Kano et al. suggest that coordinating the periodic behavior of so many legs requires decentralized control to the extent where legs are dependent on the ground reaction force feedback from the anterior leg pair. From the sensory feedback, the control implemented along the different segments of the body relating to its locomotion would be the phasing between the leg pairs. The biological specimen likely achieves control of the metachronal gait with the complexity of a CNS applying constant leg thrust performance acting on the changing environment, utilizing sensory feedback. While feedback control would be desirable, the primary objective within the control scheme is to generate the desired thrust force from a specified metachronal gait.

3.2.3 Body mechanics and control

A tertiary biological feature of interest to emulate on the robot is a millipede's flexible body, a result of the relative motion between the segments of the body. As seen in chapter 2, millipedes have the ability to shape their body by lateral, dorsoventral, and even rotational movements [23], [53] of their body segments. While this permits the ability to traverse on complex terrain and is

worthy of investigation, such features come second to implementing the capabilities of its powerful locomotion techniques. Actual millipedes, possess a very complex musculature within their body that permits them to articulate these motions of the “ball and socket” like joints between segments. While applying a mechanism that allows the three degree of freedom motions, determining the actuators and controls to the design would be dependent on space, control and power availability.

3.3 Robot Design and Manufacture

In this section, the design of a millipede robot that highlights the biological characteristics just mentioned is discussed. While limitations will always exist, particularly in attempts to emulate the capabilities of muscles with actuators, and the intellect of a complete central nervous system with simplistic control schemes, we can only try capture the aggregate motion and dynamics of interest of millipede effective powerful traveling wave gait. A comparative assessment with related existing robots, mechanisms, and control technology is done within the discussion of the design approach, indicating why such directions were taken.

3.3.1 Initial design concepts

One of the initial inspirations of developing a ROV utilizing millipede locomotion in this Bioinspired Materials and Design Laboratory, was the work initiated by Dragan Avirovik [10], [11]. These works were proposed locomotion designs for a wireless capsule endoscope (WCE). Avirovik developed two similar piezoelectric ceramic driven motors, using geometries resembling an “L” and “U” as leg actuators. These motors were implemented on small platforms, and tried to emulate insect and millipede gait patterns on these devices. However, with only using four legs, the applied gait in [11] is limited in how much of the traveling wave characteristic it can capture.

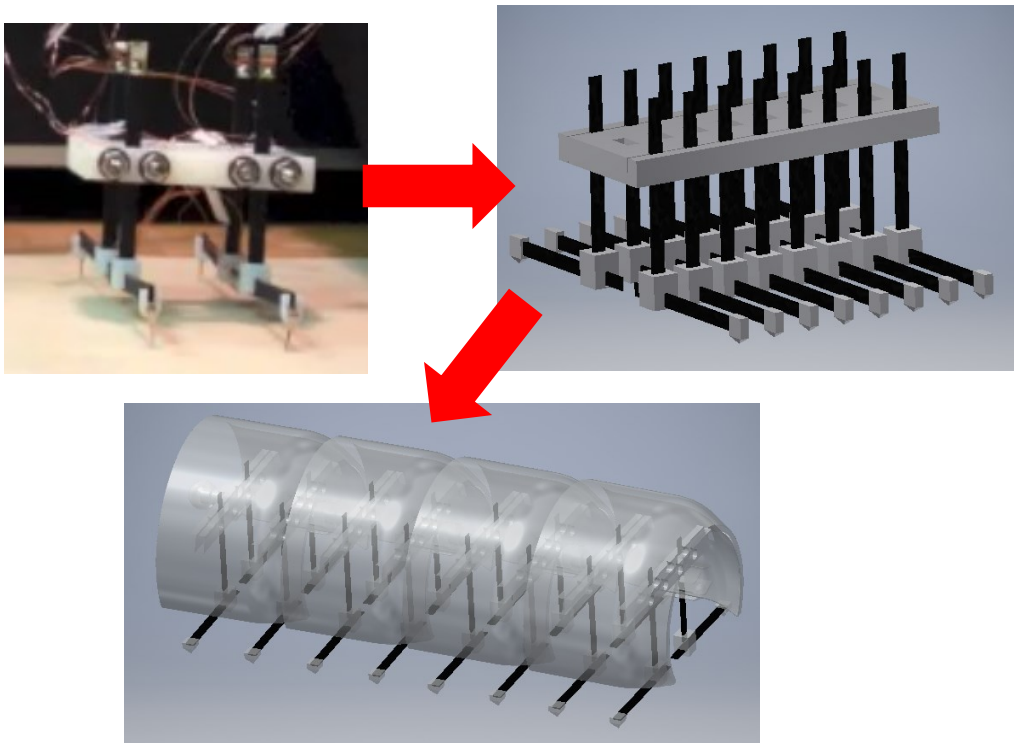

Figure 3.3: Initial conceptual design of millipede bio-mimicking robot – an extension of existing robot developed by Avirovik [9]

The initial idea for developing a millipede robot was to essential create an extension of Avirovik's L-shaped robot as seen in Figure 3.4.

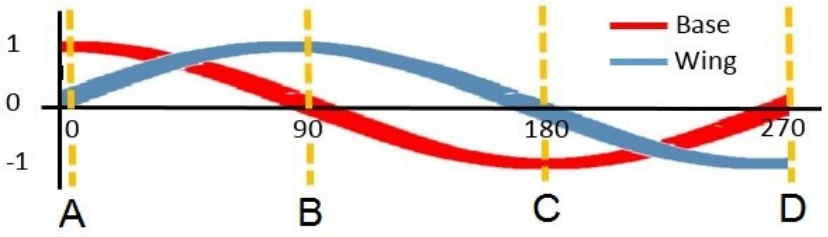

	0	90	180	270
Base Signal	1	0	-1	0
Wing Signal	0	1	0	-1

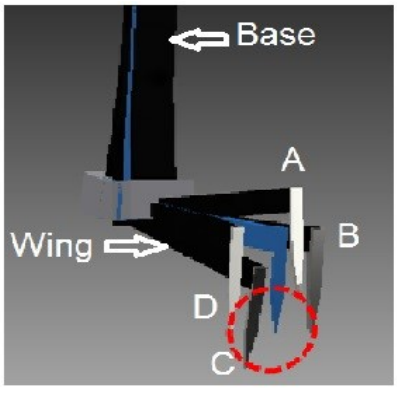

Figure 3.4: Control scheme for L-shaped piezoelectric motor leg

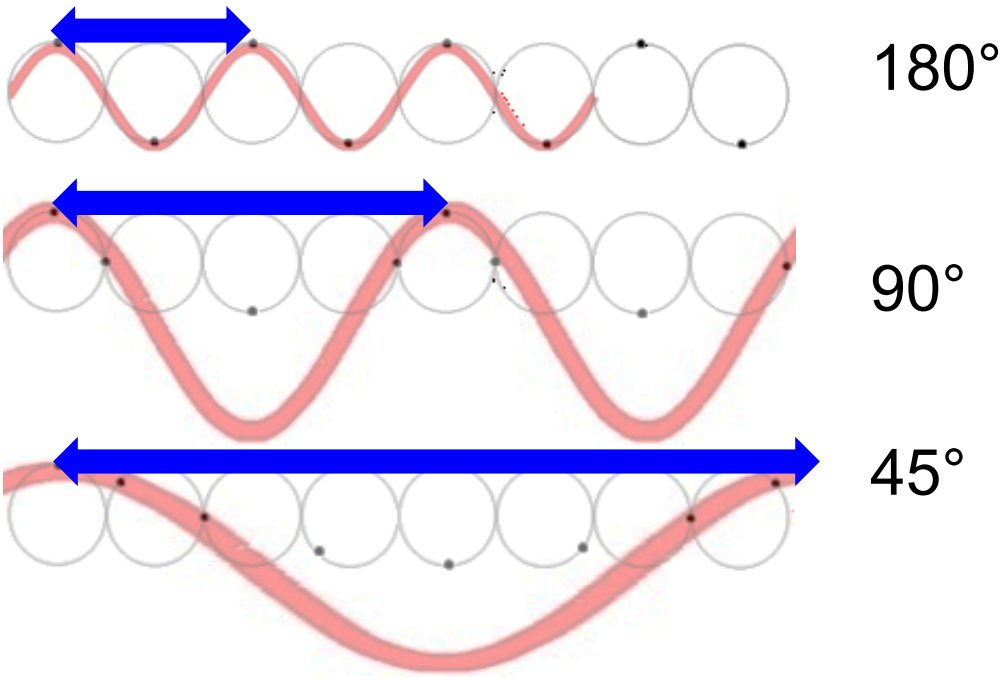

Figure 3.5: Variation of metachronal gaits achievable with two wave signal inputs to L-shaped actuator

The L-shaped motor [10] is driven by two sine wave signals that are 90° out of phase with each other actuating the two piezoelectric cermaics, resulting with the tip tracing a circular motion (Figure 3.4). Avirovik took inspiration of such trajectory from the work of Sathirapongsasuti [52]. Using this control scheme of two wave input signals, a few traveling waves can be generated with legs operating at 45°, 90°, and 180° out of phase with the adjacent pairs (Figure 3.5). However, limiting factors arise under closer inspection of the resulting metachronal gait. In comparison with the biological observations made, the mechanics of this leg design does not capture the motion needed to adequately capture the actual millipede wave modulation behavior. Without an explicitly defined duty cycle to adjust, limited wave modulation options with regards to actuator control requiring large amplifiers, as well as the limited strain of the piezo L-shaped motors making its locomotion performance frequency dependent, resulted in pursuit of another design approach.

3.3.2 Limitations of existing robot designs

Leg motion mechanisms

Prior to developing a mechanism for the legs of the millipede robot, we looked at existing design approaches used in other legged crawling robots. The legs designs in the existing robots aforementioned in chapter 1, regardless of the number of legs on the platform, generally fell short of meeting the required features of the bio-mimicking leg mechanics desired. While they all capture the two degrees of freedom of horizontal and vertical motion, most of them took the same approach as Avirovik [10], [11], of applying an input of a circular trajectory for the end of the leg with a constant angular velocity. For robots that used rigid bodied legs, typically those that used an electromagnetic motor like [6], [8], [19], results in a very low duty cycle. Taking such an approach for designing a millipede robot to emulate the wave modulations observations in chapter 2 for high thrust output would not be effective. This approach of rigid bodied legs performing circular trajectories geometrically reduce and minimize the number of legs in contact with the ground, unable to capture the "constancy in forward strokes" or increasing the number of contact points with increased wavelength. An illustration of the limitations of using a circular trajectory with a rigid bodied actuator-mechanism can be seen in Figure 3.6.

As for robot designs that used a circular input trajectory, but with some compliance by using smart materials such as piezoelectrics [5], [7], [10], [11], [20], [21] or shape memory alloys [9] or mechanically with springs [27], [28], this would begin to introduce a straight line motion during the propulsion stage of the walking motion (Figure 2.2). However, even with the compliant legs, the resulting duty cycle passively occurs and is dependent on the stiffness of actuator-mechanism. Furthermore, if the stiffness of the compliance mechanism is left constant with changes in duty cycle, the vertical load distribution over the legs in contact with ground introduce significant

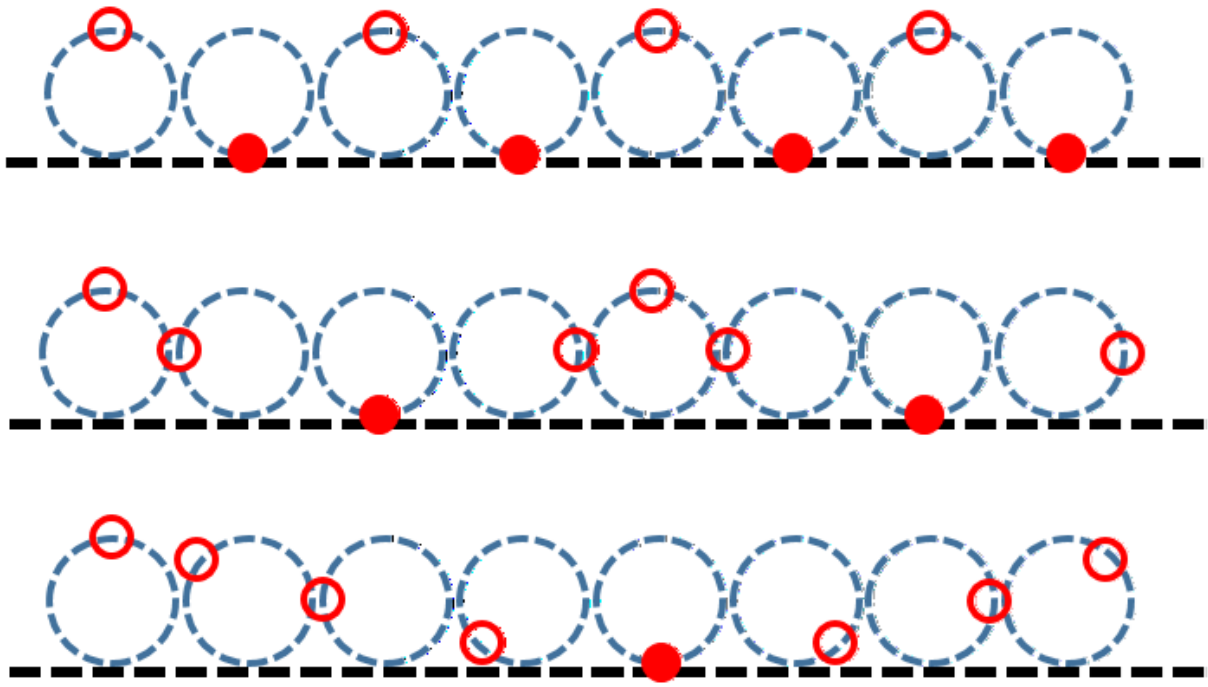

Figure 3.6: Limitation of circular path trajectory of rigid body leg. Increasing the wavelength actually reduces the number of leg in contact with ground, contrary to observations of actual millipedes

variation in individual leg mechanics (i.e. for a low duty cycle with fewer legs in contact with ground per wavelength, the legs will experience large deflections from the compliant behavior, while for a high duty cycle with more legs in contact with the ground per wavelength would experience smaller deflections). In an actual millipede the constant propulsion effort of individual legs is controlled constantly, which relates to a millipedes finer control of the vertical motion leg muscles keeping the millipede at a desired elevation. The passive occurrence does not allow one to adjust the duty cycle accordingly, which may be somewhat representative of the actual occurrence in millipedes, sacrifices the consistency and control of the individual leg efforts.

Furthermore, from the biological observations in chapter 2, the stride length performed by an individual millipede leg is a few millimeters, which is a significant amount of motion in relation to the dimension of the leg itself, and do so at a frequency around 1Hz. While piezoelectric

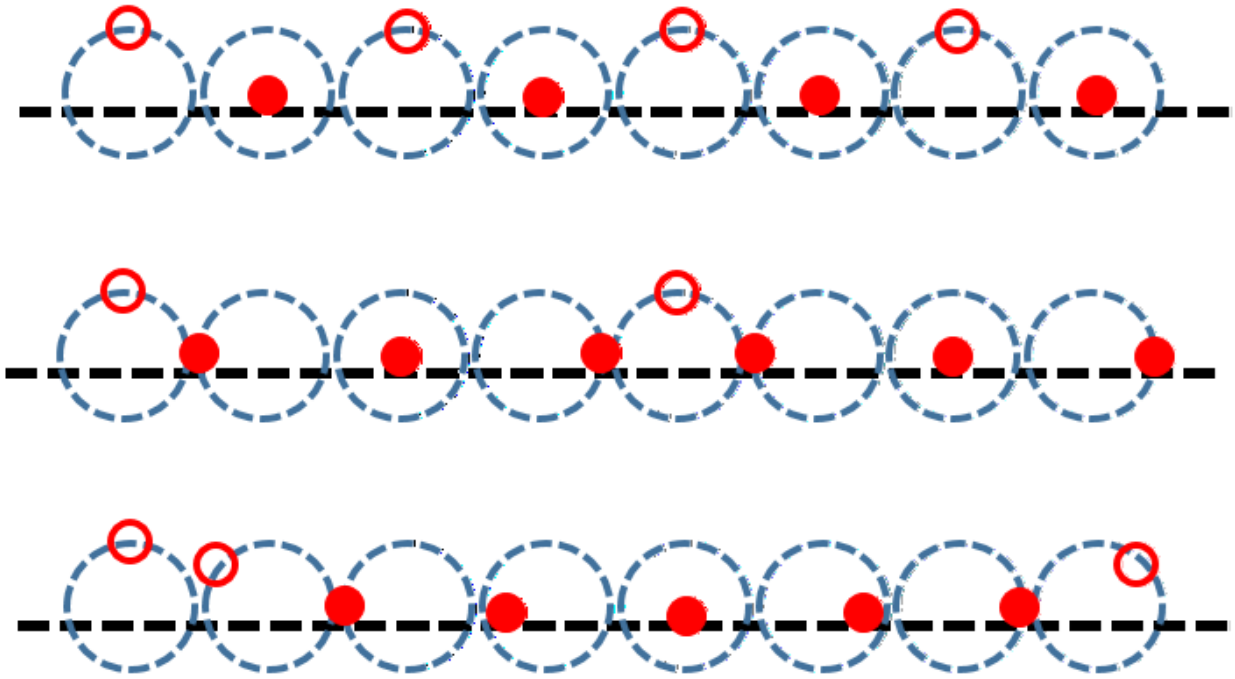

Figure 3.7: Limitation of circular path trajectory of compliant leg. While there is improvement compared to a rigid body with more legs in contact with ground, consisting with millipede observation, there is no explicit control of the duty cycle (which also influences the "constancy if forward strokes"

ceramics are effective for miniature scale robotics, the limited strain and dependency of operating would be difficult to use effectively in mimicking the millipede leg mechanics. Therefore, for the bio-mimicking design it is likely electromagnetic motors would be used.

Leg motion and co-ordination control

Stemming from the limitations of the leg mechanisms of existing robots, the lack of mechanically defined stages of elevation and propulsion, makes it impossible to manipulate the duty cycle in a controlled fashion that will allow us to explicitly investigate the relationship with total forward thrust.

As for the coordination between legs, this is essential in order to capture the traveling wave phenomenon from the aggregate behavior of individual legs. In the initial design concept of extending design of Avirovik [10], [11], control of the legs would be from an external signal generator and require large amplifiers for the piezoelectric actuators. Similar to Hoffman et al. [20], [21] controlling the leg motions would be dictated by a central external source. Being miniature scale limits these robots from having on board controllers. Larger scale robots such as the centipede robot by Koh et al. [19] and the millipede robot by Kano et al. [27], can use onboard controllers. Zinedyn [19] was a very simple mechanism driven by a single motor to drive all legs, which meant that the leg phases (thus wave characteristics) were fixed and unchangeable. Kano et al. [1] developed a decentralized control scheme, utilizing feedback control from each leg to determine its gait. While such a gait control mechanism is very robust, the cost comes to its size (75cm) and weight of on board sensors and computing power. With the primary interest of this robot design being to investigate the output thrust force of the gait, such level of feedback control could be redundant at the price of explicit control of the duty cycle.

3.3.3 Leg mechanism design and control scheme

Leg motion mechanism

As it has been discussed, for the purposes of this millipede robot design we need a mechanism that can actuate the leg so that it not only captures at least the two degrees of freedom of horizontal and vertical motion, but accomplishes a trajectory with a circular or elliptical arc during the elevation stage and a straight line motion in the propulsion phase of the stride. Also, it is desirable to keep the number of actuators to a minimum.

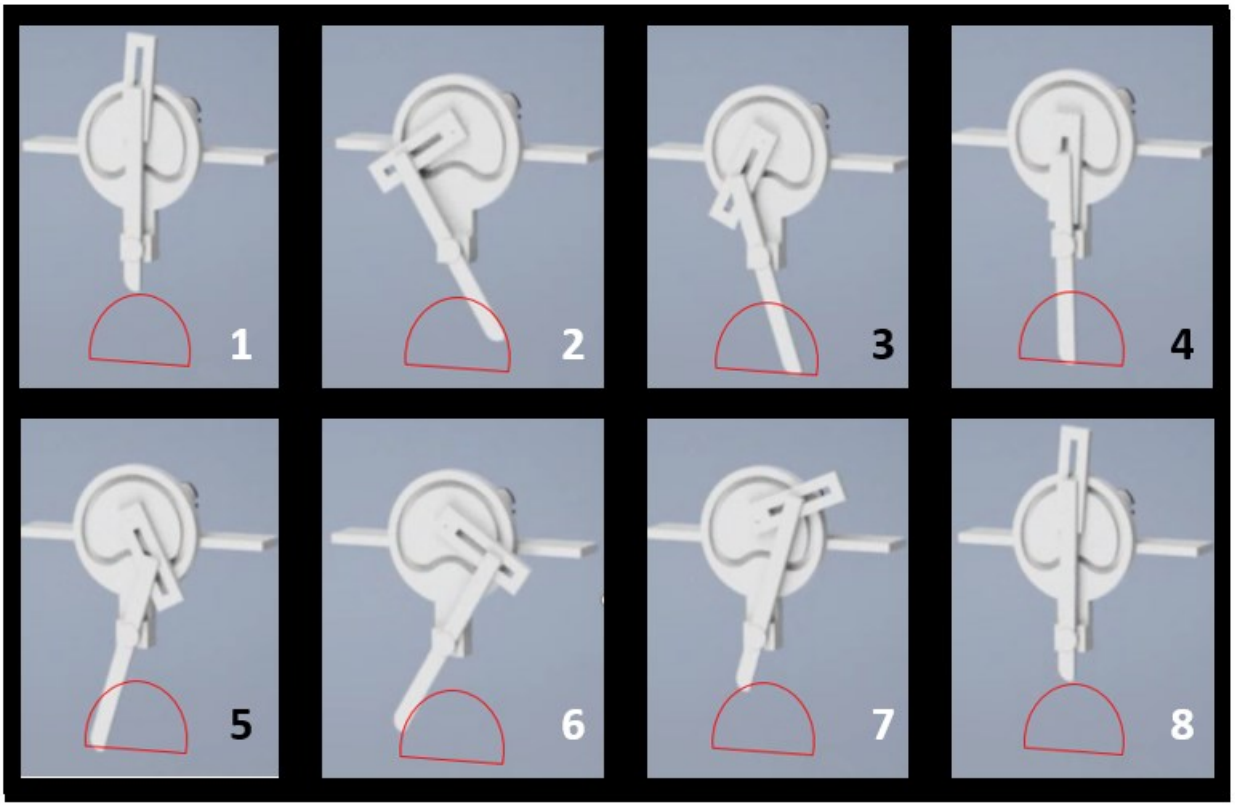

Figure 3.8: Time frame instances of leg mechanism CAD simulation. Frame instances 3, 4, and 5 the leg is in contact with the ground performing a straight line motion. Frames 1, 2, 6, 7, and 8 the leg is elevated tracing a circular path

While straight line mechanism motion is not new technology, Wan et al. developed a cam-controlled, single-actuator-driven leg mechanism for legged vehicles [63]. Unlike other straight line legged mechanisms, it does not require multiple actuators to achieve the returning motion. With this mechanism a constant rotational angular velocity input produces legs that moves at a constant speed. The proposed cam curve profile proposed is designed to have a third derivative (jerk) connectivity. Wan et al. did not build a robot using this mechanism, but did develop a simulation to perform force analysis.

Using the cam profile that Wan et al. proposed in [2], a leg mechanism was designed driven by a single electromagnetic DC motor. The resulting motion of the legs end tip is the desired profile of

an elevated arc forward stroke and straight line propulsion backstroke (Figure 3.8). This path replicates what is seen in millipede locomotion, as shown in Figure 2.2.

Leg motion control

Now that we have a leg mechanism that has explicitly defined stages of elevation and propulsion, it is now possible to adjust the duty cycle of an individual leg. As the legs' two degree of freedom motion is driven by a single motor, controlling the duty cycle will be done by adjusting the angular velocity over a specified region. From the biological observations seen in Figure 3.2, the time period of the legs elevated transfer stage (Tt) stays relatively constant regardless of the forward thrust demand, while the time period over propelling stage (Tp) increases. This observation, in combination with the constant thrust force performance, would suggest a constant torque input which would result in varying duty cycles with different load resistances. However, the nature of mechanism design involves a cam trajectory which would not permit a constant motor torque control resulting in a constant leg motion or thrust force. Also, the interest of this robot experiment is not the gait response to changing environments, but how different gaits generate changes in thrust force.

Implementing this to the leg mechanism, the angular velocity will be adjusted by the regions seen in Figure 3.9A. The blue arrow region is cam motion that drives the leg in the elevated transfer stage (Tt), while the red arrow region drives the leg during the propulsion stance.

In order to accomplish this control, the angular position of the rotary motors need to be constantly tracked, which is be achieved by using encoders. A simple PID control scheme is implemented on each motor to control the change in angular velocities throughout a revolution.

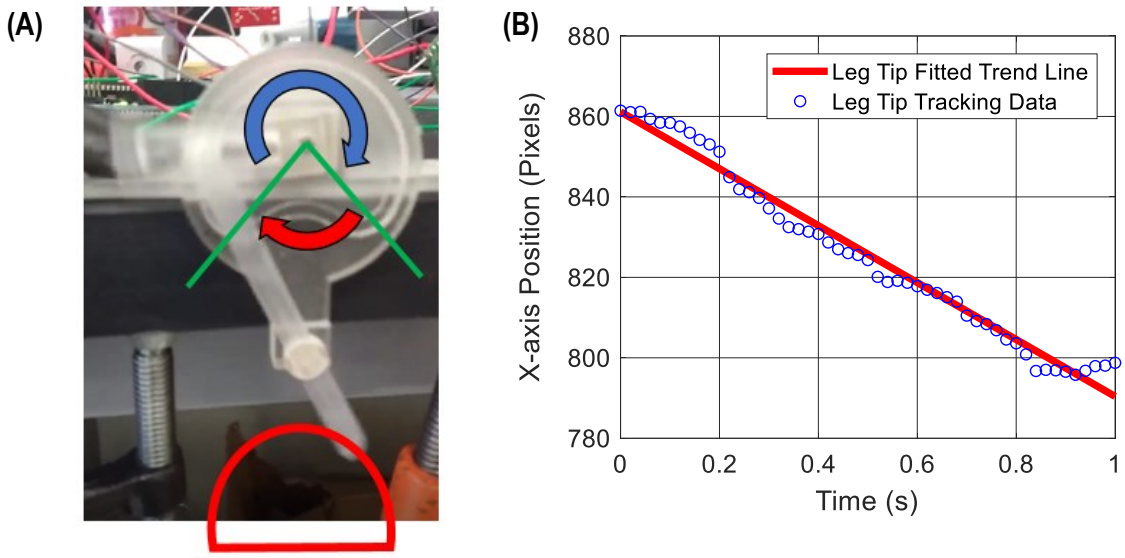

Figure 3.9: (A) Control scheme for individual leg motion: the two arrows indicate two different regions to define an angular velocity. The blue arrow indicates the region of the cam track that causes the leg to elevate, while the red arrow indicates the region where the angular velocity of the motor drives the linear motion of the leg (B) Video tracking of leg tip to verify that the leg moves at constant velocity during the straight line propulsion stance when driven with a constant angular velocity

With this leg motion mechanism and control design, the key leg motion mechanics of interest needed to emulate the metachronal gait adjustments performed by millipedes in modulating their traveling wave locomotion attaining more thrust are met. The complex biological system of the millipede leg, which consists of more than three-degree of freedom motion and several actuating muscles (Figure 2.13 and Figure 3.1), has been reduced to two-degree of freedom cam mechanism driven by a single DC motor actuator.

However, this current mechanism design does not explicitly tackle the ground reaction force profile during the propelling stride. Despite this, while no actuation is currently actively involving those dynamics modeled and observed in the previous chapter, the kinematics of the leg mechanism does take away some of the pendulum motion effects and potentially biases towards

the desired profile as the legs are essentially being retracted at initial contact and extended just prior to take off.

Leg co-ordination control

As discussed earlier, millipedes have a central nervous system (CNS), that consists of a ventral nerve cord that goes along the body, and have ganglia/nerve clusters at each leg pair. These ganglia interpret the CNS signal and relay the desired movements to the local leg pair. The presence of the ganglia decentralizes the level of control from the brain, as its relayed signal are what governs the function within the body segment. An illustration of the millipede CNS is shown in Figure 3.10A. Also aforementioned was the millipede model and robot developed by Kano et al. [27], that suggested that the decentralized control was a function of the ground reaction force feedback control of the anterior leg pair. While this approach is robust in capturing the millipede locomotion behavior, it comes at the price of having to build a rather large robot to incorporate the necessary sensors and controllers. For the purposes of this investigation, the design of the robot will be used to test specifically the traveling wave gait modulation for forward thrust performance. In this case, this level of feedback control is not required.

With the interest in characterizing the traveling wave performance against thrust force, the minimal required level of control is the duty cycle of each individual leg pair. As postulated, for the millipede robot design, we can reflect the decentralized structure of millipede control by use of a master controller (brain) providing gait parameters to slave microcontrollers (ganglia) at each body segment to generate the traveling wave form from the aggregate leg behavior. A schematic of this structure is shown in Figure 3.10B. The control scheme implemented to accomplish a variety of duty cycles and metachronal gaits is illustrated in Figure 4.3.

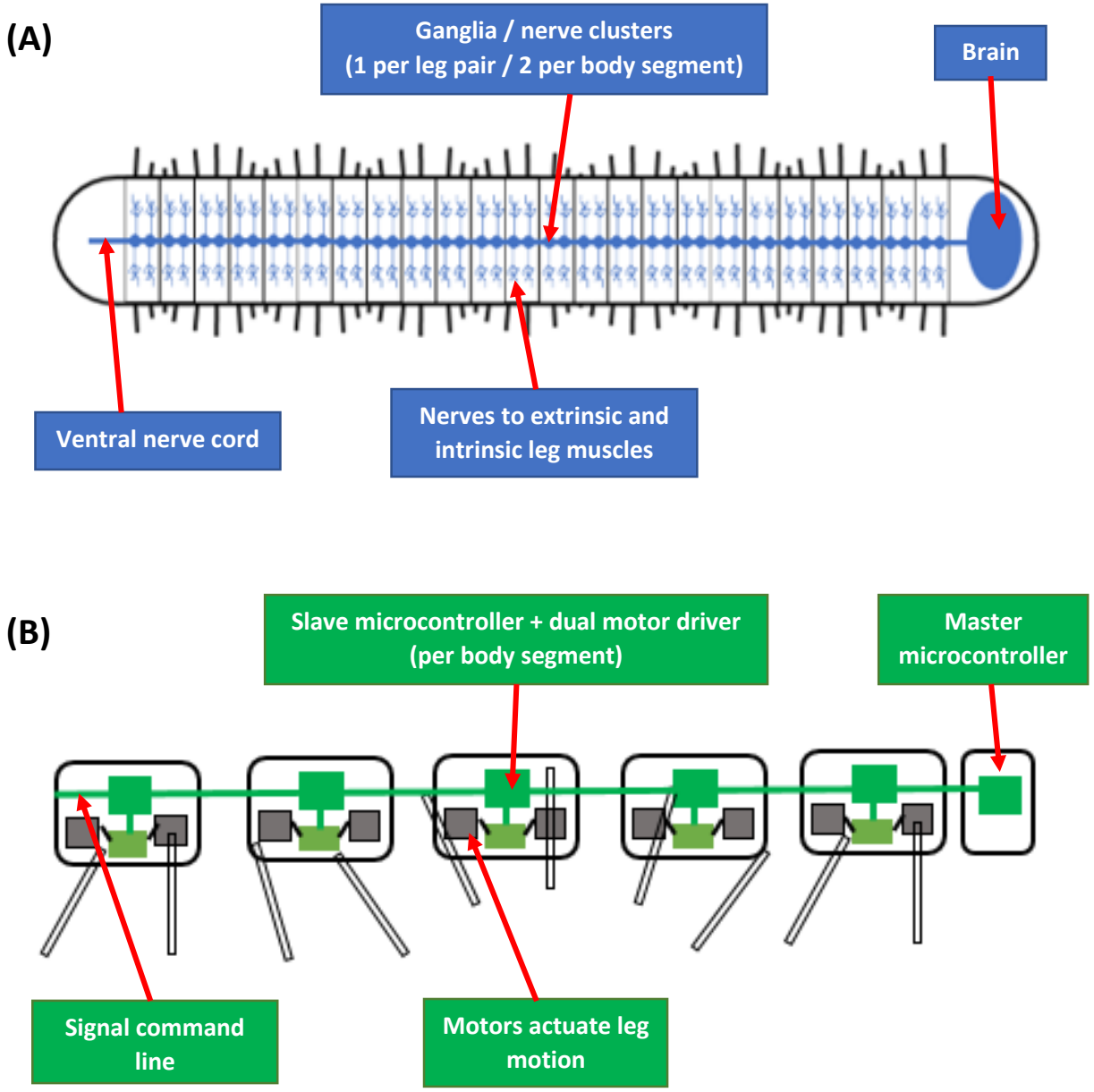

Figure 3.10: A side-by-side schematic comparison of the control structure of biological millipedes and the proposed robot, drawing a resemblance in the decentralized nature of controls. (a) A visual representation of the biological CNS of millipedes. (b) A visual representation of the electronics and control scheme of the proposed millipede robot design

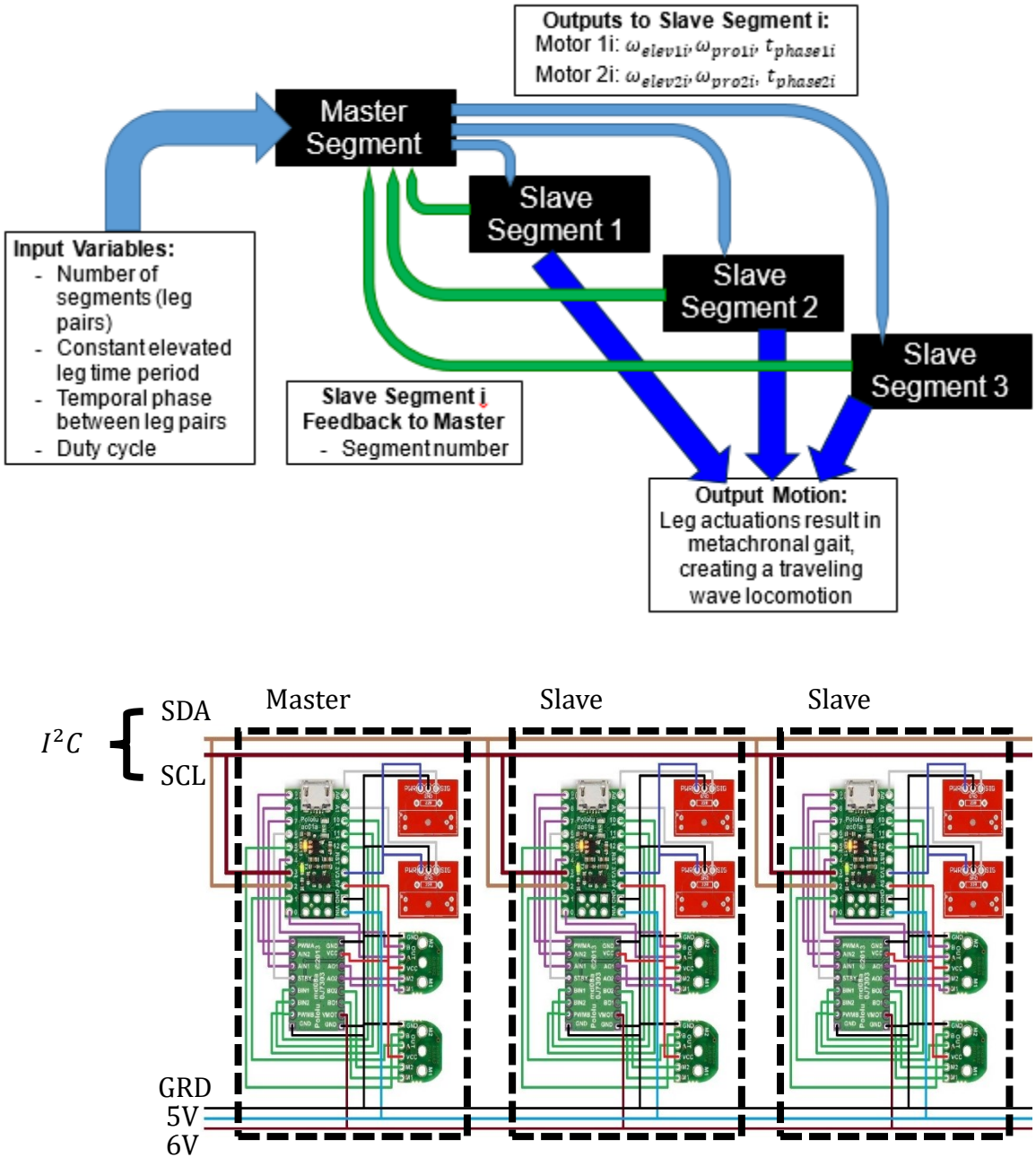

Figure 3.11: Control scheme for bio-mimicking millipede robot to perform range of metachronal gaits (top), Electronics schematic to implement I^2C communication control between segments

3.3.4 Millipede robot design and build

Now that we have a mechanism to generate the leg desired leg motions, as well as general control scheme, the complete design of the millipede mimicking robot needs to be addressed. The distinct characteristics of the millipede morphology were explored in the previous chapters. Firstly, they possess an elongated flexible segmented body, where the flexibility is attained from the combination of a complex trunk musculature and "ball and socket like" joints between segments permitting the three-degrees of freedom of lateral, dorsoventral, and rotational relative motion. Secondly, they possess many legs, with two leg pairs per body segment. Where leg pairs operate in bi-lateral phase with each other. In our bio-mimicking design we want to encompass as many of these features as possible, but with the understanding that emulating the powerful modulating traveling wave gait is the primary focus.

Starting with the design of a single segment, the first part to consider is the body which will be carrying the on board electronic controller and sensor components. The representative body of the millipede for this design consists of two components: the base and the ring/shell.

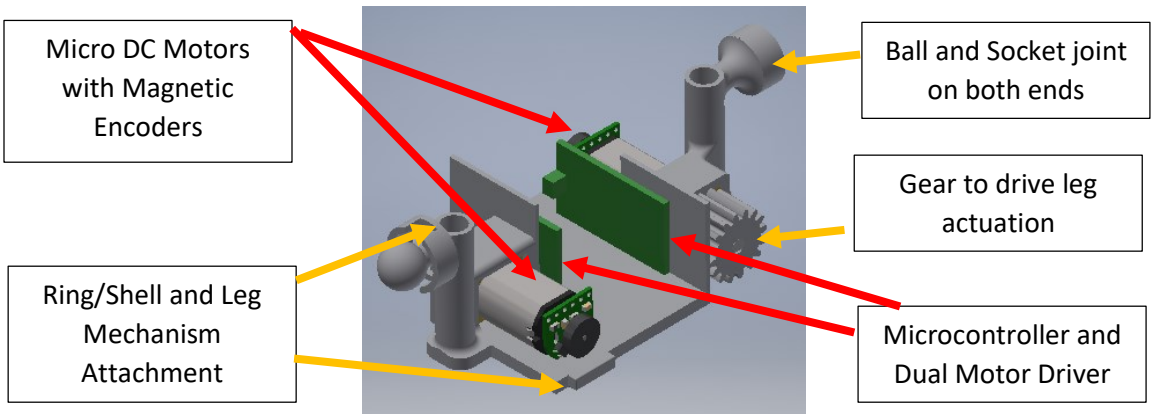

Figure 3.12: Body base of segment that consists of holding the DC motors, microcontroller, and motor driver

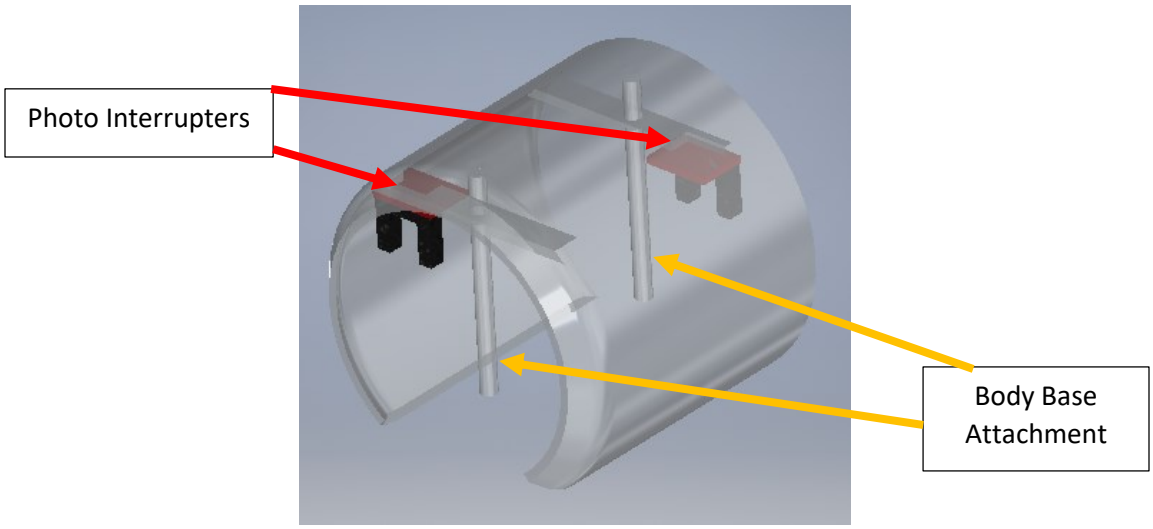

Figure 3.13: Body ring/shell of segment that also holds the photo interrupt that calibrate the leg motions

The base will provide space for a microcontroller (A-Star 32U4 Micro), a dual motor driver (TB6612FNG), and two micro DC motors (Micro Metal Gearmotor HPCB 6V with Extended Motor Shaft) each with magnetic encoders (12CPR). The base design also incorporates "ball and socket like" joint endings to attach to the adjacent segment. While actuation of the body motion is not currently in the design, the degrees of freedom for those motions, if actuation is implemented in the future, are there. With the base being the central component of an individual segment, it has press fit attachment points to the ring/shell and leg mechanisms. A schematic of the base and the encompassed components are shown in Figure 3.12.

The ring/shell of the segment body replicates the functionality of the ring/shell of the actual millipede, shielding the internal components from outside disturbance. But also for this robot design, it will also be the supporting frame for the photo interrupters (GP1A57HRJ00F). The photo interrupters are used to indicate and calibrate an initial leg position and act as reference point. In this design configuration the referenced initial position (or 0° angle of rotation) would be when

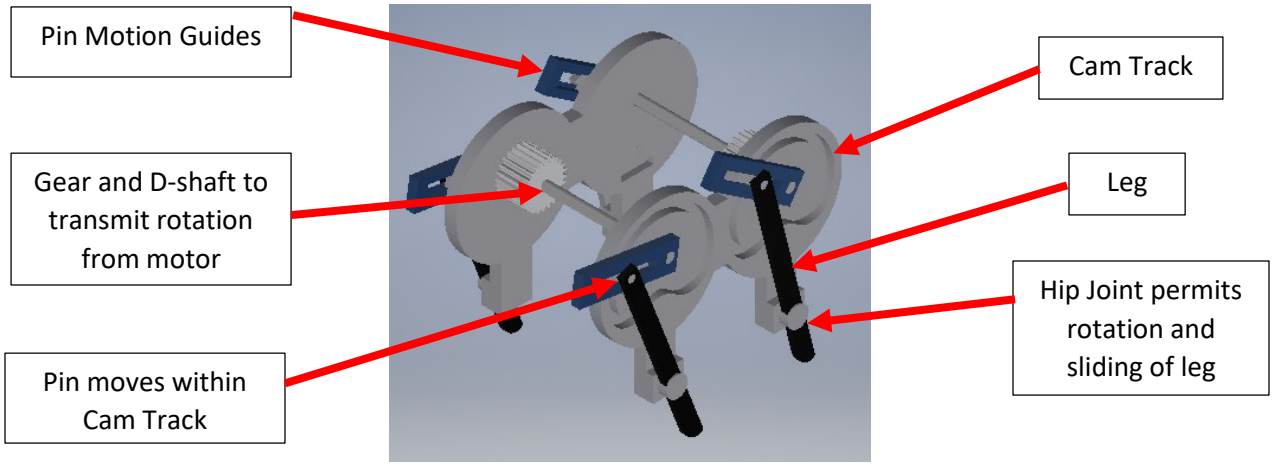

Figure 3.14: Leg mechanisms for a segment: a leg pair, which operate in phase with each other, is driven by a single actuator

the legs are retracted and the end tips are closest to the body. A schematic of the body ring/shell component is shown in Figure 3.13.

The last major component of a body segment is the leg mechanism. As there are two leg pairs (4 legs) per body segment, and each leg pair operates in bilateral phase with each other, a single pair of legs can be driven by the same actuator. The rotation of the motors is transmitted through gears and a D-shaft. The D-shafts are attached to the pin motion guides (dark blue in Figure 3.14). The

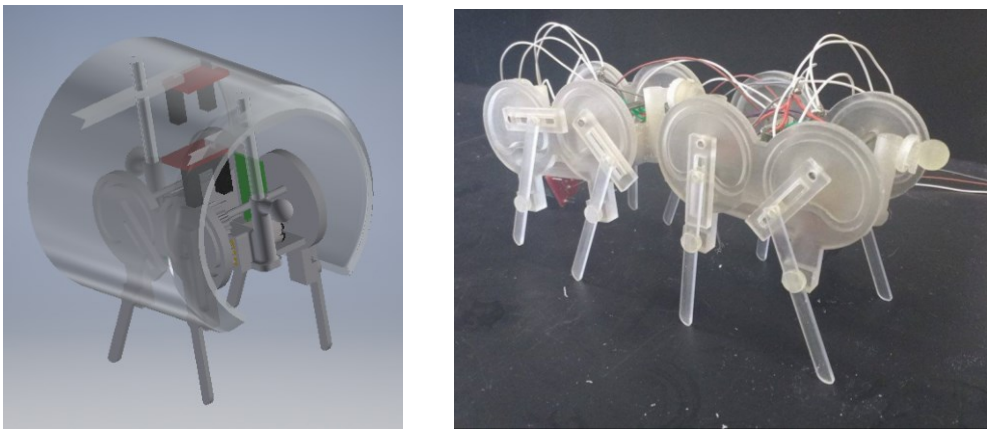

Figure 3.15: (left) CAD assembly of a single segment, (right) built assembly of two segments (in progress)

pin in the cam track is attached to the top end of the leg, therefore as the motion guide drives the pin around the track, the leg follows. The leg is hinged at the hip, and permits linear sliding motion, as a result the bottom tip of the leg creates the desired trajectory discussed earlier. A full schematic of the leg mechanism components is shown in Figure 3.8.

Combining these three main components (base, ring/shell, and leg mechanism) a complete segment is assembled. With nature of the millipede morphology, generating a full millipede body consists of simply reiterating the build process. For this first initial robot, the components were rapidly constructed prototypes using a 3D printer (Objet). A CAD assembly of a single and initial fabrication are shown in Figure 3.15.

Design and manufacturing adjustment

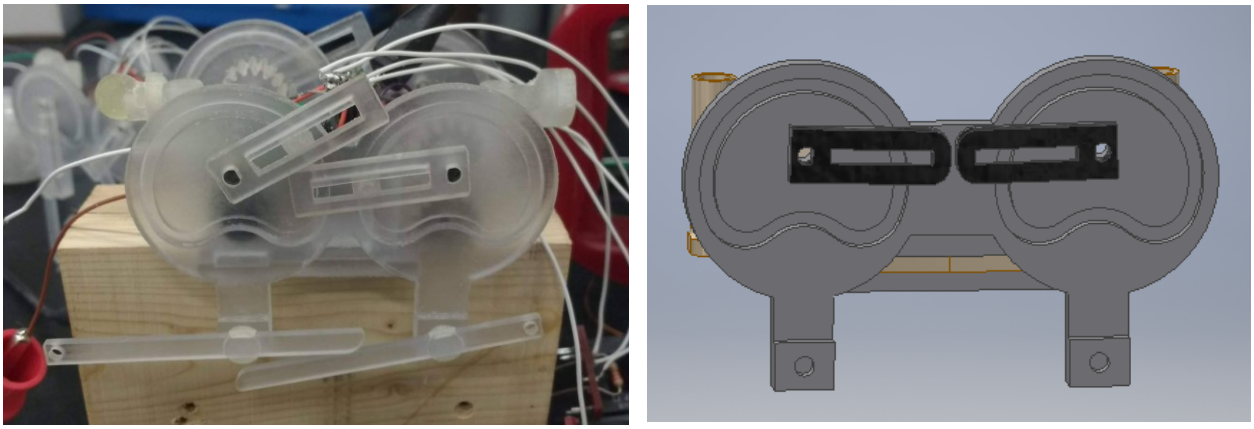

Figure 3.16: Pin motion tracks need to be redesigned to avoid collision with adjacent leg mechanism

Testing the initial robot mechanism, several issues were encountered that required design adjustments. The first issue to arise with the mechanism design was that adjacent leg pairs would collide with each other, as shown in Figure 3.16. While ideally with the leg phase difference that we expect from by applying the millipedes gait would permit overlapping trajectories of the leg mechanisms, for a robot application, instances where a leg falters, would not only disrupt the gait

because of its performance but would also cause issues with the adjacent leg pair. Such an occurrence could also cause the DC motor to stall and draw large currents. To avoid this, the spacing between leg pairs needed to be increased slightly, and also shortening the sliders as much as possible. Increasing the size of the segment is not desired, but is necessary in order to permit locomotion if a leg pair were to falter.

Another aspect of the design that was encountered, was the pin attached to the leg was found to get jammed when sliding within the cam design [63] when the motor was operating at lower angular velocities. The initial design was modified to utilize a ball-bearing at the pin within the cam sliding mechanism (seen in Figure 3.17). The bearing, in combination with the use of Teflon eliminated the jamming and smoothened the motion of the leg mechanism.

During the manufacturing process, issues with the 3D printers (Objet and FormLabs) were encountered. Therefore, the design was modified to allow manufacturing and assembly primarily via laser cutting. Without access to rapid prototyping capabilities of a 3D printer, and with the primary focus of the study relating to thrust force of straight forward motion, the initial design of a ball-and-socket joint attachment between segments was reduced to a hinge joint that permitted flexion replicating the dorsoventral degree-of-freedom observed in millipedes.

Furthermore, after initial attempts of having the robot walk, it was observed that there was a lack of vertical support of the robots' body anterior, posterior, as well as between segments at the hinge joints. In actual millipedes, this vertical support holding the body off the ground is created not only by the legs, but the morphology permitting leg pairs to be very closer to one another reduced vertically unsupported regions, in combination with the bodies complex musculature between

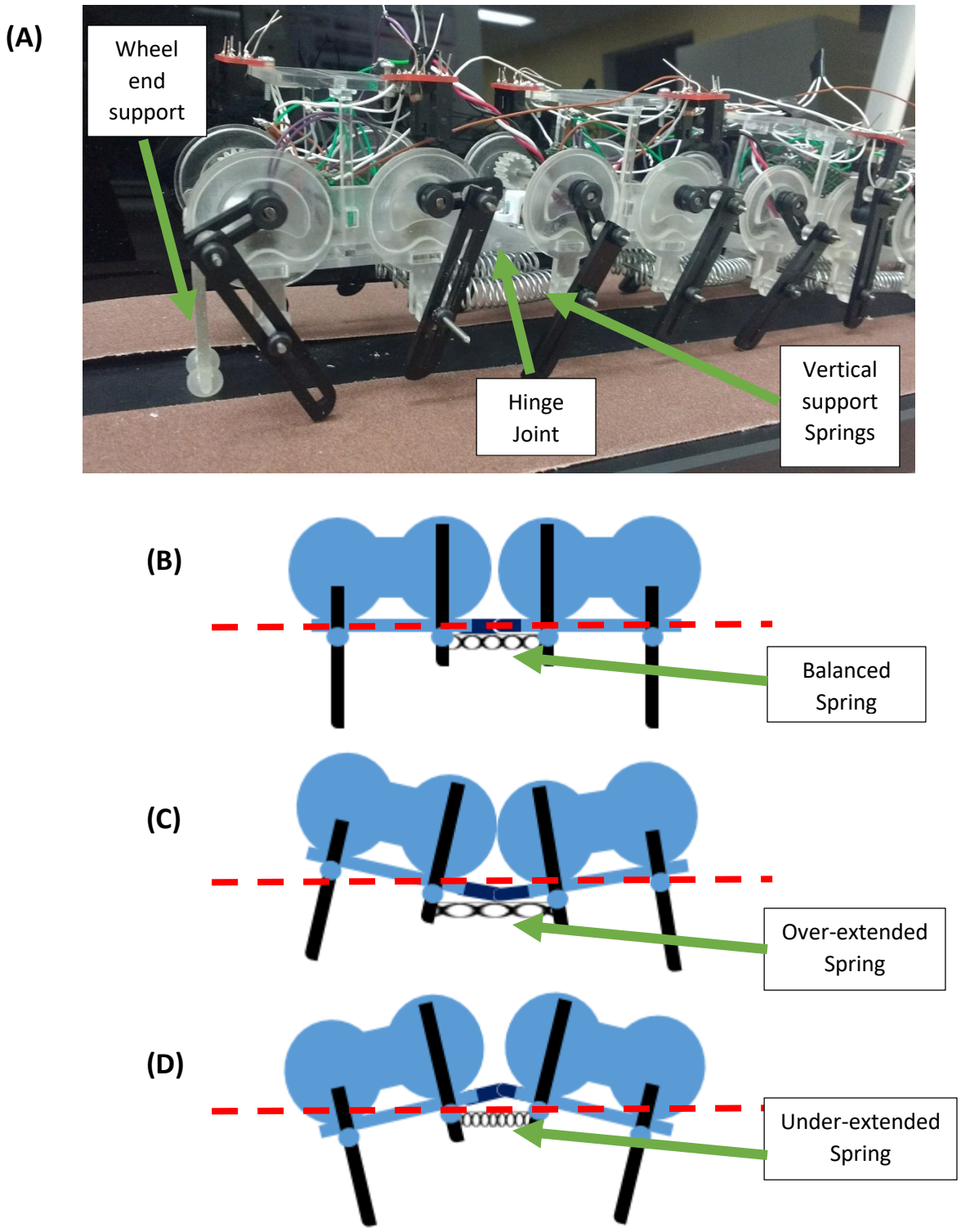

Figure 3.17: (A) Adjusted design with laser cut manufacture, (B) Spring force between segments (to emulate millipede body muscles) is tuned so there is no angle between them when there is no vertical support provided by the elevated legs, (C) If spring force is too small the joint between body segments will lead to the body sagging below the horizontal body axis, (D) If spring force is too large the joint between body segments will raise above the horizontal body axis due to an over contraction

segments permitting articulate movements. For this robot initial design, articulate motion control between segments is not a primary focus (perhaps in future work), therefore to compensate for musculature activity seen in actual millipedes for this morphology, springs were placed between segments, across the hinge joints to provide an upright stability that still permitted some degree of flexion. As shown in Figure 3.17B-D, the spring was tuned so that the segments were aligned parallel to the ground. For the posterior and anterior end of the robot, a wheeled support was attached to permit elevation of the leg pairs at either end.

3.4 Conclusion

In this chapter a millipede-inspired robots' mechanisms and control were designed and manufactured, with the purposes of mimicking the modulating metachronal gait exhibited by millipedes in order to control their axial thrust force in the direction of motion. From the bio-mechanics study in Chapter 2, it was found the primary factors governing their thrust force capabilities was the duty cycle and number of body segments. The robot developed was designed to permit explicit control of the duty cycle over an arbitrary number of segments/legs.

Chapter 4 – Implementation of Traveling Wave Modulation on Millipede-mimicking Robot

4.1 Introduction

In the previous chapter a millipede mimicking robot was developed for the purposes of better understanding and trying to replicate millipede locomotion, with particular interest in their ability to handle large resistive axial loads by generating effectively large thrust forces in the direction of motion, utilized in situations such as burrowing and climbing. The focus of this chapter is to determine if the impressive powerful forward thrust performance exhibited my millipedes can be emulated by the robot by the adjusting same gait variables and morphological parameters observed in the bio-mechanics study in chapter 2.

4.2 Methods

4.2.1 Experimental setup

The aim of this experiment is to determine the thrust capabilities of the developed millipede robot (chapter 3) using a variation of gaits and morphology, and determine if they are consistent with the model developed in bio-mechanics model in chapter 2. With the biological specimens in chapter 2, the two experiments performed to reveal the gait variation responses to increased thrust force demand were the controlled inclined slope and the burrowing stage. However, these two approaches have limitations which would make them less effective to utilize on testing the millipede-mimicking robots' capabilities. The inclined slope effectively encouraged a behavioral

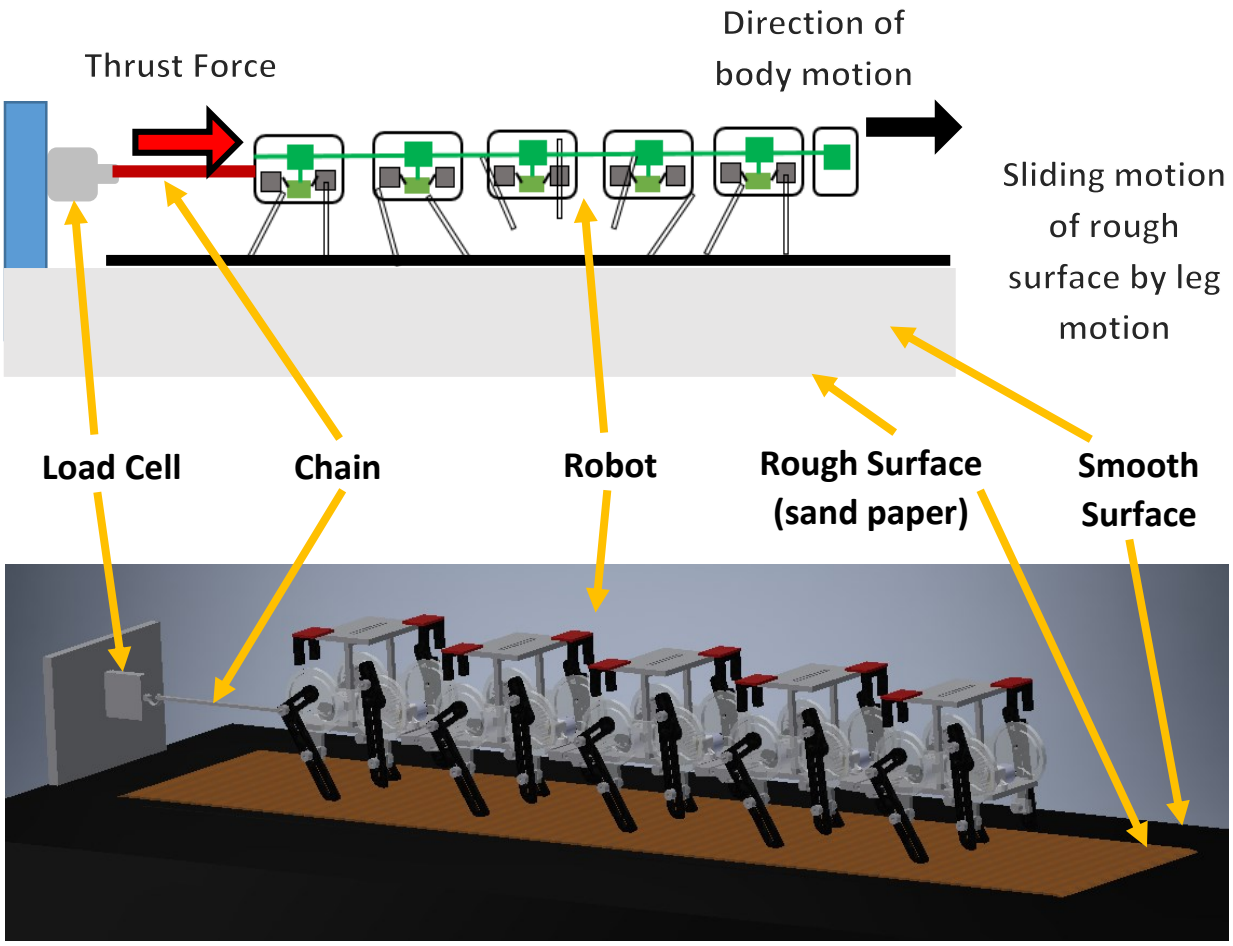

Figure 4.1: Experiemtal setup to determine the millipede robot locomotion thrust capabilities, measured directly from a load cell

response corresponding to an increase in axial load by reduction of traction. While the biological specimens may not use biological adhesion techniques demonstrated by insects and other small animals (such as beetles, ants, geckos, etc [46]), they do have sharp tarsal claws [23], which in combination with many compliant legs, each with various degrees of freedom, help them to be able to climb steep inclines on a flat surface (sand paper roughness of grit 400). To implement such a technique with the robot would be difficult, as the robot has rigid legs made of acrylic, without any adhesion techniques applied. Being significantly larger, even with a rough surface, a lot of slipping would occur at large inclined surface angles, and potential damage to the robot is

undesirable. As for emulating a setup similar to the burrowing stage for the robot would be possible, having the robot push against incrementally increasing loads. This could however lead to a difficult assessment of performance given the potential traction issues. On the biological specimen, it appears the presence of sensory feedback and the constant effort provided by an individual leg allows the millipede to apply the appropriate gait for the thrust force demanded. Even the robot developed by Kano et al. [27] utilized such sensory feedback, without explicit constant control effort on the legs would make it difficult to or compare fairly. With the robot build in chapter 3, the application of a constant torque at each leg, with a defined temporal phase was considered to accomplish the responsive nature of variation in duty cycle. However, given the nature of the mechanism, which permits explicitly defined regions of the stride cycle, applying a constant torque across the cam profile [63] would not generate a constant velocity or consistent performance. While the mechanism cannot be driven with constant torque, it can be controlled with determined velocities for both the propulsion and transfer stages. It was determined that the leg during the stance phase of the mechanism, when operated at a constant angular velocity, produced a linear motion of constant velocity (Figure 3.9B).

Instead of encountering increasing loads to test the robot, we will directly measure the output resultant force as a product of changing the duty cycle and/or number of body segments. To do this, the experimental platform in Figure 4.1 was designed. As shown, the robot will be attached directly to a load cell by a rigid body chain or rope. The robot will then walk on a rough surface sliding on top of a smooth surface, which will be driven by the walking motion of the legs. To maximize traction, the sliding rough surface will be made of sand paper. As a result, the thrust generated by the robot gait will be transmitted to the chain pulling on the load cell.

4.2.2 Millipede robot characteristics

Prior to testing the thrust force capabilities of the millipede robot, the robot needs to be characterized to allow us to fairly compare its variation in performance to the biological specimens.

In the bio-mechanics study and modeling (chapter 2), we look at and analyzed both morphological features and behavioral characteristics of the millipede specimens to develop a model. A list of those same variables of interest for the robot are shown in table 4.1. From our model parametric study, it revealed that behavioral variables, stride length and leg temporal phase, remained relatively constant and had negligible effects on the total output thrust force of the gait. This assisted in the robot design, as the stride length was taken to be constant, which dictates the leg temporal phase, or number of legs elevated per wave from the relationship determined in equation 2.25. The other two behavioral variables explored were the individual leg thrust force and duty cycle. The results from the modeling section in chapter 2 suggested that individual leg effort or force of the millipede specimens stayed constant, while the duty cycle was the primary changing factor in achieving change in thrust performance.

Table 4.1: Robot Segment Parameters

Robot Segment Morphological Parameters	
Weight	1.2N
Diameter	0.05m
Length	0.09m
Leg Spacing (d)	0.047m
Stride Length	0.04m

With the duty cycle being the controlled input variable of the robot system in this experiment, the individual leg thrust force needed to be determined, and verified that its performance over varying

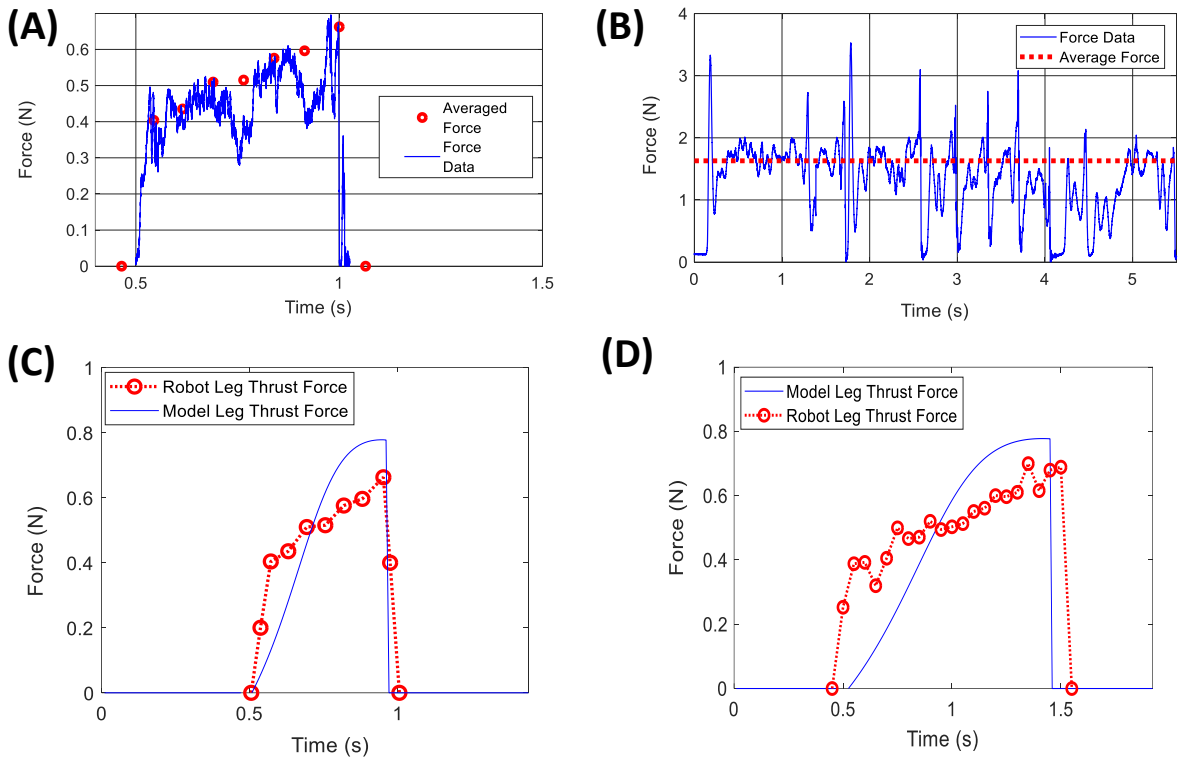

Figure 4.2: (A) Averaged force compared to force data of individual leg with a duty cycle of 0.33 (B) Averaged force compared to force data of three body segments (6 legs) walking at 0.5 duty cycle (C) Individual leg thrust force for a duty cycle of 0.33 (D) Individual robot leg thrust force for a duty cycle of 0.5

duty cycles reflected constant effort. In the biological specimens, the maximum thrust force of a single leg pair is determined by the musculature of the segment. For the robot, the thrust force of a single leg needs to be determined experimentally. To do this, the experimental stage designed earlier in this chapter was used for a single leg pair operating at different duty cycles.

The experimental results of the individual robot leg thrust force seen in Figure 4.2 were averaged over several stride cycles. While the robot thrust force profile during the propulsion phase does not quite match the profile developed in the model, they both perform in a similar temporally asymmetric fashion, where the thrust force increases from foot landing up to foot elevation. Considering that the numerous biological muscles and joints in actual millipedes was reduced to a

mechanism driven by single actuator to operate two legs (single pair) for this robot design, this is a reasonably close emulation of the individual leg pair effort and behavior.

4.2.3 Variation in duty cycle

The primary behavioral variable governing the thrust force from the millipede bio-mechanics model was the duty cycle. The variation in duty cycle observed in actual millipedes ranged between 0.3 and 0.7, which corresponded to resulting thrust forces of the specimens' body weight to twice its body weight respectively. Applying gait duty cycles within that range to the robot would result in the gait variations shown in Figure 4.3. Whether this corresponds to the same thrust force ratio of the full robot body weight will be dependent on the thrust force of individual legs.

4.2.4 Variation in number of body segments

The model also indicated that the morphological parameter with significant influence on the total thrust force is the number of body segments and/or legs. For this experiment we will test the robot operating with 1 up to 5 body segments, which corresponds to 10 leg pairs, enough legs to generate an effective traveling wave phenomena from the metachronal gait and maintain upright support. An example of the 5 segmented robot demonstrating the traveling wave locomotion shown in Figure 4.3B.

4.3 Results and Discussion

For this experiment we controlled the two variables, duty cycle and number of body segments and/or legs, on the millipede robot in order to try emulate the behavior observed in the biological millipede specimens, with regards specifically to their forward thrust capabilities. Furthermore, such experimentation could further validate the bio-mechanics model developed in this work.

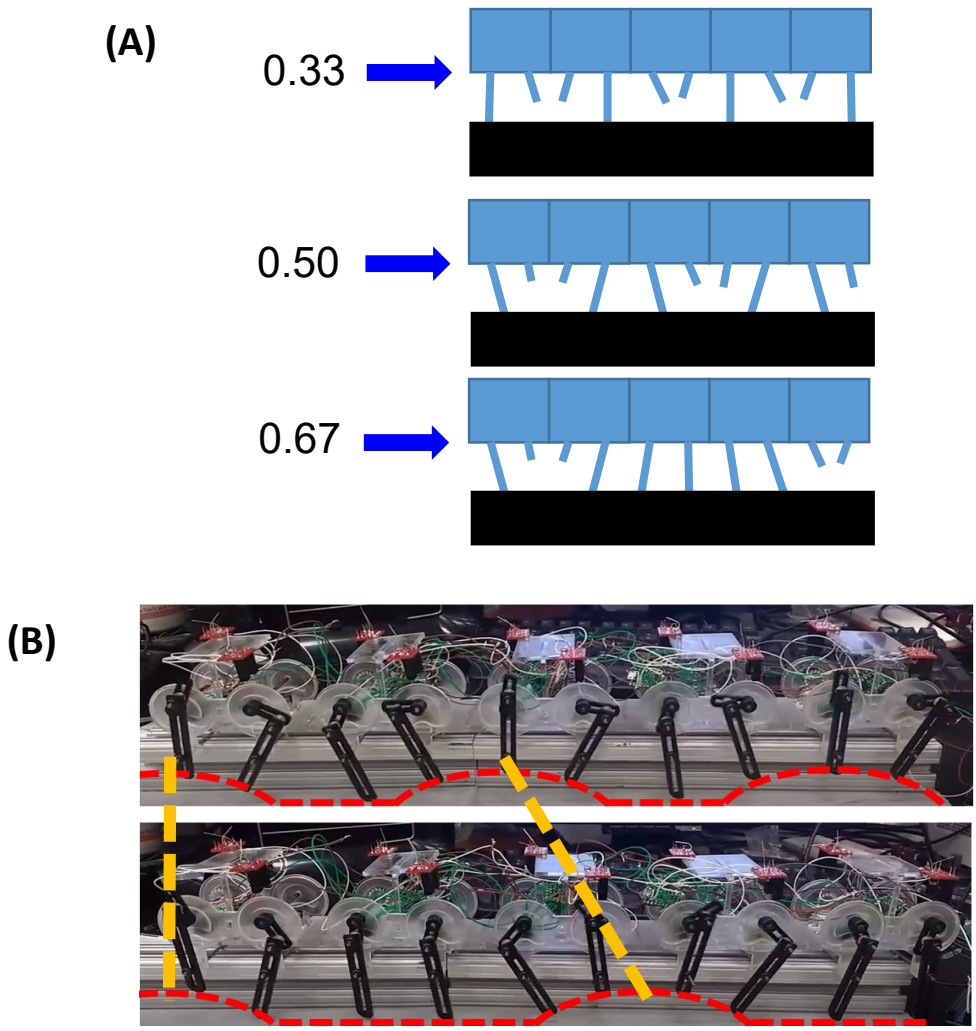

Figure 4.3: (A) Schematic of duty cycles to apply in robot experiment (B) Examples of low and high duty cycles applied to robot creating a metachronal gait

4.3.1 Model expectations

Prior to testing the thrust force capabilities of the actual millipede robot, simulations were performed using the dynamic model in chapter 2, using the measured morphological parameters and determined behavioral variables, with input sweeps of duty cycle and number of body segments. Note that for the designed robotic platform, there were no body segments without legs representing the anterior and posterior ends found on the biological millipedes. As a result, the

asymptotic behavior of gait variables relation to thrust output (dimensionless force) against increasing number of body segments, like those observed in Figure 2.22, did not exist.

As a result, looking at the trend of dimensionless force against number of body segment and duty cycle, no longer revealed an asymptotic trend towards the maximum or 'ideal' scenario. Back in chapter 2, it was revealed that millipedes grew to a length encompassing a number of body segments where the gained thrust force per body segment was at approximately 90% of the dimensionless force asymptotic value. This can be seen on the surface plot in Figure 2.22C.

While growing to that limit would likely be one factor in dictating the biological millipedes body length and number of legs, another factor would possibly relate to their gait limitations. There was commonality also revealed in the model and experimentation, relating to the dimensionless wavelength, as shown in Figure 2.16A. This could perhaps be another means to determining the desired morphology of number of body segments/legs.

4.3.2 Analysis of variation in duty cycle

As previously mentioned, the behavioral gait variable tested in this experiment was the duty cycle. The duty cycles implemented were in the range exhibited by the biological specimens, shown in Figure 4.3 between 0.3 and 0.7.

Looking at the dimensionless force against the change in duty cycle from the experiments conducted on the robotic platform appear consistent with the simulation model results just mentioned, shown in Figure 4.4D and E (Figure 4.2B). The slight deviations likely relate to the different force profiles of the individual legs, in that the robot was not able to capture all the articulate movements of the biological legs. Furthermore, there was evidently moments where the legs would slip, which may have influenced the averaging of an already noisy signal reading. To

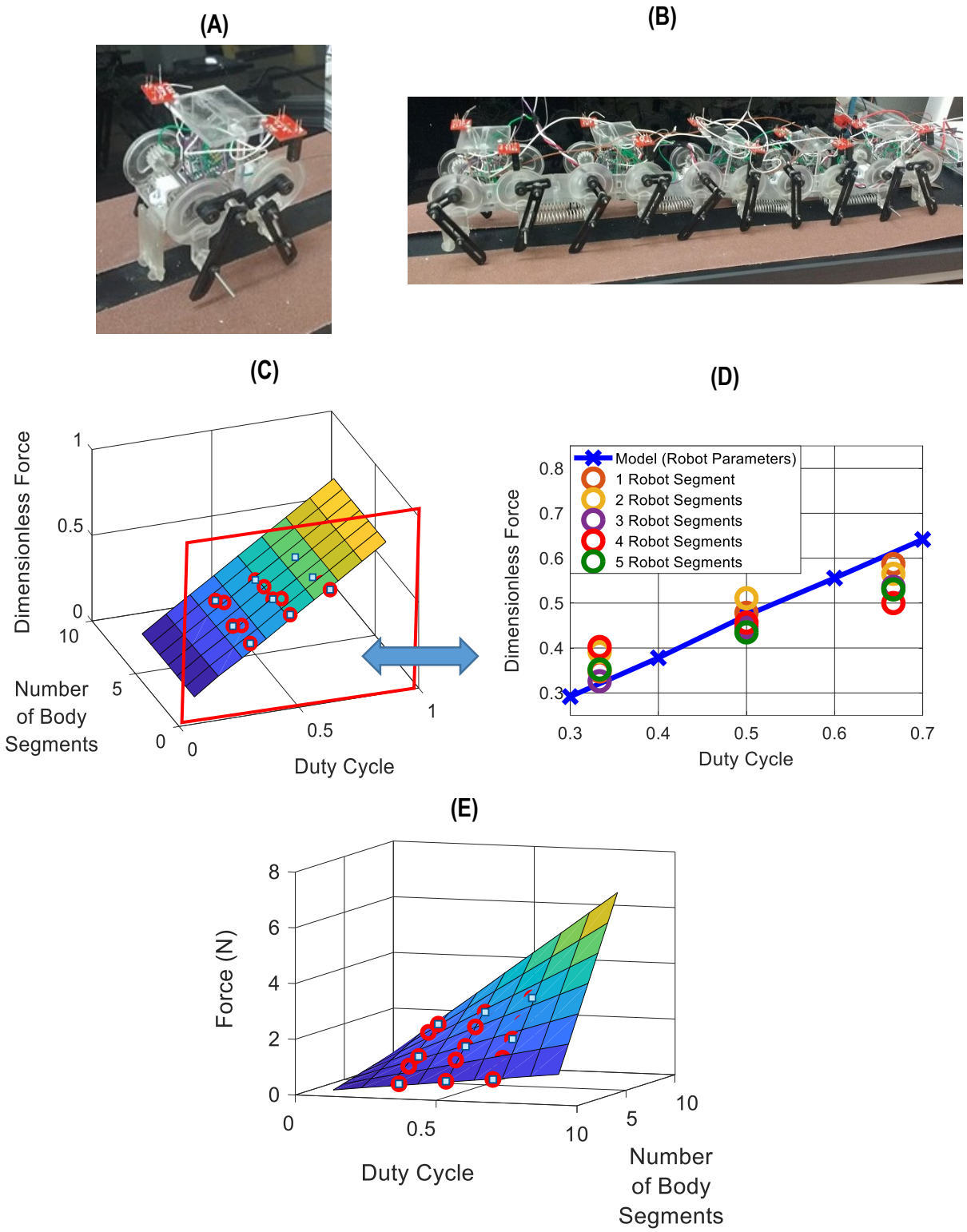

Figure 4.4: Millipede robot (A) Single body segment (B) Full body consisting of 5 segments (C) Simulation model comparison of Dimensionless force vs number of body segments vs duty cycle (D) Dimensionless force vs duty cycle (E) Absolute total thrust force vs number of body segments vs duty cycle

try reduce such affects, a logarithmic average was taken, which was similarly done for all reading from the load cell.

4.3.3 Analysis of variation in number of body segments

The morphological parameter investigated is the number of body segments, which is probably the most intriguing characteristic of millipedes' relating to the body length and numerous pairs of legs. We have discussed from the simulation modeling of the robot, the elimination of the asymptotic behavior regarding the dimensionless thrust force performance with the increasing number of body segments. The actual robot performed in a manner consistent with the model results, indicating that the total thrust force performance gained per body segment added was constant (Figure 4.4C and D). While this does not allow us to determine the desired body length based on that alone, where the biological specimens revealed a consistency of about 90% of the asymptotic value, there are still advantages of increasing total thrust force with added body segments. This is clearly illustrated in Figure 4.4E.

4.3.4 Analysis of traveling wave modulation

From the initial simulation model of the robot, it was found we could not determine the desired body length of robot, given the morphological segment parameters, with the lack of anterior and posterior end segments that did not have legs actively assisting the locomotive efforts. One aspect found common between the millipedes was the dimensionless wavelength, as shown in Figure 2.16A. The dimensionless wavelength defined in equation 2.20 was completely determined from the geometry of the millipedes'. The equation took inspiration from Manton's [23] revelation that the volume of the body segment was proportional to the leg musculature, and thus effort capabilities. Comparing biological specimens, dimensionless wavelength equation takes an assumption of matching muscular density (leg thrust force relative to the body segment weight).

While this is a reasonable assumption, the ratio of segment weight with individual leg thrust force (which was unknown prior to modeling) was determined for both species. It was found that for both species, the individual leg forward thrust effort was equivalent to twice their body segment weight, providing affirmation of the assumption. In order to make a fair comparison, the equivalent ratio representative of the body segments and legs muscular force density of the robot needed to be determined. The individual leg thrust force was only 2/3 of the weight of the body segment weight, which is much smaller compared to the biological specimens. To compensate for this difference, the dimensionless wavelength equation was updated to incorporate the leg force effort, shown in equation 4.1.

$$\lambda_{DL} = \left(\frac{\lambda}{L}\right)\left(\frac{DN}{L}\right)\left(\frac{W_{segment}}{F_{leg}}\right) \tag{4.1}$$

where F_{leg} is the maximum forward thrust force of an individual leg and $W_{segment}$ is the weight of a single body segment.

This adjustment to the dimensionless wavelength formulation allows a comparable value taking into consideration the strength of the individual legs relative to the body. Surface plots of dimensionless wavelength versus number of body segments versus duty cycle were generated for segment parameters for both millipede species and the robot, shown in Figure 4.5.

From Figure 4.5A and B, we can see that the dimensionless wavelength for both species operate approximately between 0.5 and 1, corresponding to the duty cycle range of 0.3 to 0.7, for their actual body length. Reduction of the number of body segments of either species, would result in rapidly increasing dimensionless wavelengths, which would be undesirable introducing stability issues previously discussed in the bio-mechanics modeling chapter 2. For the robot, the dimensionless wavelength curve is of values between the range of around 0.5 and 1, corresponding

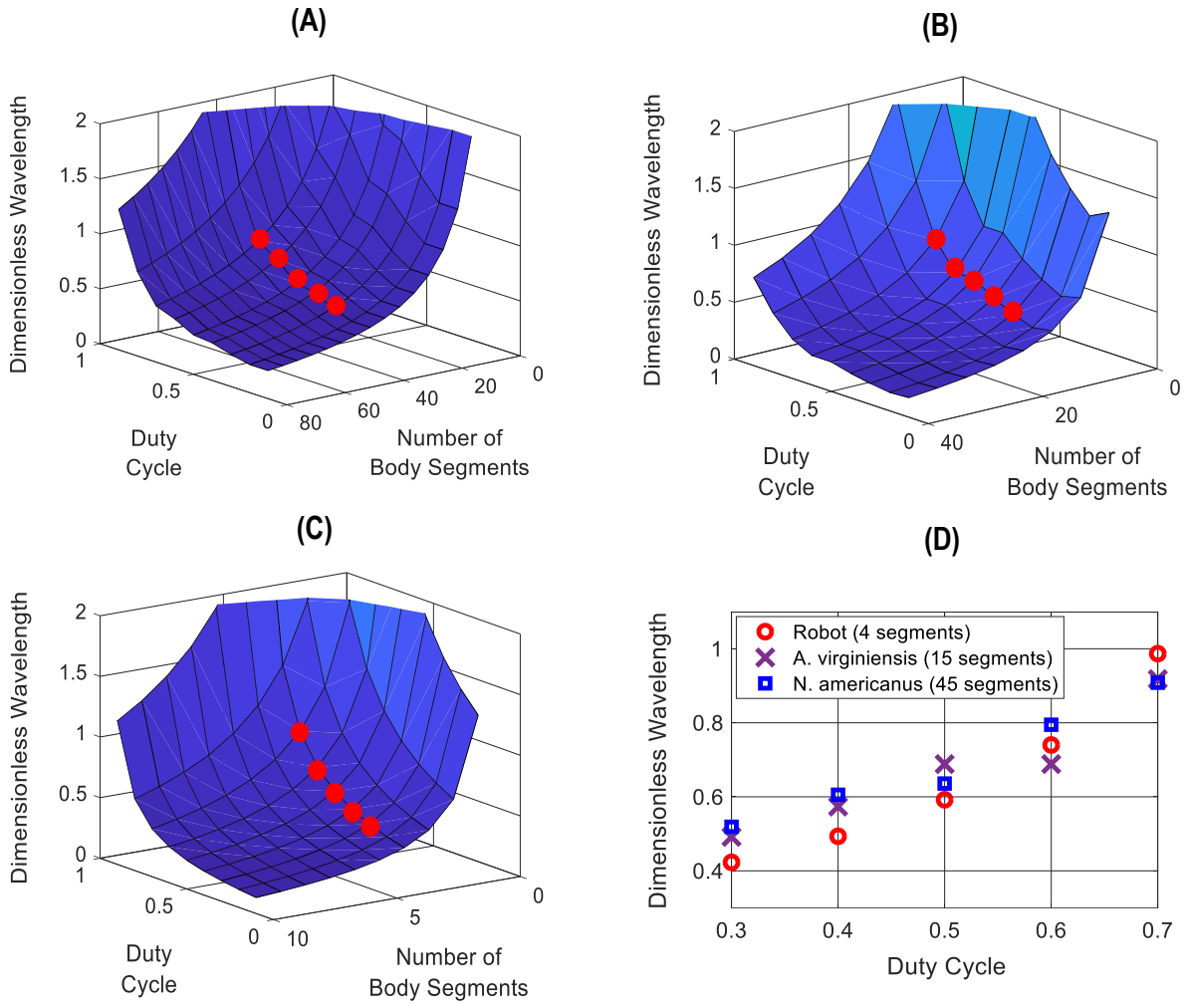

Figure 4.5: Dimensionless wavelength vs duty cycle vs number of body segments for (A) *N. americanus* (45 legged segments) (B) *A. virginiensis* (15 legged segments) (C) millipede robot (4 legged segments), and (D) Comparing the dimensionless wavelength with the actual millipede morphologies, and desired robot morphology

to a duty cycle range of 0.3 and 0.7, at 4 body segments (shown in Figure 4.5C). A comparison of these dimensionless wavelengths, at the millipedes actual number of legged body segments, and the robot with 4 segments is shown in Figure 4.5D.

Given that 4 segments is the desired number of body segments, we can back calculate the ideal sizes of the posterior and anterior ends for a millipede of such segment morphology. Performing a

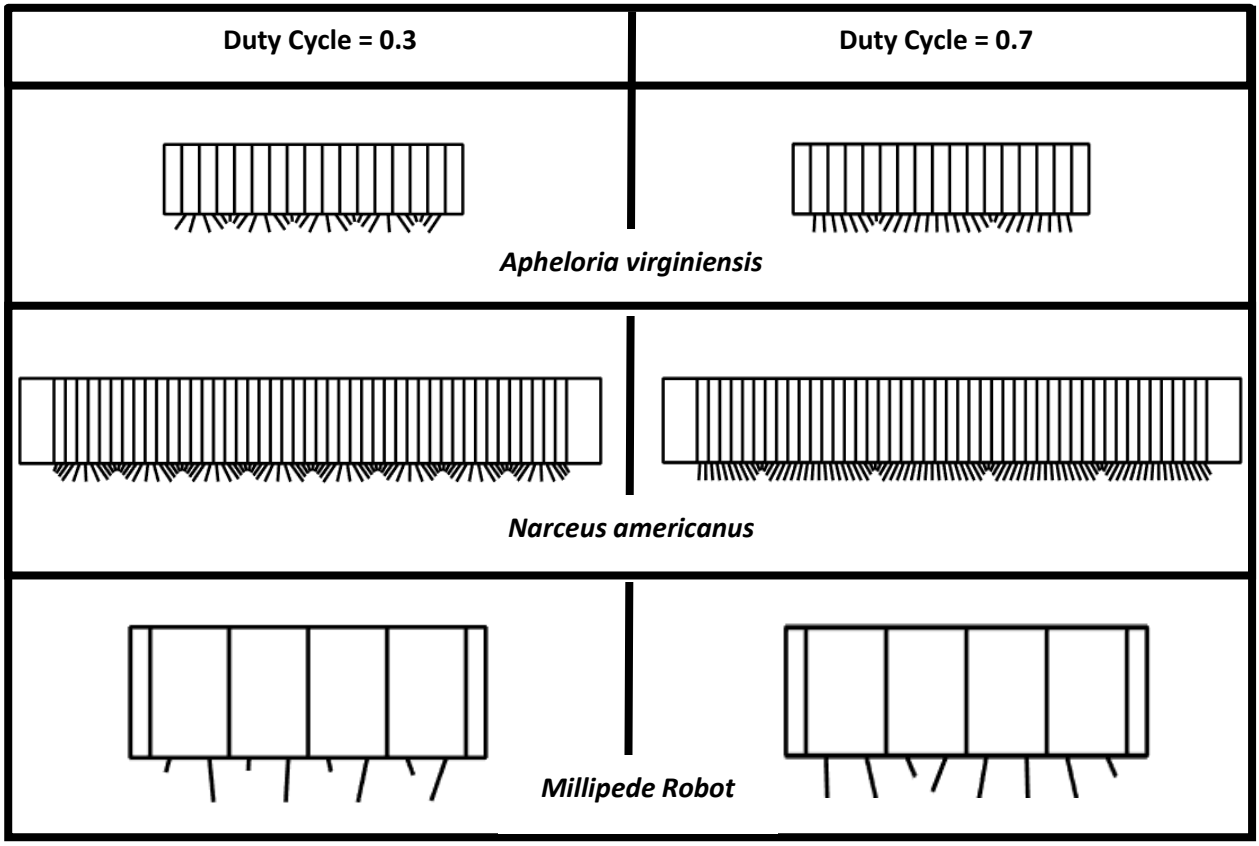

Figure 4.6: A simulation model generated visual comparison of the range of ideal wavelengths between the millipede specimens and robot

sweep of the various end segment sizes, for a body length encompassing of 4 segments, it was determined that the anterior and posterior ends would approximately a quarter of the weight of an average segment. The curve in Figure 4.7 corresponds to such morphology, which results in a thrust force approximately 90% of the asymptotic value cap seen in actual millipedes in chapter 2.

With the millipede robot morphology and gait, we can also determine the cost of transport for the robot. Given that we can determine the electrical input into the robot system, and that the model compared to the robot provide consistent outcomes, the model was used to determine the COT. For the power input, the average electrical power was initially used. In the calculation. However, the actual mechanical input to the system was actually less with the DC motors operating at

approximately 20% efficiency (both shown in Figure 4.8A). As it can be seen in Figure 4.8 the cost of transport for the robot is relatively high compared to the actual millipedes and other biological terrestrial animals. This is likely due to the energy losses not just from the motor, but the robots' mechanisms utilized to achieve locomotion. The higher COT is common in most terrestrial robots [64], as engineering and technology continue to try emulate the efficient locomotion techniques observed in nature.

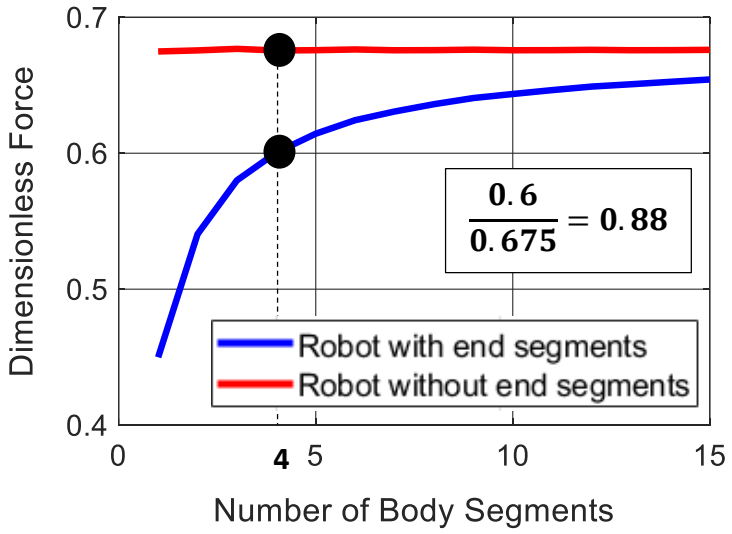

Figure 4.7: Model of millipede robot morphology of 4 segments, with anterior and posterior segments, each weighing a quarter of the average legged segment

4.4 Conclusion

In this chapter the developed millipede robot was tested to emulate the traveling wave metachronal gait exhibited in actual millipedes to handle large resistive loads. The robots' performance was consistent with the experimental and simulation modeling results in chapter 2, when controlling the variable parameters of duty cycle and number of body segments. Both these factors influenced the thrust force of the robot, as anticipated by the model.

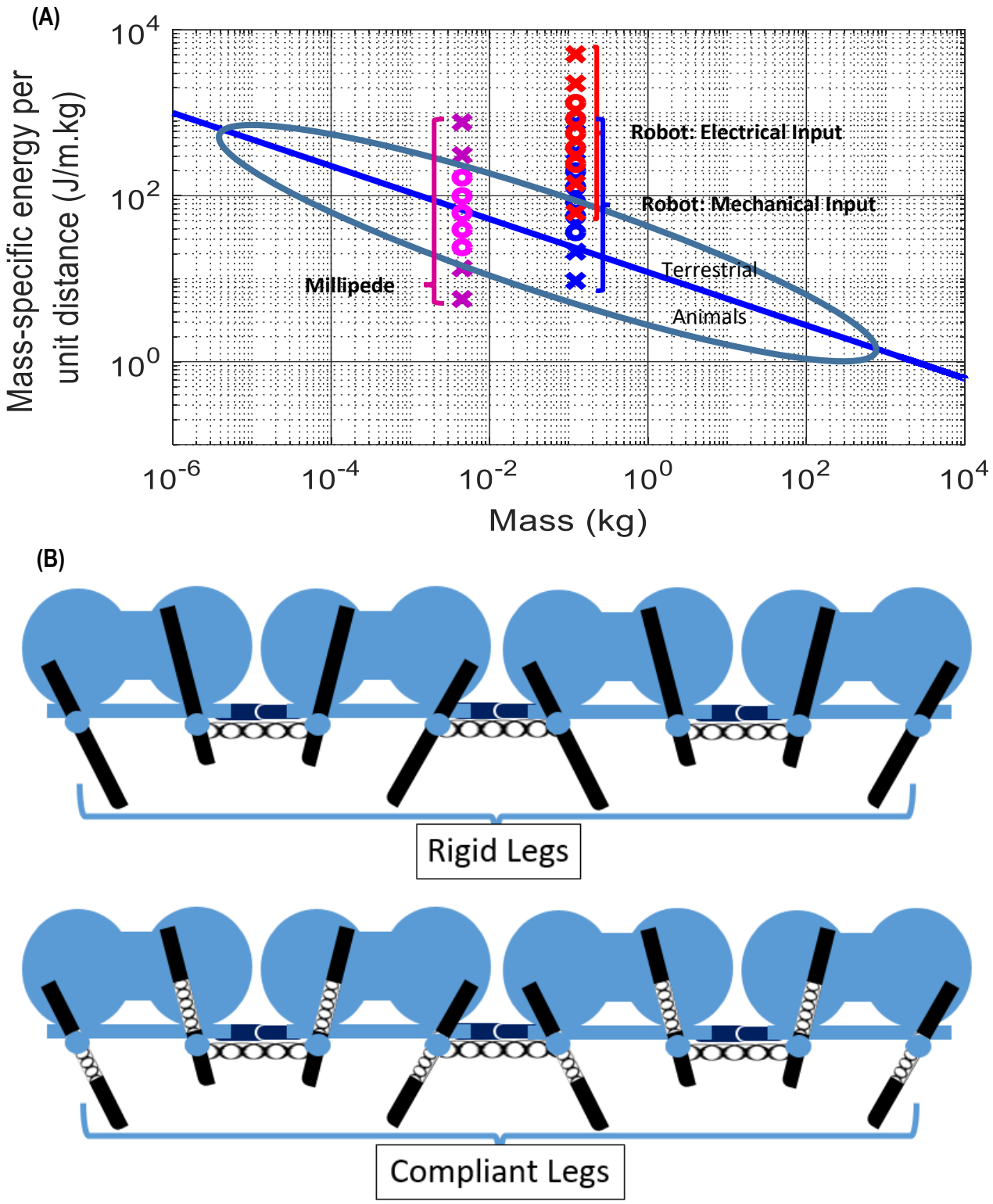

Figure 4.8: (A) Cost of transport comparison of robot (electrical and mechanical inputs) with an actual millipede (B) Potential future robot leg design adjustment to minimize slipping behavior by introducing compliant lets

In chapter 2, determining the number of body segments appeared to relate to morphology of the anterior and posterior ends, due to the extra weight that did not assist in the propelling the body forward. For the robot these did not exist. To determine the desirable number of segments on the robot, the dimensionless wavelength was investigated. This wave characteristic was shown to be common in chapter 2 between both millipede species. However, to determine such measure to the robot fairly, the formula for dimensionless wavelength needed to be adjusted to take into the account the legs strength relative to the weight it was moving. Doing so resulted in a desirable number of body segments of 4 for the robot.

The current robot utilizes a design of rigid legs (Figure 4.8B) that accomplishes the two degrees of freedom of an elevated and propulsive stance via the mechanism described in chapter 3 and [63]. However, with the rigid legs slipping did occur in various instances, as can be seen in Figure 4.2B when the force readings displays instantaneous drops. One improvement that could be implemented to the design in future iterations of the robot is incorporating springs making the legs compliant (Figure 4.8C). While the deformation of the circular trajectory of the leg end is accomplished with the cam mechanism design, a compliant nature of the legs with springs would likely result in better contact with the surface. Implementing such a design could allow tuning of the leg compliance, such that the weight of the body is suspended at a desired elevation enabling continuous leg contact through the duration of the stance phase. Furthermore, with the uniaxial spring mechanism, the resulting ground reaction forces will be accentuated and increased with deformation experienced by the spring at mid-stance, potentially reducing the slipping behavior observed by the current robot.

Chapter 5 – Design, Manufacture, and Testing of Rumen ROV Locomotion Mechanism

5.1 Introduction

In the previous chapters, the focus has been on developing a strong fundamental understanding of the millipede traveling wave locomotion through modeling, biological experiments and observations (chapter 2), and emulating them on a millipede-inspired robot (chapters 3 and 4), with the intent of extracting an effective locomotion method to apply on a rumen ROV.

Prior to designing, the specifications for a rumen ROV design can be broken down into three main categories:

1 – Capable of exhibiting actively controlled locomotion within the rumen which comprises of an environment of varying material densities that stratifies both vertically and horizontally.

2 – Carry onboard sensors (pH, O_2, temperature, etc.) and have space to potentially collect samples.

3 – While initial designs maybe inserted through the cannula, ideally the design can be miniaturized into a bolus design that is swallowable by the cow.

In this chapter, the focus will be on the development, design, and testing of a millipede-inspired locomotion mechanism that meets the first specification listed above. Once this has been achieved, second and third features can be incorporated through design optimizations and miniaturizations of the component and drive electronics.

5.2 Initial prototype concept designs of rumen ROV capsule

While there are two bolus-based designs commonly used to track rumen characteristics, nothing commercially exists that incorporates an integrated active locomotion mechanism to permit traversing within the rumen itself. There is limited literature on addressing such problem specifically. Most of the prior research related to the development of active locomotion in-vivo has been done extensively for pillcam endoscopic capsule robot applications [65]. Several of these prior studies have incorporated active locomotion mechanisms, while others have primarily focused on anchoring capabilities, relying on the muscular contractions driving the device passively. Such devices include the work done by Avirovik et al. ([10], [11], [16]), where traveling wave and millipede legged locomotion was considered, however, the utilization of piezoelectric actuators resulted in the limited strain capabilities that would be ineffective in an environment as dynamic as the rumen. Other legged or appendage mechanism designs include Ref.'s [47]–[49], [66], [67]. Studies that focused on utilizing micro-adhesive techniques allowing the device to stay anchored in a desired place can be found in Ref.'s [42]–[45], [68]. Other locomotion mechanisms that utilize motors and shape memory alloys are discussed in Ref.'s [48], [51], [69]. The nature of these designs have been discussed in chapter 1.

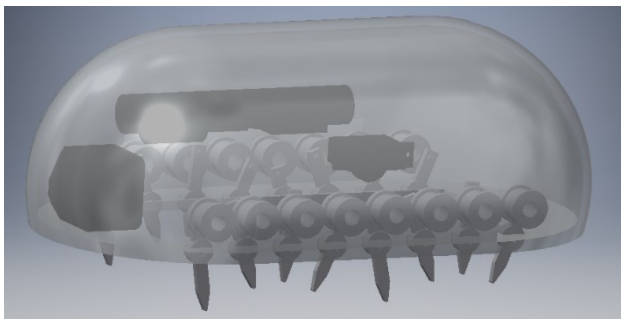

Figure 5.1: Initial simplistic millipede inspired locomotion applied to rumen ROV capsule design

Prior to the completion of the investigation in previous chapters on studying millipede locomotion, some initial designs were considered, based on some of the already existing locomotion technology and inspiration from biological mechanisms. From initial observations, the traveling wave, whether via flexible body or metachronal appendages, appeared to be a common extractable feature between locomotion mechanisms exhibited by nature for animals that would effectively burrow in high density (granular substrates) or low density (fluid) environments, such as Fish, Ctenophores, Scincus Scincus (sand swimmers), millipedes, worms etc. With this conceptual approach some initial mechanisms were designed:

Figure 5.1, was a millipede inspired design utilizing legs actuating in a metachronal gait fashion, generating a larger amplitude traveling wave, compared to [11]. However, this simplistic design certainly lacks the modulating wave locomotion burrowing techniques discussed in the previous chapters. Also, for a bolus design, the large protruding legs may cause discomfort and are likely to result in potential damage as large appendages.

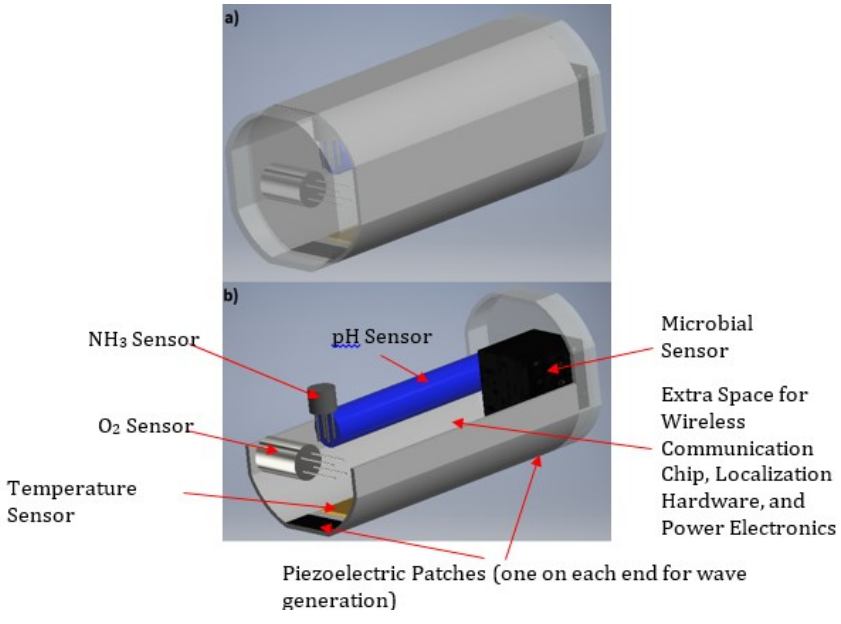

Figure 5.2: Conceptual design of using traveling wave beam driven by piezoelectric actuators to generate locomotion

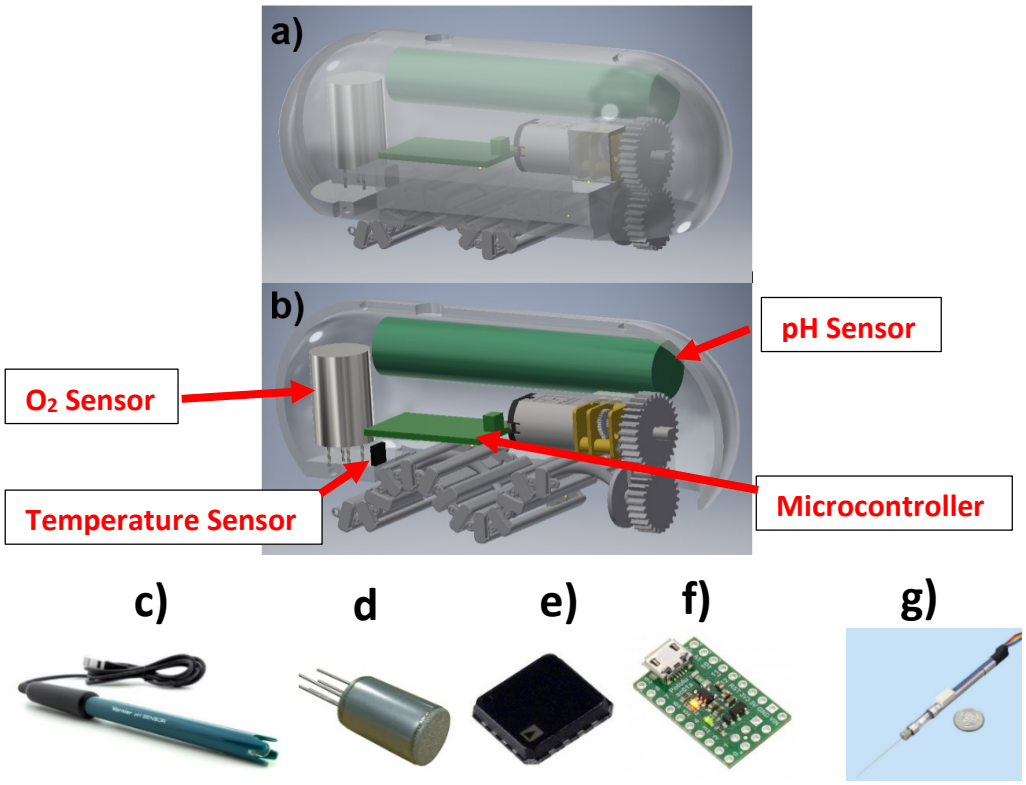

Figure 5.3: [fair use]
Proposed millipede inspired locomotion platform as a multi-sensing node (A) enclosed capsule platform, (B) open platform view of sensors and locomotion components, (C) Vernier pH sensor, (D) SST Sensing O_2 sensor, (E) ADT7420 Temperature sensor, (F) A-Star 32U4 Microcontroller, (G) Takasago Fluidic Systems SAP series syringe pump

Figure 5.2 takes inspiration from Avirovik et al. [16] who proposed potential locomotion from the traveling mechanical wave of a beam driven by piezoelectric ceramics. However, the limiting factor of this design would be the small strain achieved by the low amplitude traveling waves, while effective of a perfectly flat surface, in the difficult cluttered and viscous environment of the rumen larger amplitude actuation would be required to generate thrust.

An initial working prototype concept was designed by combining the features from the two designs shown in Figure 5.1 and 5.2, and taking inspiration from the single actuator wave-like (SAW) robot developed by Zarrouk et al. [18]. This SAW locomotion is a large amplitude traveling wave

(the mechanism design was discussed in chapter 1). While the wavelength or amplitudes cannot be modulated, it is driven by a single rotary motor that can adjust its angular velocity.

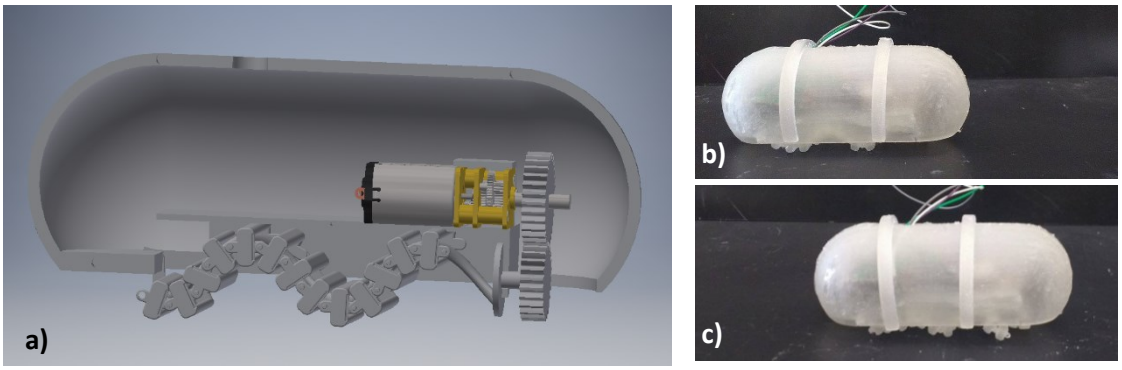

Figure 5.4: (A) Design of initial working prototype of rumen ROV capsule utilizing SAW mechanism (Zarrouk et al. 2016 [18]). (B)-(C) Time frame capture of prototype ROV device in motion

Figure 5.3 shows a concept design that is capable of holding the desired number of sensors on board the device in combination with control needed for such a locomotion mechanism. Figure 5.4 shows the locomotion design and demonstrates that the bolus capsule design is capable of locomotion (although not tested in a rumen environment). This was the initial conceptual prototype, which was incrementally improved to develop the optimum locomotion mechanism and improve performance based on the understanding of millipede locomotion.

5.3 Design of Millipede-inspired High Thrust Force Locomotion Mechanism

From initial observation of millipede locomotion and existing technologies, the focus was on traveling wave locomotion techniques. After carefully studying the locomotion technique exhibited by millipedes, it was found that to attain a powerful thrust, millipedes will modulate the

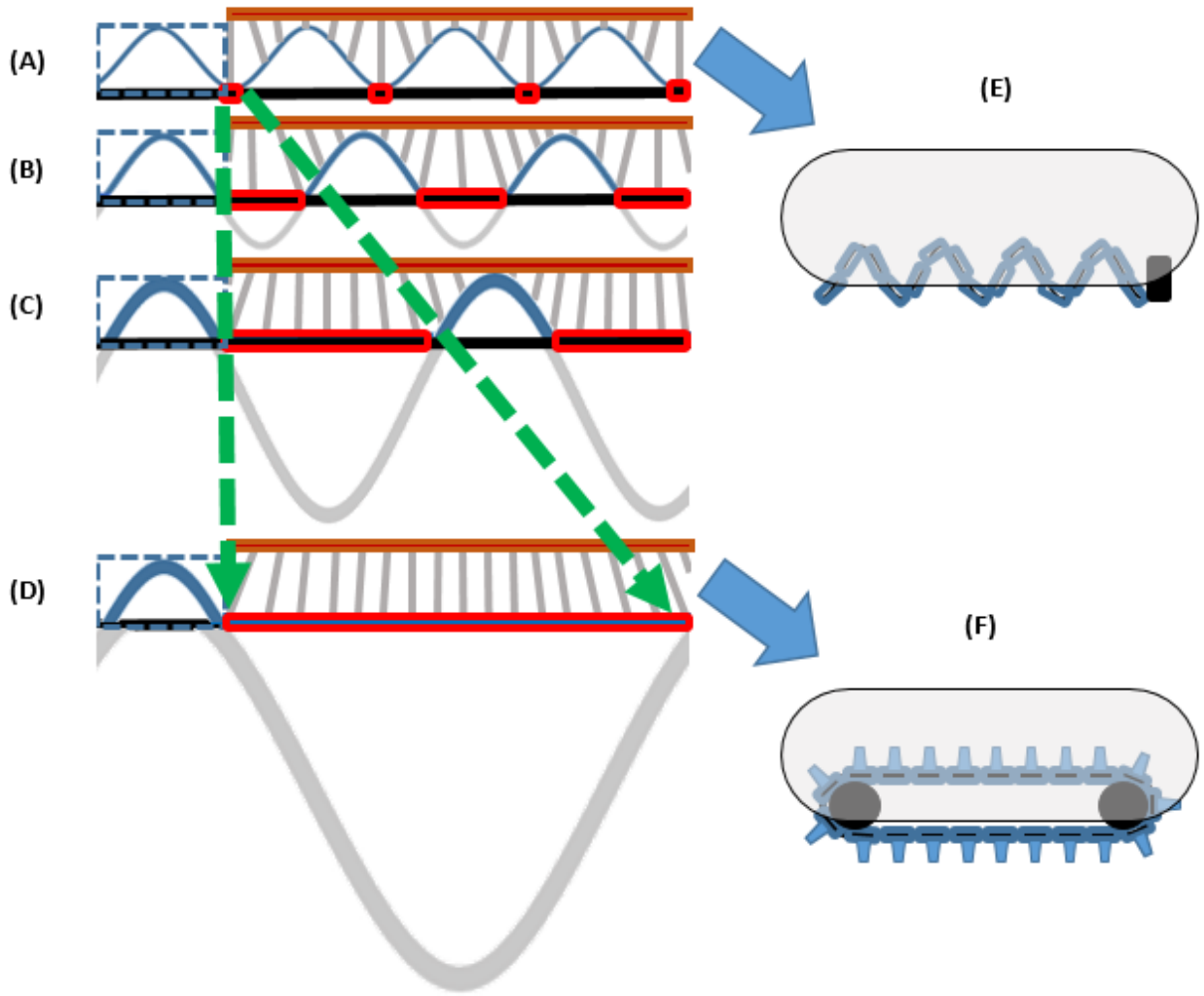

Figure 5.5: (A) Extrapolated illustration of traveling wave locomotion of lowest duty cycle and forward thrust force (B) Illustration of millipede low duty cycle and low forward thrust force (C) Illustration of millipede high duty cycle and low forward thrust force (D) Extrapolated illustration of traveling wave locomotion of highest duty cycle and forward thrust force

traveling wave characteristics (increasing length, amplitude, and mechanically clipping) by adjusting their metachronal gait. A visual of how this wave was modulated can be seen in Figure 5.5B and 5.5C. The effective traveling wave generated from an actual millipedes metachronal gait is clipped, possessing more than a single leg in contact with the ground per wave in order to support and carry its own weight forward. Figure 5.5B corresponds to a lower duty cycle gait, while Figure 5.5C illustrates a higher duty cycle.

Comparing these generated traveling wave gaits, to the locomotion technique implemented in the initial concept design in the previous section, would suggest that the traveling wave of the SAW mechanism [18] resembles the traveling wave generated by a metachronal gait of a very low duty cycle, and thus low thrust force (Figure 5.5A and E). Such a gait would be more effective for high speed, however not desirable for handling large resistive loads. To increase the thrust force of the locomotion technique, the wave form generated will need to be modulated both in wavelength and amplitude, however the wave form needs to be offset to emulate the 'constancy in forward strokes' as discussed in chapter 2 resulting in a mechanically clipped traveling wave form. To better understand the 'constancy in forward strokes' characteristic of the wave during the modulations, wavelength and amplitude modulations of the mechanically clipped wave were studied to try develop a single mechanism that could be easily actuated (some initial waveform modulation in wavelength and amplitude were determined using the models in chapter 2, such as shown in Figure 2.3). However, while this was an interesting design space to potentially pursue for fundamental

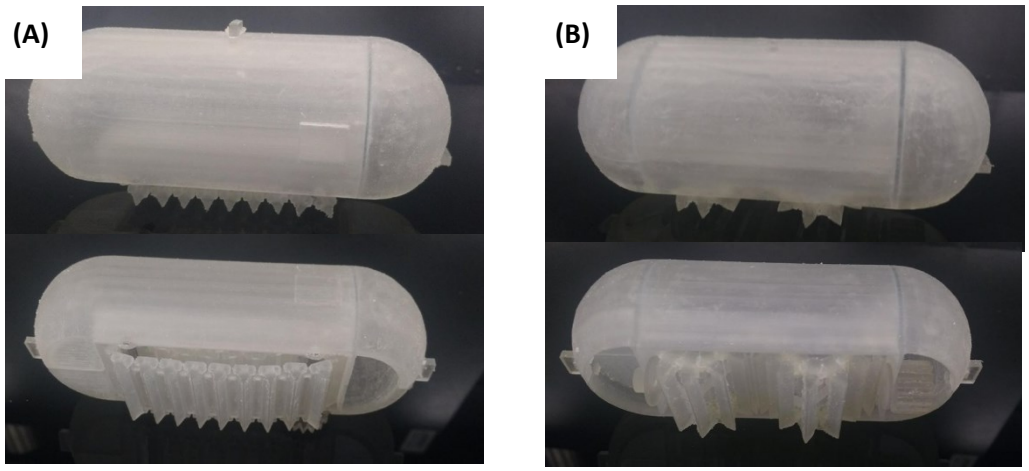

Figure 5.6: (A) Tread locomotion mechanism robot (B) Helix traveling wave locomotion mechanism (Zarrouk [18] SAW design)

Figure 5.7: Tread locomotion mechanism robot being tested for thrust force using experimental setup in chapter 4

understanding, for application in miniature robotic locomotion for the rumen ROV, this leads to the question of determining the desirable gait for the operation. For this specific application, the desired locomotion mechanism should be capable of handling large resistive forces against the desired direction of motion, as the rumen presents a high dense mud-like substrate.

If we extrapolate locomotion technique to generate maximum thrust force, the result is illustrated in Figure 5.5D and F, corresponding to duty cycle 1. While actual millipedes could physically demonstrate a gait of a duty cycle approaching 1, this would result in body velocity exponentially approaching zero (which in turn exponentially increases the cost of transport), and furthermore they may encounter issues of upright stability due to an increased dimensionless wavelength. However, in a robot design, other mechanisms can be used to accomplish this without having to deal with issues of stability and velocity. By extrapolating the modulated clipped traveling wave, the locomotion features reduce to a technique that resembles tank treads, conveyor belt or a wheel which have a continuous propulsion, which would eliminate issues of stability and low velocity. Such design would essentially be an extrapolation of the Whegs [46] mechanism mentioned in chapter 1. In comparison, this tread design accomplishes the advantage of legs or appendages, but

can also accomplish a maximum duty cycle of 1, while the Whegs design cannot attain the same continuous propulsion.

5.3.1 Comparative test of locomotion mechanisms

To test the hypothesis illustrated in Figure 5.5, the robots in Figure 5.6 were developed and compared with regards to their thrust force capabilities. Both robots were placed in the same experimental setup as the millipede robot in the previous chapter to measure forward thrust force. For comparing the thrust force between the two difference mechanisms, the same input angular velocity of the dc motor actuator was applied. For both devices, five different angular velocities were used as input. The results of the thrust output force (measured in dimensionless force, which is the ratio of the thrust force and the capsule robot weight) are shown in Figure 5.8. As shown in this figure, the tread design does provide a larger thrust force compared to the traveling wave design as hypothesized from our understanding of millipede locomotion behavior.

It is worth noting that this test was performed on a flat surface compared to a viscous and dense environment in which burrowing behavior would occur. In such environment, the volume displacement would need to be taken into account, which both mechanisms will be able to handle, just in a different fashion [70]. The traveling wave generated by the full body oscillatory behavior would generate a volume displacement related to its wave amplitude, while the traveling wave generated by the metachronal behavior of numerous appendages depends on the summation of volume displaced by each appendage or leg. The application of oscillatory body dynamics are typically larger animals with a focus for speed. The use of appendages are usually found in relatively smaller animals for burrowing via compaction (and some excavation) in a wet soil (plastic/granular) environment is consistent with observations found in [38], [70].

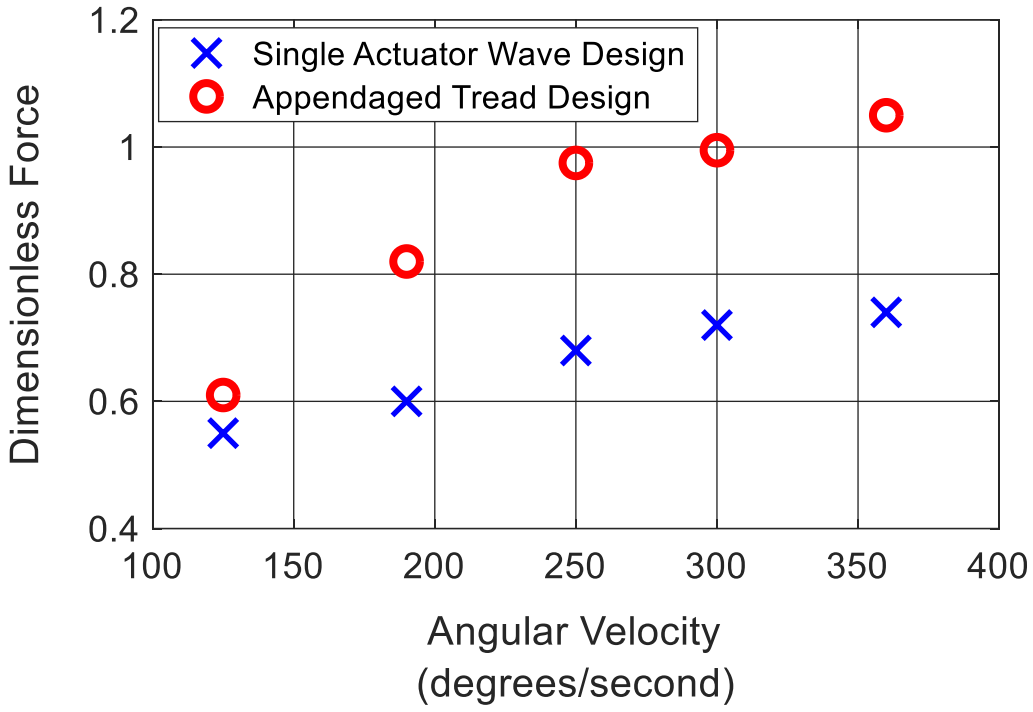

Figure 5.8: Comparative test between the tread locomotion mechanism and traveling wave mechanism: Dimensionless force vs Input motor angular velocity

From the observation on burrowing stage and using information from existing literature, we understand that the metachronal behavior of a system consisting of numerous appendages is effective for high thrust in burrowing applications of high density, plastic and/or wet granular environments. For a device to traverse within the rumen environment we need to also address whether such locomotion would be effective in fluid environments. The systems with many appendages found in nature operating in fluid come in the form of cilia. One species that utilizes these in a metachronal fashion is the ctenophore [71]. Similar to the millipede leg, the motion of cilia consists of a forward and backstroke,that could correspond to the elevation and propulsion stages of a leg. Such comparison can be seen in Figure 5.9. While the millipede leg typically operates on a solid surface or within a soil substrate which experiences plastic deformation, cilia function in a fluid environment.

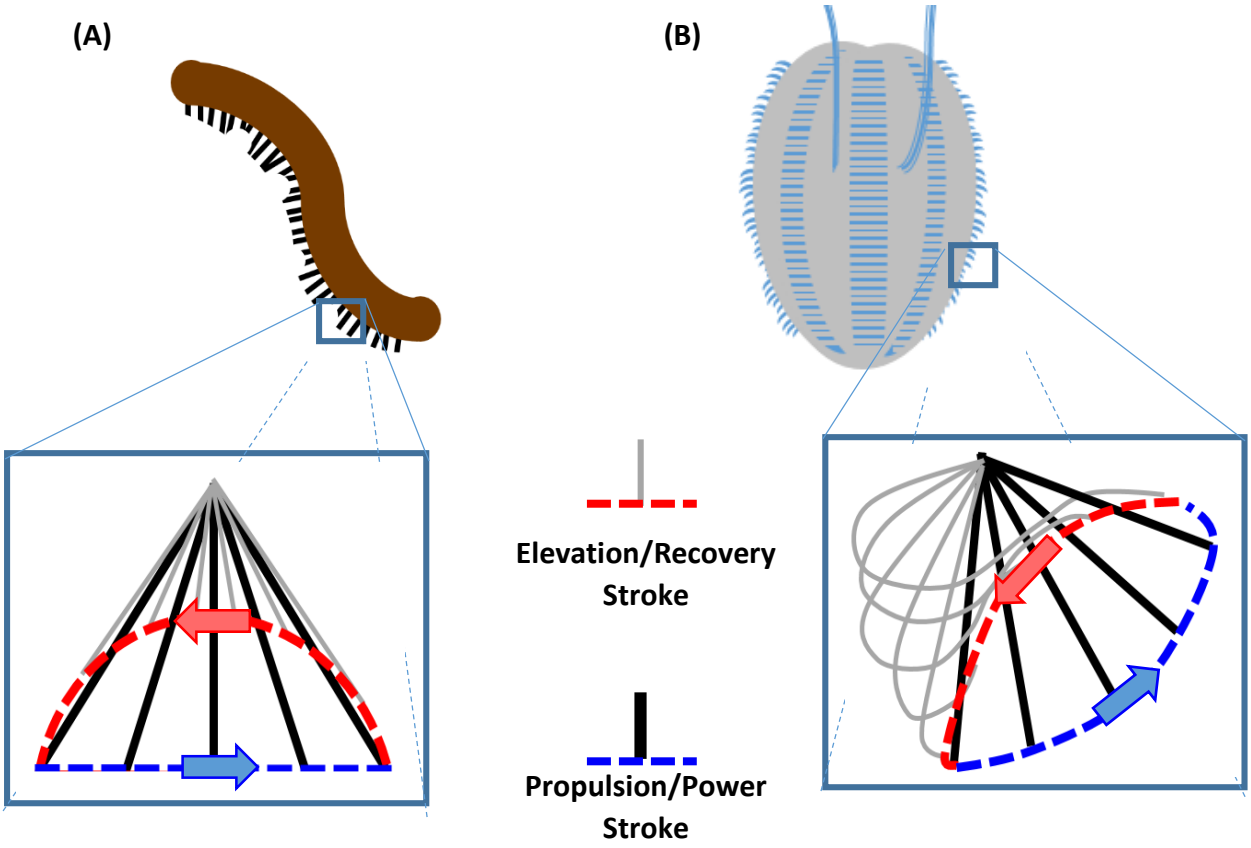

Figure 5.9: (A) Millipede leg motion (Propulsion stance and Elevated phase) (B) Ctenophore cilia motion (Power stroke and Recovery stroke)

Similar to burrowing activities [70], fluid propulsion characteristics differ between the full body wave locomotion compared to appendages metachronal behavior. Locomotion using a traveling wave along the body are generally used by larger and faster swimmers like fish, relying on inertial effects (high Reynolds number) caused by large body undulations or movements. On the other hand, locomotion from metachronal behavior of cilia, while slower, relies on the movement of small actuators and is characterized by viscous stresses or vorticity (low Reynolds number).

From these observations, while both the body traveling wave and metachronal behavior of appendages are utilized in nature for locomotion on the surface, burrowing, and swimming, for the rumen ROV application the series of appendages approach is advantages. For the rumen ROV,

operating in a mud-like environment is essential, requiring the maximum thrust force capabilities which has been demonstrated. Furthermore, knowledge of this locomotive behavior in ctenophore would suggest that the rumen ROV locomotion mechanism is at least functional in fluid environments, emulating multiple power strokes simultaneously. Such an example can be found looking at existing vehicle locomotion mechanisms, an appendaged tread design can be found in the Air Hogs Thunder Trax [72] remote-control all-terrain vehicle, which demonstrates swimming capabilities. While the body wave motion could work, this locomotion found in nature is more effective at high speed at the price of large body dynamics, compared to resisting large loads without significant physical disturbance to the surrounding environment.

5.3.2 Directional control design and testing

The developed millipede-inspired mechanism, in Figure 5.6A, is unidirectional and without steering capabilities on its own. Millipedes, as observed and discussed in chapter 2, can control their direction by use of an elongated segmented body consisting of a complex musculo-skeletal system with articulate joints. The ball-and-socket joint present between the body segments permitted 3-degree-of-freedom movements to effectively move in 3-dimensional space. While this

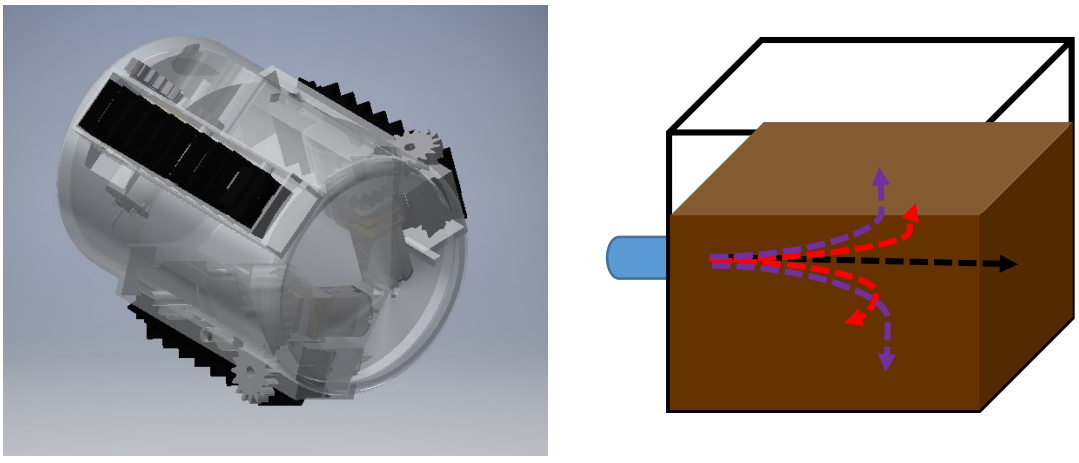

Figure 5.10: Rumen ROV locomotion mechanism with directional control via differential steering

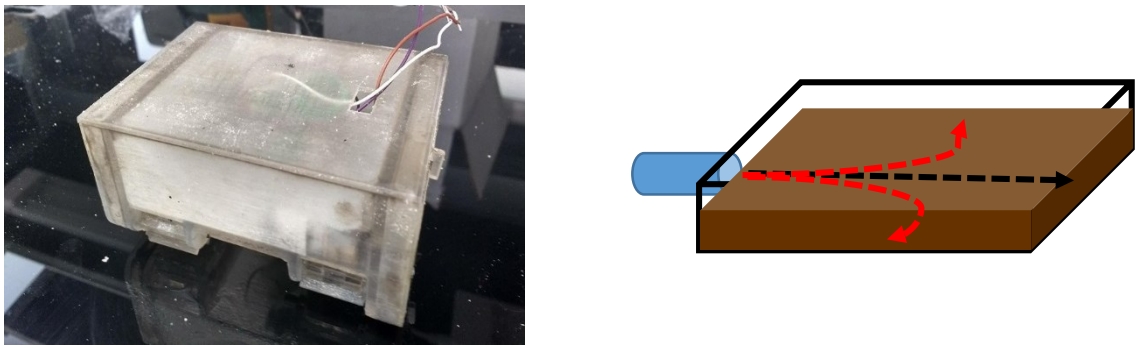

Figure 5.11: 2-dimensional locomotion mechanism with directional control via differential steering

may be effective in burrowing instances for a millipede, in the case of the rumen ROV application, incorporating a flexible body is not desirable in the dynamic environment of the rumen. This is because the rumen ROV's primary function requires a variety of on board sensors which need to be cased and protected from damage, as well as introducing more degrees of freedom in the robot design introduces new actuators and control schemes further complicating the mechanism.

Taking inspiration from both robotic platforms ([44], [72]) and biology (ctenophores [71]), the approach of differential steering was implemented to develop a rumen ROV capable of traversing the 3-dimensional environment of varying substrate densities. Such an approach involved utilizing the tread appendage mechanism design, and replicating it around the body of the capsule device. As shown in Figure 5.10, a minimum of three tracks were placed on the capsule in order to traverse in 3-dimensional space, each requiring a single actuator to control the direction or velocity of propulsion. Controlling the motors of each of the treads with different velocities permits the driver to induce a torque on the capsule.

While in application, the device would operate submersed in the rumen content three-dimensionally (Figure 5.10), to test the locomotion mechanism in such an environment is difficult. To simplify the process of testing if the mechanism is capable of operating in the highly dense and

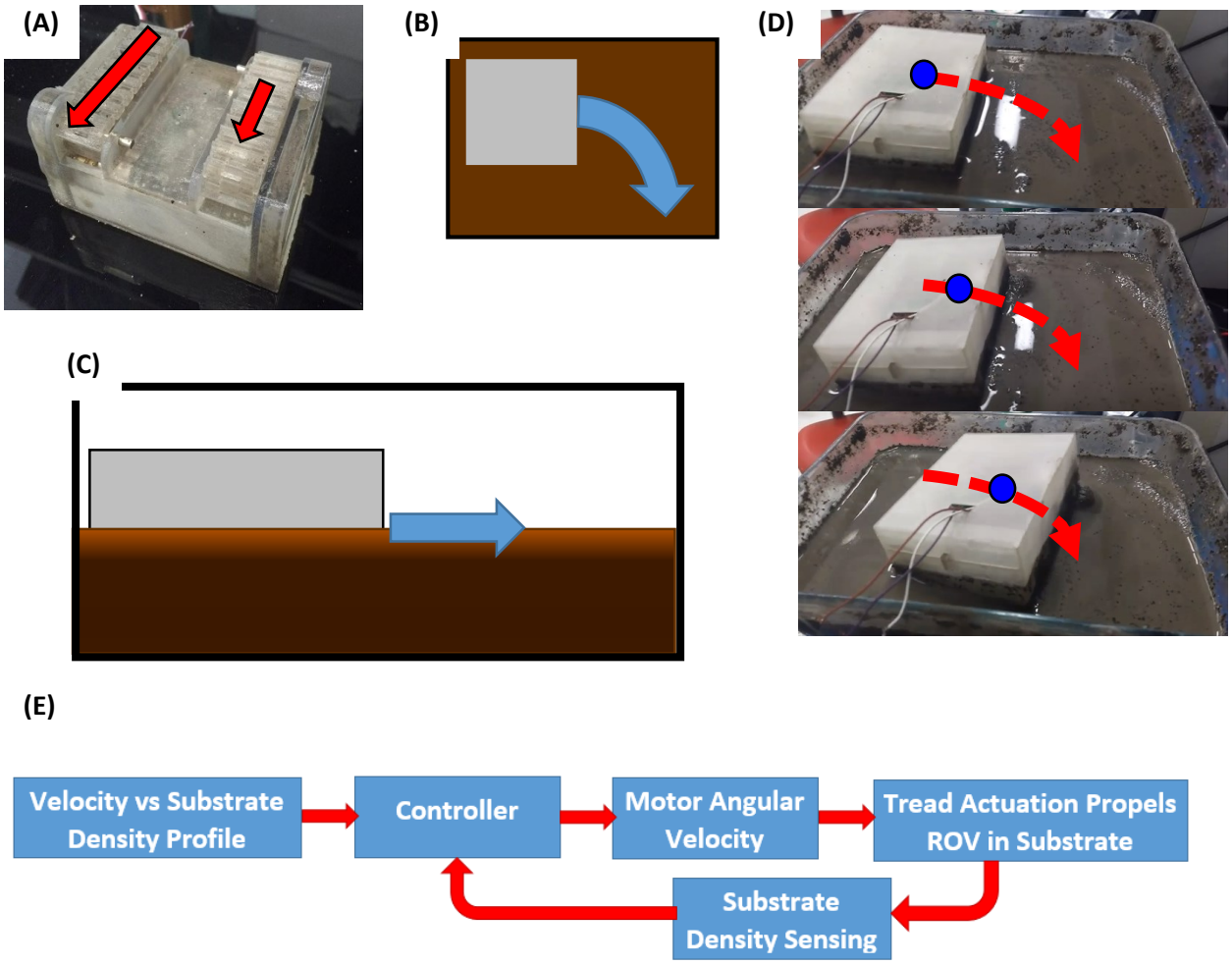

Figure 5.12: Two-dimensional experimental observation (A) Differential steering control, (B) Expected turning behavior, (C) Appendage tread locomotion mechanisms submerged underneath surface of mud (soil/sand/water mixture) to test burrowing capabilities, (D) Time frames of observation (E) Block diagram of potential closed-loop control scheme

viscous environment, a two-dimensional approach was taken (Figure 5.11). Observing operation in the two-dimensional case still allows us to test the ability to burrow through the substrate and differential steering control. To do this, a simple vehicle was assembled consisting of appendage tread designs (Figure 5.11). For this observational experiment, the vehicle was driven such that one tread set was faster than the other, which would result in turning the device (Figure 5.12A and B). To test the burrowing capability of the locomotion mechanism, the treads were placed fully

submersed underneath the surface of a mud mixture of soil, sand, and water, to emulate the dense and viscous nature of the rumen environment (Figure 5.12C).

Figure 5.12D shows a time lapse frame sequence of the device operating in the substrate. The mechanism was functioning in fully submersed condition in the dense mixture and achieved steering control. The device experienced some elevation during the locomotive effort, as there was no resistance above the surface, which would be existent in a fully submersed condition. The appendage tread design was able to traverse through the substrate, suggesting that the mechanism will be promising in the rumen environment.

5.4 Conclusion

In this chapter, the locomotion mechanism for a rumen ROV was investigated and developed. For a device operating in the rumen environment, the primary focus was the ability to traverse within the highly dense and viscous substrate present in the rumen. In the previous chapters, investigations were focused on the locomotion techniques utilized by millipedes for burrowing. Such locomotion ability with burrowing capability can be very promising in the rumen ROV application. While the traveling wave locomotion is one of the primary features associated with the millipede gait, and is commonly used in the design of miniature robots, extrapolating the manner in which millipedes modulate their behavior reveals a different ideal locomotion technique. Modulating their metachronal gait to achieve a complete travelling wave form actually reflects the strategy for maximizing speed, but at the price of reduced thrust force. On the other extreme, the traveling wave form is reduced to a continuous propulsion, resembling a conveyor belt or tread locomotion design. The effective thrust force results from the summation of many appendages overlapping in the propulsive phase. Actual millipedes cannot achieve this extreme

because of morphological limitations, related to the nature of musculoskeletal joints. However, this concept can be extracted and emulated on a robot locomotion mechanism, driven by a rotational actuator. Experiments were performed to confirm this hypothesis, that the appendage tread design generates a higher thrust force than a sinusoidal wave form.

The appendage tread design was also tested to demonstrate locomotion against large resistances presented by high density and viscosity mud substrate. Furthermore, the mechanism when replicated on the same device, displayed the ability of differential steering. While the locomotive mechanism has been demonstrated, applying open-loop differential steering control, the ideal case would be to incorporate a closed-loop automated control system. The actuation of the appendage tread mechanisms should be determined by the nature of the substrate it is currently encountering, which will vary in density. Actual millipedes encounter their surroundings using their antennae as sensors, which provide feedback to dictate their locomotive behavior. For a rumen ROV, sensing the current substrate density to indicate if encountering a mud-like or water-like environment would be needed to determine the ideal angular velocity for the tread to operate at, as simple control scheme is shown in Figure 5.12E. The nature of the sensor would need to be determined, whether using larger mechanical mechanisms or potentially even bacteriabots. While this goes beyond the context of the work in this chapter, in potential future work it would be determined by the desired performance and scale of the rumen ROV application.

The work in this chapter abstracted the key behavior in millipede locomotion to effectively burrow, and reflected such concepts on a mechanism to apply on a rumen ROV design. The mechanism was successful in traversing in a rumen-like substrate, and demonstrated the ability directional control.

Chapter 6 – Conclusions and Future Work

In this dissertation, the locomotion mechanism inspired by millipede was developed for a miniature remotely operated vehicle (ROV) designed for dynamic sensing within the rumen. The data gathered by the vehicle will improve our understanding of animal's physiology and real-time influence of changes in environmental factors. Such interest is drawn from the need to improve safety and food production efficiency. In the larger context, the developed mechanism for in-situ sensing would assist the implementation of precision animal agriculture.

The rumen dynamic environment and varying content densities present complexity to maneuver the mobile sensing node or rumen ROV. To resolve this issue, a bio-inspired approach was adopted in this thesis to design ROV with required thrust capabilities. Fundamental investigations were conducted focusing on understanding the origin of impressive large thrust forces exhibited by millipedes. An extensive bio-mechanics study comprising of controlled experiments on millipedes in combination with analytical modeling, was described in chapter 2. In chapters 3 and 4 a millipede-inspired robot was designed, fabricated, and tested. The millipede robot was used to validate the developed analytical model and validate model was used to provide guidance for the design and development of robotic platform. The experiments on robot confirmed the conclusions that millipedes' duty cycle (behavior variable) and number of body segments (morphology parameter) were the key factors in their thrust force abilities. In chapter 5, the millipede locomotion model was used to develop the design for a rumen ROV locomotion mechanism that can sustain environments of large resistances to motion. The locomotion mechanism was tested in the

environment consisting of large resistive forces, and results were used to guide the development of efforts in directional control.

Following sections provide discussion on future work related to various aspect of this dissertation covering millipede bio-mechanical locomotion model providing understanding of the variation in thrust force capabilities (chapter 2), the development of a millipede-inspired robot to extend the learning through controlled experimentation and emulate key factors indicated from the model (chapters 3 and 4), and lastly utilizing these foundational concepts of millipede locomotion to design a locomotion mechanism for a rumen ROV.

6.1 Millipede Simulation Model

6.1.1 Summary

In chapter 2, a detailed analysis on the bio-mechanics of millipede locomotion was performed. Millipedes were studied because of their ability to generate large thrust force abilities demonstrated in tasks such as burrowing and climbing. It was found that their bodies utilized the elongated segmented morphology to accomplish directional control and conform to varying surface or substrate, and traversed with a metahchronal gait, generating a traveling wave mode of locomotion. The ability to handle a large variety resistive loads comes from modulation of the metachronal gait. To investigate the gait adjustments when encountering increasing resistive loads in the direction of motion, the specimens were subjected to two different experimental stages. The experimental stages involved a platform encouraging gait variation by introducing various incline surfaces, and the other was a stage developed to try to emulate the burrowing phenomenon.

For both experiments, video tracking analysis was performed for determining the kinematics, gait behavior and morphological parameters. From the data, a dynamic (quasi-static) simulation model was developed to investigate the variables that have significant influence on the thrust output. The results indicate that the primary factors in controlling the generated thrust force in the direction of motion were the duty cycle of the gait (a behavioral variable), and the number of body segments/legs (a morphological parameter).

6.1.2 Future work

The developed simulation model investigated the effects of various parameters, from the gait behavior to morphology, on the generation of thrust force in the direction of motion. This was of interest on two fronts, the first was the specific application of developing the rumen ROV locomotion mechanism that can effectively operate in that complex environment. The second was to extract and reveal the fundamental mechanics that make millipedes effective in burrowing. In doing so the thesis tries to answer questions related to the traveling wave locomotion behavior and influence of morphology on the locomotive performance. These discussions broaden our understanding and open up new design spaces for designing locomotion of miniature robotics.

While the model provides an avenue for illuminating such a design space, there are several other aspects of millipede locomotion that it does not capture in the current form. The simulation model is currently only two-dimensional, and the analysis has been performed by deriving the effects on the axial loads (or resistive forces in the direction of motion). In future, modeling of the articulate movements in turning, climbing, and rotation would be of great interest. Such model would allow us to determine the essential governing factors used by millipedes to achieve precise energy efficiency movements, whether it be the range of motion of the segment joints, the relative size of the segments, the bodies musculature, etc.

There are two other facets of the millipede locomotion that would be of significant interest in further understanding of the gait modulations to achieve effective burrowing. The first would be modeling the effects of the metachronal traveling wave gait when vertical or radial loads are encountered (perpendicular to the direction of motion), and secondly the changes in gait variation beyond the desirable resistance, e.g. when encountering (axial) loads over twice their weight. These gait behaviors were observed in the experiments, and revealed relatively sporadic behavior. A few initial speculations of changes in gait behavior (effecting the generated traveling wave locomotion) are that changes occur with the other gait variables which initially stay relatively constant, such as leg phase (constant forward strokes profile), stride length, and most importantly the individual leg effort. While the model was indicative that changing the other gait variables did not have a significant (if any) effect on the thrust force, that all can change if the effort of the individual leg is adjusted. Essentially, the gait modulations with increased resistance in the axial direction was representative of a system operating in a space constrained by several fixed parameters, reducing the control of locomotion down to a primary variable. Adjusting the individual leg effort opens up that space, where the other previously fixed variables need to be redefined to constrain the locomotive system or are free variables of their own.

While the current model can provide understanding of the millipede locomotion behavior and morphological advantages for their specialized performance in burrowing, the simulation model can certainly be further developed in its robustness, to capture more dynamic aspects of its locomotion.

6.2 Millipede-inspired robot

6.2.1 Summary

In chapters 3 and 4, a millipede-inspired robot was designed based upon the primary characteristics of millipede locomotion observed and modeled in the prior chapter. The robot was fabricated and tested to quantify the millipede gait variations responsible for improving thrust force.

In the development of the robot, while it is desirable to mimic the biological creature completely, limitations in engineering technologies require prioritizing the elements of its behavior and morphology in order to capture the desired millipede gait characteristics. Similar to the simulation model, the priority was on understanding the ability to increase thrust force in the direction of motion using the metachronal gait. Chapter 3 illustrates the process of designing and manufacturing the robots' mechanisms and controls, prioritizing the study with influence of duty cycle and number of body segments on thrust force in straight line locomotion.

In chapter 4, the robot was tested to explicitly determine if we can emulate the varying thrust force behavior demonstrated by observations on millipede and predicted by the model. The results indicate that the robot performance was consistent with the model kinematics and dynamic predictions, indicating that the conclusions drawn from the model regarding the parameters that dictate thrust force abilities are significantly relevant.

6.2.2 Future work

There are two different directions to pursue with regards to the millipede-inspired robot. The first direction is similar to the evolution of simulation model which emphasizes understanding of structural, behavioral, and physiological parameter influencing the gait dynamics. The robot was developed focused on testing primarily the influence of duty cycle and number of segments on the

thrust force capabilities. In this direction, the next steps for the robot design would be to test variation in the other gait parameters (such as stride length, phase difference, etc.) to quantify their influence on the robot locomotion. Further, high resolution 3D body motion analysis can be included to emulate the articulately controlled 3-degree-of-freedom motion between segments.

Regarding the gait behaviors, implementing variations on the current robot design are possible. In the current robot morphology, the distance between leg pairs (d) is fixed, with a stride length determined with a fixed leg length and the larger radius of the cam mechanism. Both these variables dictate the phase, as given by equation 2.25. Adjusting the leg length will introduce changes in stride length, which would change the leg phase. While this leg phase observed in the biological specimens, likely relate to the vertical support created by the bodies musculature, for the robot, like the model, these parameters can be adjusted independently.

Incorporating the 3-degree-of-freedom movement between body segments can be accomplished using a ball-and-socket joint (Figure 3.12), rather than a hinge joint (which was used in the current robot). Furthermore, incorporating control of body movement would be intriguing. Currently the robot uses springs between body segments in order to maintain upright vertical support. One direction that can be considered to provide actuation control and support is use of shape memory alloy springs between segments to articulate the joint, similar to that in Ref. [15]. Improving the robot in parallel with simulation model by testing different variables will allow further validation in pursuit of better understanding of the locomotion capabilities of millipedes.

The second direction would be pursuit to more closely match the biological performance. Currently the robot is significantly larger (> x10 in volume) due to limitations in available actuators and manufacturing processes for rapid prototyping. While there are on-going efforts to improve and miniaturize traditional actuators like DC motors, shape memory alloys, and piezo-electric

materials, they still possess limitations that fall short of the ability of muscle fibers found in biology. Current research that may eventually narrow the gap in mimicking the biological specimens are efforts made with "Bio-bots". Whether in the form of developing bio-actuators from skeletal muscle cells (such as work done in Ref. [73]–[75]) or control of actual biological animals with neural engineering (such as Ref. [76]). Figure 6.1 shows both approaches.

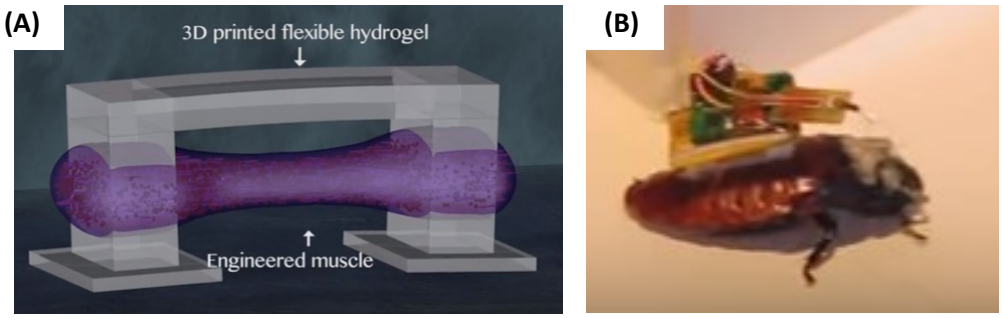

Figure 6.1: [used with permission]
Example of "Biobots" (A) Developed bio-actuator from skeletal muscle that can be externally stimulated for control (B) RoachBot – control of the cockroach animal via attached electronic backpack

The development of bio-actuators using muscle tissue, would open a large design space for engineering miniature locomotion techniques, particularly in bio-inspired or mimicking applications. An actuator capable of miniaturization, while exhibiting large force and repeatable high strain, would allow to implement a millipede robot design that operates at closer spatial scales. With regards to the neural engineering approach, if this could be achieved, explicit control of a millipedes' locomotion would allow us to directly implement a wide range of different gaits and observe the resulting behaviors.

6.3 Millipede-inspired Rumen ROV

6.3.1 Summary

One of the primary goals of this dissertation was to develop a locomotion mechanism relevant for the remotely operated vehicle traversing within the rumen environment. The rumen can be as large

as 100L in volume, containing 90kg of content varying in consistency and experiencing perturbations from violent muscular contractions. A variation in density stratifies vertically, from a low viscous water-like fluid mixture to high viscous conditions resembling oatmeal or mud.

In chapter 5, such locomotion mechanism was developed taking inspiration from millipedes. The fundamental principles of millipede locomotion that made them effective burrowers were extracted and translated into the design in order to achieve high thrust force capabilities against an environment providing resistance to motion. The modulations of the traveling wave behavior observed in millipedes were extrapolated to the extremes, which corresponded to either high velocity or high thrust force. To achieve high thrust force performance, the waveform is essentially reduced to a tread-like locomotion mechanism. To test this hypothesis, a simple experiment was done comparing the thrust force abilities of an unclipped traveling waveform mechanism against the tread locomotion mechanism. The results shown in Figure 5.8 confirmed the conclusions.

To achieve directional control, this locomotion mechanism was replicated around a capsule design, to achieve differential steering. For experimental and observational purposes, a 2-dimensional representation of viscous and dense environment was used. A simple vehicle was assembled, possessing two appendaged treads to implement differential steering. The vehicle was tested in the soil, sand, and water (mud) mixture to try replicate the varying and highly viscous and dense environment of the rumen. The mechanism demonstrated the ability to operate in such environments with effective directional control and high enough thrust force to traverse the mud substrate.

6.3.2 Future work

The work done in this dissertation demonstrated a locomotion mechanism that can handle the varying substrate environment with directional control. While the mechanism has successfully traversed in the high viscous environments and demonstrated directional control, the next step would be to test the 3-dimensional design (Figure 6.2) ex-vivo with actual rumen content, followed eventually by in-vivo experiments.

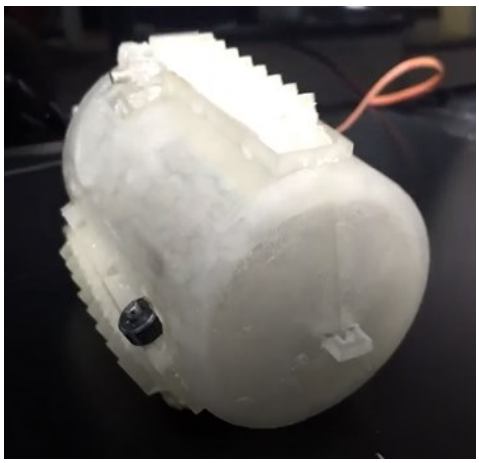

Figure 6.2: Developed 3-dimensional concept design of functioning rumen ROV locomotion mechanism with directional control via differential steering

While the focus of this work has been on the locomotive mechanism, future investigation on the desirable shape of the capsule that can be most effective in traversing within the rumen content should be done in order to determine optimal performance. Variation in shapes are even seen between the millipede species investigated in chapter 2, when utilizing a large surface for compaction burrowing (*N. americanus)* or narrower for burrowing by insertation (*A. virginiensis)*. The fact that the rumen ROV is substantially larger would also need to be considered. Furthermore, monitoring and sensing features on the rumen ROV will need to be integrated in the capsule design. Lastly, miniaturizing the device (while considering the scalability of the existing sensor technologies) would be desirable for ease of implementation.

References

[1] J. Gookin, D. Foster, A. Harvey, and D. McWhorter, "An Animated Model of Rumen Motility," 2009. [Online]. Available: https://projects.ncsu.edu/project/cvm_gookin/rumen_motility.swf. [Accessed: 02-Oct-2017].

[2] "Smaxtec - Inside Monitoring." [Online]. Available: https://www.smaxtec.com/en/.

[3] "Dascor." [Online]. Available: http://www.dascor.com/index.html.

[4] H. Nogami, S. Arai, H. Okada, L. Zhan, and T. Itoh, "Minimized bolus-type wireless sensor node with a built-in three-axis acceleration meter for monitoring a Cow's Rumen conditions," *Sensors (Switzerland)*, vol. 17, no. 4, 2017.

[5] T. Ho, S. Choi, and S. Lee, "Development of a Biomimetic Quadruped Robot," *J. Bionic Eng.*, vol. 4, no. 4, pp. 193–199, 2007.

[6] R. J. Bachmann, F. J. Boria, R. Vaidyanathan, P. G. Ifju, and R. D. Quinn, "A biologically inspired micro-vehicle capable of aerial and terrestrial locomotion," *Mech. Mach. Theory*, vol. 44, no. 3, pp. 513–526, 2009.

[7] G. Fischer, M. Gogola, E. Garcia, and M. Goldfarb, "Development of a piezoelectrically-actuated mesoscale robot quadruped," *J. Micromechatronics*, vol. 1, no. 3, pp. 205–219, 2001.

[8] P. Birkmeyer, K. Peterson, and R. S. Fearing, "DASH: A dynamic 16g hexapedal robot," in *2009 IEEE/RSJ International Conference on Intelligent Robots and Systems, IROS 2009*, 2009, pp. 2683–2689.

[9] A. M. Hoover, E. Steltz, and R. S. Fearing, "RoACH: An autonomous 2.4g crawling hexapod robot," in *2008 IEEE/RSJ International Conference on Intelligent Robots and Systems, IROS*, 2008, pp. 26–33.

[10] D. Avirovik and S. Priya, "Crawling-inspired robot utilizing L-shape piezoelectric actuators," in *2013 IEEE/ASME International Conference on Advanced Intelligent*

Mechatronics: Mechatronics for Human Wellbeing, AIM 2013, 2013, pp. 894–899.

[11] D. Avirovik, B. Butenhoff, and S. Priya, "Millipede-inspired locomotion through novel U-shaped piezoelectric motors," *Smart Mater. Struct.*, vol. 23, no. 3, p. 037001, 2014.

[12] A. K. Eigoli and G. R. Vossoughi, "Locomotion modes of a novel piezo-driven microrobot: Analytical modeling and performance evaluation," *Mech. Mach. Theory*, vol. 52, pp. 248–266, 2012.

[13] K. A. Daltorio, A. S. Boxerbaum, A. D. Horchler, K. M. Shaw, H. J. Chiel, and R. D. Quinn, "Efficient worm-like locomotion: Slip and control of soft-bodied peristaltic robots," *Bioinspiration and Biomimetics*, vol. 8, no. 3, 2013.

[14] A. A. Calderon, J. C. Ugalde, J. C. Zagal, and N. O. Perez-Arancibia, "Design, fabrication and control of a multi-material-multi-actuator soft robot inspired by burrowing worms," *2016 IEEE Int. Conf. Robot. Biomimetics, ROBIO 2016*, pp. 31–38, 2016.

[15] H. Yuk, D. Kim, H. Lee, S. Jo, and J. H. Shin, "Shape memory alloy-based small crawling robots inspired by C. elegans," *Bioinspiration and Biomimetics*, vol. 6, no. 4, 2011.

[16] D. Avirovik, V. V. N. S. Malladi, S. Priya, and P. A. Tarazaga, "Theoretical and experimental correlation of mechanical wave formation on beams," *J. Intell. Mater. Syst. Struct.*, vol. 27, no. 14, pp. 1939–1948, 2016.

[17] D. Zarrouk and M. Shoham, "Analysis and Design of One Degree of Freedom Worm Robots for Locomotion on Rigid and Compliant Terrain," *J. Mech. Des.*, vol. 134, no. 2, p. 021010, 2012.

[18] D. Zarrouk, M. Mann, N. Degani, T. Yehuda, N. Jarbi, and A. Hess, "Single actuator wave-like robot (SAW): Design, modeling, and experiments," *Bioinspiration and Biomimetics*, vol. 11, no. 4, 2016.

[19] D. Koh, J. Yang, and S. Kim, "Centipede robot for uneven terrain exploration: Design and experiment of the flexible biomimetic robot mechanism," in *2010 3rd IEEE RAS and EMBS International Conference on Biomedical Robotics and Biomechatronics, BioRob 2010*, 2010, pp. 877–881.

[20] K. L. Hoffman and R. J. Wood, “Passive undulatory gaits enhance walking in a myriapod millirobot,” in *IEEE International Conference on Intelligent Robots and Systems*, 2011, pp. 1479–1486.

[21] K. L. Hoffman and K. L. Hoffma, “Design and Locomotion Studies of a Miniature Centipede-Inspired Robot,” 2013.

[22] S. M. Manton, “The evolution of arthropodan locomotory mechanisms - part 3: The locomotion of Chilopoda and Pauropoda,” *J. Linn. Soc. London*, vol. 42, pp. 118–166, 1951.

[23] S. M. Manton, “The evolution of arthropodan locomotory mechanisms - part 4: The structure, habits and evolution of the diplopoda,” *J. Linn. Soc. London*, vol. 42, pp. 299–368, 1953.

[24] P. E. Marek, W. A. Shear, and J. E. Bond, “A redescription of the leggiest animal, the millipede Illacme plenipes, with notes on its natural history and biogeography (Diplopoda, Siphonophorida, Siphonorhinidae),” *Zookeys*, vol. 241, pp. 77–112, 2012.

[25] A. Minelli, *Treatise on Zoology - Anatomy, Taxonomy, Biology. The Myriapoda, Volume 2*. BRILL, 2016.

[26] A. Minelli, *Treatise on Zoology - Anatomy, Taxonomy, Biology. The Myriapoda, Volume 1*. BRILL, 2011.

[27] T. Kano, K. Sakai, K. Yasui, D. Owaki, and A. Ishiguro, “Decentralized control mechanism underlying interlimb coordination of millipedes Decentralized control mechanism underlying interlimb coordination of millipedes,” 2017.

[28] K. Yasui, K. Sakai, T. Kano, D. Owaki, and A. Ishiguro, “Decentralized control scheme for myriapod robot inspired by adaptive and resilient centipede locomotion,” *PLoS One*, vol. 12, no. 2, pp. 1–12, 2017.

[29] J. Park, K. Kim, and S. Kim, “Sliding Mode Control of Locomotion for a Biomimetic Robot Inspired by Pillbugs,” *Time*, pp. 2392–2396, 2010.

[30] S. M. Manton, “The Evolution of Arthropodan Locomotory Mechanisms.– Part 5. the

Structure, Habits and Evolution of the Pselaphognatha (Diplopoda).," *J. Linn. Soc. London, Zool.*, vol. 43, no. 290, pp. 153–187, 1957.

[31] S. M. Manton, "The Evolution of Arthropodan Locomotory Mechanisms.– Part 6. Habits and Evolution of the Lysiopetaloidea [Diplopoda], some principles of leg design in diplopoda and chilopoda, and limb structure of diplopoda.," *J. Linn. Soc. London, Zool.*, vol. 43, no. 290, pp. 488–554, 1957.

[32] S. M. Manton, "The Evolution of Arthropodan Locomotory Mechanisms.– Part 7. Functional requirements and Body Design in Colobognatha (Diplopoda), together with comparative account of diplpod burrowing techniques, trunk musculature and segmentation," *J. Linn. Soc. London, Zool.*, vol. 44, pp. 384–460, 1960.

[33] S. Hopkins and H. Read, *The biology of millipedes*. Oxford University Press, 1992.

[34] H. M. Wilson, "Muscular anatomy of the millipede Phyllogonostreptus nigrolabiatus (Diplopoda: Spirostreptida) and its bearing on the millipede 'thorax,'" *J. Morphol.*, vol. 251, no. 3, pp. 256–275, 2002.

[35] B. J. Borrell, "Mechanical properties of calcified exoskeleton from the neotropical millipede, Nyssodesmus python," *J. Insect Physiol.*, vol. 50, no. 12, pp. 1121–1126, 2004.

[36] W. Liu, S. Golovatch, T. Wesener, and M. Tian, "Convergent evolution of unique morphological adaptations to a subterranean environment in cave millipedes (Diplopoda)," *PLoS One*, vol. 12, no. 2, pp. 1–21, 2017.

[37] P. Marek, "Ultraviolet-induced fluorescent imaging for millipede taxonomy," *Res. Ideas Outcomes*, vol. 3, p. e14850, 2017.

[38] J. J. Bowen and D. I. Hembree, "Neoichnology of two spirobolid millipedes: improving the understanding of the burrows of soil detritivores," *Palaeontol. Electron.*, vol. 17, no. 1, pp. 1–48, 2014.

[39] A. Francisco, C. S. Fontanetti, and R. C. F. Nocelli, "The nervous system of the neotropical millipede Gymnostreptus olivaceus Schubart, 1944 (Spirostreptida, Spirostreptidae) shows an additional cell layer," *Anim. Biol.*, vol. 65, no. 2, pp. 133–150, 2015.

[40] P. Marek, “Marek Lab - Systematic Entomology.” [Online]. Available: http://jointedlegs.org/.

[41] G. Newport, “On the Structure , Relations , and Development of the Nervous and Circulatory Systems , and on the Existence of a Complete Circulation of the Blood in Vessels , in Myriapoda and Macrourous Arachnida . First Series Author (s): George Newport Source : Phi,” *Philos. Trans. R. Soc. London*, vol. 133, no. 1843, 2018.

[42] M. E. Karagozler, E. Cheung, J. Kwon, and M. Sitti, “Miniature endoscopie capsule robot using biomimetic micro-patterned adhesives,” *Proc. First IEEE/RAS-EMBS Int. Conf. Biomed. Robot. Biomechatronics, 2006, BioRob 2006*, vol. 2006, pp. 105–111, 2006.

[43] P. Glass, E. Cheung, and M. Sitti, “A legged anchoring mechanism for capsule endoscopes using micropatterned adhesives,” *IEEE Trans. Biomed. Eng.*, vol. 55, no. 12, pp. 2759–2767, 2008.

[44] L. J. Sliker, M. D. Kern, J. A. Schoen, and M. E. Rentschler, “Surgical evaluation of a novel tethered robotic capsule endoscope using micro-patterned treads,” *Surg. Endosc. Other Interv. Tech.*, vol. 26, no. 10, pp. 2862–2869, 2012.

[45] J. Kwon, E. Cheung, S. Park, and M. Sitti, “Friction enhancement via micro-patterned wet elastomer adhesives on small intestinal surfaces,” *Biomed. Mater.*, vol. 1, no. 4, pp. 216–220, 2006.

[46] S. N. Gorb, M. Sinha, A. Peressadko, K. A. Daltorio, and R. D. Quinn, “Insects did it first: A micropatterned adhesive tape for robotic applications,” *Bioinspiration and Biomimetics*, vol. 2, no. 4, 2007.

[47] M. Quirini, R. J. Webster, A. Menciassi, and P. Dario, “Design of a pill-sized 12-legged endoscopic capsule robot,” *Proc. - IEEE Int. Conf. Robot. Autom.*, no. April, pp. 1856–1862, 2007.

[48] S. Park *et al.*, “Multi-functional capsule endoscope for gastro-intestinal tract,” *2006 SICE-ICASE Int. Jt. Conf.*, pp. 2090–2093, 2006.

[49] H. M. Kim *et al.*, “Active locomotion of a paddling-based capsule endoscope in an in vitro and in vivo experiment (with videos),” *Gastrointest. Endosc.*, vol. 72, no. 2, pp. 381–387,

2010.

[50] H. Liang, Y. Guan, Z. Xiao, C. Hu, and Z. Liu, “A screw propelling capsule robot,” *2011 IEEE Int. Conf. Inf. Autom. ICIA 2011*, no. 2009, pp. 786–791, 2011.

[51] R. Carta *et al.*, “Wireless powering for a self-propelled and steerable endoscopic capsule for stomach inspection,” *Biosens. Bioelectron.*, vol. 25, no. 4, pp. 845–851, 2009.

[52] J. Sathirapongsasuti, N. Punnanithi, and P. Wimonkittiwat, “Walking with a millipede,” in *Intel ISF*, 2004.

[53] A. Garcia, S. Priya, and P. Marek, “Understanding the locomotion and dynamic controls for millipedes: Part 1 - Kinematic analysis of millipede movements,” in *ASME Conference of Smart Materials, Adaptive Structures and Intelligent Systems*, 2015, pp. 1–10.

[54] J. N. Siddall, “The wave mode of walking locomotion,” *J. Terramechanics*, vol. 1, no. 4, pp. 54–73, 1964.

[55] J. Fang, C. Jiang, and D. Terzopoulos, “Modeling and animating myriapoda,” *Proc. 12th ACM SIGGRAPH/Eurographics Symp. Comput. Animat. - SCA ’13*, no. i, p. 203, 2013.

[56] Y. Tanaka, K. Ito, T. Nakagaki, and R. Kobayashi, “Mechanics of peristaltic locomotion and role of anchoring,” *J. R. Soc. Interface*, vol. 9, no. 67, pp. 222–233, 2012.

[57] D. Spinello and J. S. Fattahi, “Peristaltic Wave Locomotion and Shape Morphing with a Millipede Inspired System,” *J. Nonlinear Sci.*, vol. 27, no. 4, pp. 1093–1119, 2017.

[58] S. Kuroda, I. Kunita, Y. Tanaka, A. Ishiguro, R. Kobayashi, and T. Nakagaki, “Common mechanics of mode switching in locomotion of limbless and legged animals,” *J. R. Soc. Interface*, vol. 11, no. 95, pp. 20140205–20140205, 2014.

[59] R. M. Alexander, “Models and the scaling of energy costs for locomotion,” *J. Exp. Biol.*, vol. 208, no. 9, pp. 1645–1652, 2005.

[60] L. Matthey, L. Righetti, and A. J. Ijspeert, “Experimental study of limit cycle and chaotic controllers for the locomotion of centipede robots,” *2008 IEEE/RSJ Int. Conf. Intell. Robot. Syst. IROS*, pp. 1860–1865, 2008.

[61] K. Tsujita, K. Tsuchiya, and A. Onat, “Decentralized Autonomous Control of a

Quadruped Locomotion Robot," *Proc. AMAM 2000*, pp. 1–8, 2000.

[62] S. Aoi, T. Tanaka, S. Fujiki, T. Funato, K. Senda, and K. Tsuchiya, "Advantage of straight walk instability in turning maneuver of multilegged locomotion: A robotics approach," *Sci. Rep.*, vol. 6, no. July, pp. 3–8, 2016.

[63] X. Wan and S. Song, "A Cam-Controlled, Single Actuator-Driven Leg Mechanism for Legged Vehicles," in *International Mechanical Engineering Congress and Exposition*, 2004.

[64] S. Kim and P. M. Wensing, "Design of Dynamic Legged Robots," *Found. Trends Robot.*, vol. 5, no. 2, pp. 117–190, 2017.

[65] C. Quaglia, E. Buselli, R. J. Webster, P. Valdastri, A. Menciassi, and P. Dario, "An endoscopic capsule robot: A meso-scale engineering case study," *J. Micromechanics Microengineering*, vol. 19, no. 10, 2009.

[66] P. Valdastri, R. J. Webster, C. Quaglia, M. Quirini, A. Menciassi, and P. Dario, "A new mechanism for mesoscale legged locomotion in compliant tubular environments," *IEEE Trans. Robot.*, vol. 25, no. 5, pp. 1047–1057, 2009.

[67] M. Simi, P. Valdastri, C. Quaglia, A. Menciassi, and P. Dario, "Design, fabrication, and testing of a capsule with hybrid locomotion for gastrointestinal tract exploration," *IEEE/ASME Trans. Mechatronics*, vol. 15, no. 2, pp. 170–180, 2010.

[68] P. Glass, E. Cheung, H. Wang, R. Appasamy, and M. Sitti, "A motorized anchoring mechanism for a tethered capsule robot using fibrillar adhesives for interventions in the esophagus," *Proc. 2nd Bienn. IEEE/RAS-EMBS Int. Conf. Biomed. Robot. Biomechatronics, BioRob 2008*, pp. 758–764, 2008.

[69] B. Kim, S. Park, and J. O. Park, "Microrobots for a capsule endoscope," *IEEE/ASME Int. Conf. Adv. Intell. Mechatronics, AIM*, pp. 729–734, 2009.

[70] K. M. Dorgan, "The biomechanics of burrowing and boring," *J. Exp. Biol.*, vol. 218, no. 2, pp. 176–183, 2015.

[71] J. R. Blake and M. A. Sleigh, "Mechanics of ciliary locomotion," *Biol. Rev. Camb. Philos.*

Soc., vol. 49, no. 1, pp. 85–125, 1974.

[72] "Air Hogs - Thunder Trax." [Online]. Available: http://www.spinmaster.com/product_detail.php?pid=p20978.

[73] C. Cvetkovic *et al.*, "Three-dimensionally printed biological machines powered by skeletal muscle," *Proc. Natl. Acad. Sci.*, vol. 111, no. 28, pp. 10125–10130, 2014.

[74] R. Raman *et al.*, "Optogenetic skeletal muscle-powered adaptive biological machines," *Proc. Natl. Acad. Sci.*, vol. 113, no. 13, pp. 3497–3502, 2016.

[75] V. Chan, K. Park, M. B. Collens, H. Kong, T. A. Saif, and R. Bashir, "Development of miniaturized walking biological machines," *Sci. Rep.*, vol. 2, 2012.

[76] B. T. Latif and A. Bozkurt, "Roach Biobots," no. october, pp. 27–30, 2017.